# MANAGEMENT OF PHASE UNBALANCE IN LOW VOLTAGE DISTRIBUTION NETWORK (LVDN) WITH DISTRIBUTED GENERATORS AND DIVERSE LOAD

*A thesis*
*submitted in fulfillment of the award of the degree of*

**Doctor of Philosophy**

submitted by

**Jayakumar P**

Under the Supervision of

**Dr. Reji P**

and

**Dr. Meenakshy K**


**Department of Electrical Engineering**
**Government Engineering College, Thrissur**
**University of Calicut**
**(2022)**

*Dedicated to my family*

# ACKNOWLEDGMENTS

It is a great pleasure to express my respect and deep sense of gratitude to my Ph.D. supervisor, **Dr. Reji P**, Professor (Rtd.), Department of Electrical Engineering, Government Engineering College Thrissur, for her guidance, enthusiastic involvement and persistent encouragement during the planning and development of this research work. I also gratefully acknowledge the efforts of thoroughly going through and improving the manuscripts, without which this work could not have been completed. I would also like to extend my special thanks to **Dr. Meenakshy K**, Professor, Department of Electrical Engineering, Government Engineering College Thrissur, my Ph.D. co-supervisor, for the timely help extended during the course of the investigation.

I acknowledge the help and encouragement from **the Principal**, Government Engineering College Thrissur, and the **Head of the Department**, Department of Electrical Engineering, for providing all the facilities to carry out the work.

I really want to convey my heartfelt gratitude to the Doctoral Committee members, **Dr. T.N.Padmanabhan Nambiar**, former chairman and Professor, Amrita Vishwa Vidyapeetham, Coimbatore, **Dr. Ashok S**, Senior Professor, Department of Electrical Engineering, National Institute of Technology, Calicut, **Dr. B.Jayanand** and **Dr. M.Nandakumar**, Professors, Department of Electrical Engineering, Government Engineering College, Thrissur, for their constructive suggestions, support and guidance for shaping the research work.

I acknowledge the support from the **AICTE** and the authorities of the **Kerala State Electricity Board Limited, Vydyuthi Bhavanam**, as well as the aid from staff at the section offices that helped me during the investigation.

The blessings and inspiration of my parents and teachers have enabled me to complete this assignment. I owe a debt of gratitude to all of them. My wife's patience, love, and encouragement along this journey are commendable. Sincere thanks are due to my colleagues, friends, and all the other people whose names do not appear here, for helping me either directly or indirectly at all even and odd times.

Finally, I am indebted and grateful to the Almighty for enabling me in this endeavor.

**Jayakumar P**

# ABSTRACT

The Low Voltage Distribution Network (LVDN) faces new challenges due to the high integration of Distributed Generators (DGs) and Electric Vehicle (EV) chargers. Being the last link between the utility and the consumer, any issue at this level is important. But it is usually non-technically managed with a lot of imperfections. The line impedances are inherently unbalanced and power flows due to single-phase sources and loads are difficult to forecast. So, maintaining of phase balancing in an LVDN is difficult. Furthermore, certain orders of harmonics that cancel during balanced operation persist in unbalanced conditions. This intensifies the harmonic problem caused by power electronics-based non-linear sources and loads. High neutral current and Neutral-to-Earth Voltage (NEV) due to zero sequence components generated by phase unbalance and harmonics is an issue in the present-day distribution system. Moreover, the unbalanced harmonic operation of LVDN reduces the efficiency and lifespan of equipment and devices connected to the system.

In this work, a realistic feeder model that accounts for the non-ideal state and imperfections of an LVDN was proposed for studying the impact of DG integration. A parameter approximation method using limited data is suggested for distribution system operators lacking smart meters and data loggers. A Kerala low-voltage distribution feeder is modelled using theoretical and realistic methods. Comparison of results from the models with the actual data shows the validity of the proposed realistic model. Before allowing DG interconnection at a location, the feasibility has to be analysed and strategic conclusions have to be derived. As the theoretical model may lead to wrong conclusions, the realistic model is more reliable for deciding the DG penetration limit. Analysis of the Kerala real feeder was done with the proposed realistic model to study the impact of DG integration to reduce adverse effects. Situations of high DG penetration and reverse power flow at LVDN were analysed and their impacts on voltage spread, unbalance, and line loss were highlighted for decision making.

A low-cost, sustainable solution for improving the power quality of LVDN was also proposed. The new neutral grounding strategy can limit the propagation of harmonics. In this case, neutral current is utilised to improve the power quality without any additional equipment. The new neutral grounding method was implemented in the European Low Voltage Test Feeder and compared with the existing system. It is found to be effective at damping the propagation of various harmonics. Additionally, the neutral-to-earth voltage and earth fault current were also found to be reduced.

But there was a slight increase in line loss. The dynamic response of the system under load variations was also verified and found satisfactory.

During unbalanced harmonic operation, the neutral current is reported as high. In this work, a novel custom power device has been developed for reducing zero sequence unbalance that contributes to neutral current. The device is also capable of providing some ancillary services. The developed prototype was tested under balanced and unbalanced conditions of source and load. The results show that the device successfully reduces the zero-sequence components. Also, the device supplies reactive power more judiciously to improve the power factors and significantly reduce the neutral current. Experimental analysis demonstrates the ability of the device to reduce harmonics in the system.

Concisely, this research work considers the high neutral current contributed by the zero-sequence components of phase unbalance and harmonics as one of the main challenges in LVDN. The suggested low voltage feeder model using minimum field data allows a more realistic analysis to decide the limit of DG penetration. As a sustainable solution, the novel neutral grounding strategy can improve the power quality of an LVDN. Above all, the new custom power device developed can reduce the zero-sequence components while providing ancillary services such as adaptive power factor correction, neutral current reduction, and harmonic mitigation.

# Contents

# List of Figures

# List of Tables

# List of Acronyms/Abbreviations

| | |
|---|---|
| ACSR | Aluminium Conductor Steel Reinforced |
| AT | Ampere Turns |
| BEE | Bureau of Energy Efficiency |
| BSS | Battery Storage System |
| DG | Distributed Generator |
| DL | Dynamic Load |
| DNO | Distribution Network Operator |
| DSO | Distribution System Operator |
| DSTATCOM | Distribution Static compensator |
| EMC | Energy Management Centre |
| EPRI | Electric Power Research Institute |
| ESS | Energy Storage System |
| EV | Electric Vehicle |
| FGN | Fully Grounded Neutral |
| G2V | Grid-to-Vehicle |
| HT | High Tension |
| IEEE | Institute of Electrical and Electronics Engineers |
| KSEB | Kerala State Electricity Board |
| LT | Low Tension |
| LV | Low Voltage |
| LVDN | Low Voltage Distribution Network |
| LVUR | Line Voltage Unbalance Rate |
| MV | Medium Voltage |
| MuCE | Mutual Compensator Extractor |
| NEMA | National Electrical Manufacturers Association |
| NEV | Neutral-to-Earth Voltage |
| OpenDSS | Open Distribution System Simulator |

| | |
|---|---|
| PCC | Point of Common Coupling |
| PF | Power Factor |
| PV | Photovoltaic |
| PVUR | Phase Voltage Unbalance Rate |
| RDAP | Radial Distribution Analysis Program |
| SGN | Singly or Selectively Grounded Neutral |
| SLG | Single Line to Ground |
| TDD | Total Demand Distortion |
| TFWG | Test Feeder Working Group |
| THD | Total Harmonic Distortion |
| V2G | Vehicle-to-Grid |
| V2H | Vehicle-to-Home |
| VUF | Voltage Unbalance Factor |
| ZSB | Zero Sequence Blocker |
| ZSF | Zero Sequence Filter |
| ZSS | Zero Sequence Suppressor |

# List of Symbols

| | |
|---|---|
| $n$ | Neutral |
| $a, b, c,$ | 3 phase terminals, lines or coils |
| $a', b', c'$ | 3 phase terminals at load side |
| $X, X'$ | Reactance matrix |
| $R, R'$ | Resistance matrix |
| $Z, Z'$ | Impedance matrix |
| $L$ | Inductance |
| $g$ | Ground |
| $N$ | Number of turns |
| $r$ | Radius of toroid core |
| $\Phi$ | Magnetic flux |
| $V_a, V_b, V_c$ | Phase voltages at source side terminals $a, b, c$ |
| $V_{a'}, V_{b'}, V_{c'}$ | Phase voltages at load side terminals $a', b', c'$ |
| $I_a$ | Current in phase 'a' |
| $I_b$ | Current in phase 'b' |
| $I_c$ | Current in phase 'c' |
| $I_n$ | Current in neutral line |
| $V_m$ | Voltage in the compensator coil |
| $I_m$ | Current in the compensator coil |
| $X_c$ | Capacitive reactance |
| $X_{aa}$ | Reactance due to self-inductance of phase 'a' coil |
| $X_{bb}$ | Reactance due to self-inductance of phase 'b' coil |
| $X_{cc}$ | Reactance due to self-inductance of phase 'c' coil |
| $X_{ab}$ | Reactance due to mutual inductance between phase 'a' and 'b' lines |
| $X_{bc}$ | Reactance due to mutual inductance between phase 'b' and 'c' lines |
| $X_{ac}$ | Reactance due to mutual inductance between phase 'a' and 'c' lines |

| | |
|---|---|
| $X_{am}$ | Mutual reactance between phase 'a' and compensator coils |
| $X_{bm}$ | Mutual reactance between phase 'b' and compensator coils |
| $X_{cm}$ | Mutual reactance between phase 'c' and compensator coils |
| $Z_{aa}$ | Self impedance of phase 'a' line |
| $Z_{bb}$ | Self impedance of phase 'b' line |
| $Z_{cc}$ | Self impedance of phase 'c' line |
| $Z_{nn}$ | Self impedance of neutral line |
| $Z_p$ | Self impedance of phase coil |
| $Z_{mm}$,$Z_m$ | Self impedance of compensator coil |
| $Z_{ab}$ | Mutual impedance between phase 'a' and phase 'b' lines |
| $Z_{bc}$ | Mutual impedance between phase 'b' and phase 'c' lines |
| $Z_{ac}$ | Mutual impedance between phase 'a' and phase 'c' lines |
| $R_{aa}$ | Resistance of phase 'a' line |
| $R_{bb}$ | Resistance of phase 'b' line |
| $R_{cc}$ | Resistance of phase 'c' line |
| $R_{ab}$ | Mutual resistance between phase 'a' and 'b' lines |
| $X_{mm}$ | Self reactance of compensator coils |
| $X_{mp}$, $X_{pm}$ | Mutual reactance between any phase and compensator coil |
| $X_{ma}$ | Mutual reactance between compensator coil and phase 'a' coil |
| $X_{mb}$ | Mutual reactance between compensator coil and phase 'b' coil |
| $X_{mc}$ | Mutual reactance between compensator coil and phase 'c' coil |
| $X_p$ | Self reactance of phase coils |
| $X_m$ | Self reactance of compensator coils |
| $I_A$ | Feeder head current by actual measurement |
| $V_{rA}$ | Regulation at feeder tail end by actual measurement |
| $R_T$ | Conductor resistance |
| $I_T$ | Feeder head current by theoretical model |
| $V_{rT}$ | Regulation at feeder tail end by theoretical model |
| $V_{ag}, V_{bg}, V_{cg}, V_{ng}$ | Voltages at source side of the line section |
| $V_{a'g}, V_{b'g}, V_{c'g}, V_{n'g}$ | Voltages at load side of the line section |

| | |
|---|---|
| $R_R$ | Realistic resistance computed by approximation |
| $V_0$ | Zero sequence voltage |
| $I_0$ | Zero sequence current |
| $X_0$ | Zero sequence reactance |
| $Z_0$ | Zero sequence impedance |
| $I_{ac}$ | Phase 'a' capacitor current |
| $I_{bc}$ | Phase 'b' capacitor current |
| $I_{cc}$ | Phase 'c' capacitor current |
| $I_{res}$ | Residual current |
| $V_{res}$ | Residual voltage |
| $ID$ | Inner diameter |
| $OD$ | Outer diameter |
| $N_a$ | Number of turns of phase 'a' coil |
| $N_b$ | Number of turns of phase 'b' coil |
| $N_c$ | Number of turns of phase 'c' coil |
| $N_m$ | Number of turns of compensator coil |
| $L_{aa}$ | Self inductance of phase 'a' coil |
| $L_{bb}$ | Self inductance of phase 'b' coil |
| $L_{cc}$ | Self inductance of phase 'c' coil |
| $L_{mm}$ | Self inductance of phase compensator coil |
| $[Z_{abc}]$ | Impedance matrix |
| $V_{aa'}, V_{bb'}, V_{cc'}$ | Voltages across the phase coils |
| $PN1, PN2, \ldots$ | Pole numbers |
| $Yprim$ | Primitive admittance matrix |

# Chapter 1

# Introduction

## 1.1 Background

Historically, the primary emphasis of power systems study was on centralised power generation and bulk transmission. In order to meet the rising electricity demand, alternative power generation solutions are in consideration to avoid the widespread consumption of depleting fossil fuels. To limit the environmental impact due to large-scale consumption of fossil fuels, Distributed Generators (DGs) utilising non-conventional energy sources are encouraged globally. As a result, attention has moved to dispersed generation and distribution, followed by the deregulation of the energy sector. Among the DGs, photovoltaic (PV) plants that make use of the abundant and universally available sunlight account for a significant portion. As a result of the prevailing land constraints, rooftop small PV plants integrated at distribution level are more prominent. Increased integration of DGs at the low voltage level presents new challenges for Distribution System Operators (DSOs). One of them is ensuring the quality of supplied power.

The term 'power quality' refers to the degree to which the magnitude, phase angle, frequency, and wave form of the utility voltage agree with the specified one. When one or more of the parameters deviates for an extended or brief period of time, it causes power quality problems. Low power quality can result in equipment failure, malfunction, or premature ageing. The detrimental effect of poor power quality reduces the efficiency and lifespan of consumer equipment through excessive heating and accelerated thermal ageing. It also reduces supply side efficiency by increasing losses and shortening equipment lifespan. The estimated total cost of poor power quality cannot be ignored when annual revenue losses on both the supply and consumer sides are considered. Some of the power quality concerns that must be addressed in the new scenario are debated here.

In a balanced 3 phase system, voltages or currents in each phase have the same amplitude and are offset by 120 degrees. Phase unbalance occurs when either of these conditions is violated. Phase unbalance or imbalance is quantified using a

multitude of definitions and equations that are inconsistent. Line voltage unbalance in percentage (LVUR) is characterised by the NEMA standard as the ratio of the maximum deviation of line voltage from the average line voltage to the average line voltage [1]. There are two ways to express the degree of unbalance in phase voltage terms. The rate of phase voltage unbalance(1), PVUR(1) is defined as the ratio of the maximum deviation of phase voltage magnitude from the average phase voltage magnitude to the average phase voltage magnitude. In another way, phase voltage unbalance rate(2), PVUR(2) is regarded as the ratio of the greatest difference between phase voltage magnitudes to the average phase voltage magnitude [2].

These equations consider voltage magnitudes only, leaving out phase angle information, which is also a deciding parameter of unbalance level. Furthermore, a specific level of unbalance defined by these equations may have a wide range of possible phase and line voltage values. Moreover, these definitions do not reflect the physical effects caused by phase unbalance. It is important to know the level and nature of the unbalance to fix the derating of equipment and compute additional losses produced [3].

Voltage unbalance factor (VUF) is a more rigorous definition of unbalance that includes the magnitude and phase displacement of voltages. According to IEEE 1159-2019, the voltage unbalance taking phase angle information into account can be defined for two components. Using Fortescue's theorem, an unbalanced system can be resolved into positive, negative, and zero sequence components. The negative sequence voltage unbalance factor, VUF(-), is defined as the ratio of the negative sequence component to the positive sequence component, whereas the zero sequence unbalance factor, VUF(0), is defined as the ratio of the zero sequence component to the positive sequence component. The voltage unbalance factor (VUF) is also known as the "true definition" of unbalance, but it necessitates the transformation of the unbalanced system into its sequence components.

A set of 3 positive, negative, and zero sequence components can represent a 3 phase unbalanced system. The set of positive and negative sequence components are balanced among themselves, whereas the 3 zero sequence components are equal and unidirectional. In a 3 phase, 4 wire system, the zero sequence currents combine to form a residual current, which flows as neutral current. Also, in an ungrounded system, the residual voltage can cause a neutral shift. In 3 phase rotating machines and transformers, the electromagnetic effects created by the positive and negative sequence components are balanced, whereas the zero sequence components produce lateral magnetic forces and saturation. Mechanical damage and vibrations can result from unbalanced electromagnetic forces.

Higher level integration of DGs increases the degree of uncertainty at the distribu-

tion level. PV plants up to 5 kWp are permitted to be integrated as single-phase units at a low voltage distribution level [4]. Electric vehicles (EVs) are being promoted as a way to reduce carbon footprints, and their use is increasing. The emerging vehicle-to-grid (V2G) and grid-to-vehicle (G2V) schemes significantly add dynamics at this level. Battery Storage Systems (BSS) can also change their role as a source or load, contributing to stochastic and intermittent characteristics. The stochastic behaviour and intermittent dynamic characteristics of these sources and loads create major challenges for distribution network operators in the new scenario. It is difficult to achieve a perfect division of the single phase sources and loads among the 3 phases. Even when done wisely, the dynamic operating characteristics of the units cause the operation to be unbalanced for the majority of the time. Above all, at the distribution level, the lines are not transposed, and line impedances are unequal, which causes unequal line voltage drops. As the voltage at the point of common coupling is unbalanced, even the 3 phase balanced loads draw uneven currents. So it is difficult to maintain the phase balance of a modern distribution system [5]. As most of the sources and loads at this level are dynamic and single-phase, higher level integration of low-carbon technologies contributes to the uncertainty at this level.

The majority of low carbon technologies, such as PVs and EVs, use nonlinear power electronic devices. Almost all consumer devices include power electronic switches for improved control and efficient power utilisation. These units handle non-sinusoidal currents and voltages. Non-sinusoidal voltages and currents can be decomposed into their fundamental and harmonic components. Moreover, each harmonic order can be classified as a positive, negative, or zero sequence based on the respective sequence effects produced. Many harmonics cancel themselves at neutral in a balanced environment, whereas in an unbalanced state they do not. Positive harmonics produce pulsating torques, while negative sequence harmonics create braking torques. This results in additional heating loss and mechanical vibrations in electric machines. In a 3 phase, 4 wire system, zero sequence harmonics are added at the neutral point and flow through the neutral wire.

High neutral current is an important issue in modern distribution systems. The primary reason for neutral current is phase unbalanced operation. In the new scenario, it is difficult to balance single phase sources and loads in a distribution system. Zero sequence currents generated by phase unbalance flows through the neutral line. As a result of the proliferation of power electronic based modern consumer devices and power supply equipment, the presence of harmonics in the system is significant. Zero sequence or triplen harmonics add up and contribute to neutral current. Neutral current is high in modern power distribution systems as a result of phase unbalanced

operation and harmonics. High neutral current results in neutral-to-earth Voltage (NEV), neutral heating and additional line losses.

In earlier days, the expected neutral current was low and, in order to save money, the size of the neutral conductor was only half the size of the phase conductor. However, nowadays it is no longer permitted, because the neutral current during unbalanced harmonic operation exceeds phase currents on many occasions [6–9]. Another effect of high neutral current is the hazardous rise in the voltage between neutral and the earth. Above all, if the voltage at the point of common coupling is unbalanced and distorted, even linear balanced loads can only draw nonlinear unbalanced currents.

## 1.2 Motivation for the present research work

Secondary distribution, or low voltage distribution, is the final link in a power system network that connects the utility grid to consumers. Any event at this level has a direct impact on the quality of power supplied. Moreover, secondary distribution is observed to be poorly managed, and line losses are higher. The system is usually in poor condition with defective joints, mismanaged section fuses, and arcing contacts. The theoretical models do not account for these imperfections in the system. Hence, a realistic modelling of an LVDN is required to investigate the impact of increased penetration of low carbon technologies. Frequent load addition, variation in consumption patterns, and increased penetration of DGs at this level are all causes for concern. Periodic balancing of single phase sources and loads among the phases is important for minimizing adverse effects and losses. Above all, in the emerging micro grid and smart grid topologies, phase-unbalanced operation can lead to unstable operation resulting in grid collapse, affecting system reliability. The neutral current has increased significantly as a result of phase unbalance and harmonics, resulting in an increase in the neutral-to-earth voltage. At neutral, the zero sequence currents combine and flow as neutral current. The zero sequence currents are caused by the unbalance of the zero sequence current and harmonics. Certain order harmonics, which normally cancel under balanced conditions, are present during phase unbalanced operation, resulting in significant harmonic distortion. Because of the unbalanced and distorted voltage at the point of common coupling, even balanced linear loads draw unbalanced nonlinear currents, triggering a cumulative detrimental impact on the system. As a result, it is critical to damp harmonic propagation and reduce zero sequence currents in the network.

## 1.3 Objectives of the research work

There exists more stress at the distribution level due to large-scale integration of renewable energy sources, and more attention is needed to ensure power quality and consumer satisfaction. For power distribution network there are two type of topologies namely, North American and European systems. The majority of the research and analysis is centred on North American network topology. In European distribution networks, low-voltage lines are long and supply a large number of consumers. A distribution feeder or a primary distribution line is a line that carries current from a secondary substation to a distribution substation and is the one that supplies bulk consumers, whereas a distributor or a low-voltage distribution feeder is one from which tapings are taken along its length to supply the consumer. In this thesis, the term "low voltage distribution feeder" refers to a distributor line that supplies power to an end user at a low voltage level. This work is primarily concerned with resolving some issues in low voltage power distribution systems with European network topology. The following primary research goals are taken into account.

i) **D**evelop a realistic model of the low voltage distribution network.

ii) **D**evelop an effective strategy for analysing the impact of DGs at low voltage distribution network.

iii) **I**ntroduce a sustainable solution to improve the power quality of low voltage distribution network.

iv) **P**ropose a custom power device to minimize zero sequence current due to phase unbalance.

v) **U**tilize ancillary services of the custom power device to improve the performance of low voltage distribution network.

## 1.4 Organization of the thesis

Following introduction in Chapter 1, research work presented in this thesis is organized and structured as below.

i) **Chapter 2** presents a comprehensive review of literature in the area and solutions suggested for problems of concern.

**ii)** In **Chapter 3**, the proposed realistic model of a low voltage feeder is presented. Performance analysis of the theoretical model and the proposed model and its comparison are also presented.

**iii)** A novel method for improving the power quality of low voltage distribution feeder and its benefits are presented in **Chapter 4**.

**iv)** **Chapter 5** presents the concept of a new custom power device for reducing zero sequence unbalance, providing ancillary services such as harmonic mitigation, neutral current reduction and power factor improvement.

**v)** In **Chapter 6** conclusions highlighting the major contributions of the research work are presented.

# Chapter 2

# Literature review

## 2.1 Introduction

Power transmission is the bulk transportation of electric power from remote generating locations over large distances to substations closer to demand areas. Transmission lines carry electric power at a high voltage so as to reduce line losses. In transmission systems, a 3 phase, 4 wire arrangement is commonly used. Power from the transmission system is reduced to lower voltage levels by transformers in the substation before being delivered. A distribution system is a network of lines that transport electricity from substations to consumers. Primary distribution lines have a voltage of about 11 kV (11,000 volts), while a typical home needs 230 volts. The secondary distribution system, or a low voltage distribution system, delivers power at a voltage that can be given directly to a home or business. Distributors, or low voltage distribution lines are conductors through which power is delivered to consumers from distribution transformer.

Distribution lines are commonly radial in nature, and are structured to carry power exclusively in one direction, with no provision for generators. However, distributed generators such as PVs, wind turbines, and other locally generated power sources are commonly incorporated into the grid through distribution systems. Dispersed small generating units are integrated into the grid through the distribution network. As a result of this, nowadays the distribution network is under increased stress.

In earlier days, distribution lines received less attention than transmission lines and were not well managed by operators. In regions where dispersed generators are incorporated, this is changing. In the new scenario of power generation and distribution, re-engineering and active management activities have begun to make the distribution system more efficient and reliable. Shareholders and regulatory authorities are putting pressure on distribution utilities to raise investment and enhance operational efficiency.

Transmission system and balanced power flow analysis were traditionally given more emphasis and included in power system studies. Transmission lines have a more

phase balanced operation than distribution lines. Recently, power system studies are giving more attention to the distribution side. A "distribution feeder" is defined as a line carrying current from a substation to the distribution transformer, whereas a "distributor" is a low voltage line from which tappings are taken along its length to provide supply to the consumer. In this literature, the term "low voltage distribution feeder" or "low voltage distribution network" is used to refer a distributor line supplying power to an end user at 230V.

## 2.2 Characteristics of low voltage distribution network (LVDN)

Unlike transmission lines with long runs and more or less balanced operations with 3 lines, low voltage distribution lines are comparatively short with tapings to connect consumers. Distribution lines have a 3 phase, 4 wire configuration operating at more or less unbalanced conditions most of the time. The American style of distribution has some differences compared to European networks [10]. Most of the studies in this regard were conducted on American style networks and many software tools are available for the purpose [10, 11].

Both European and American systems are radial and have identical voltages and power carrying capacities. The primary distinctions are in topology, configuration, and applications. The transformers in European systems are larger, and there are more customers per transformer. Most European transformers are three phase and range in size from 300 to 1000 kVA. North American systems offer single phase units rated at 25 or 50 kVA. The secondary system in North America has been standardised at 120/240 V. A circuit serving the same load in the European system can travel four times the distance with twice the voltage as in North America. Each system type has advantages and drawbacks. In general, North American designs cause less customer disruption. Less primary is used in European systems, and practically all of it is on the major feeder backbone. When the main feeder fails, all customers on the circuit are disrupted. To achieve the same level of reliability, the European system requires additional switches and other equipment. Both systems are employed outside of Europe and America, and adoption follows colonial history, with European system being more commonly adopted [12].

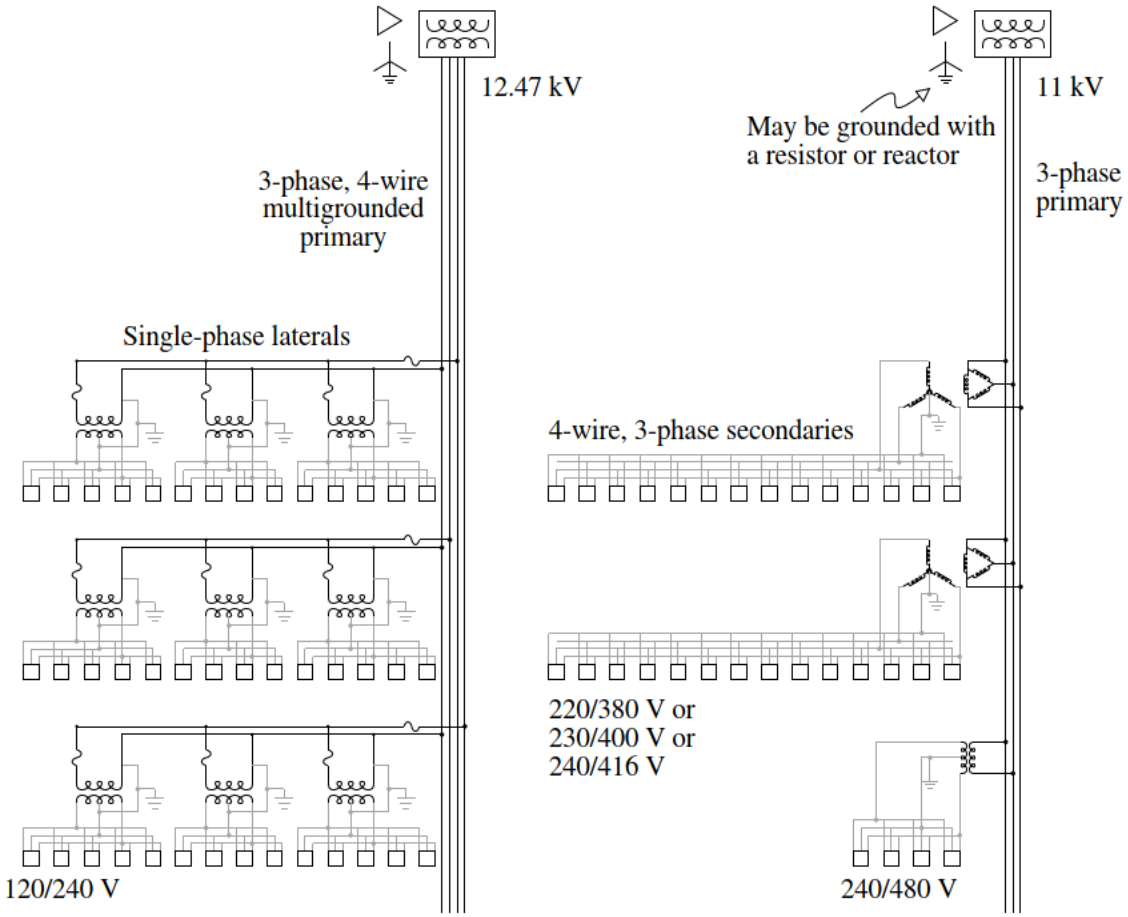


**Figure 2.1:** Topology difference of North American and European distribution systems [12]

### 2.2.1 Distributed generation (DG)

A lot of renewable energy based dispersed or distributed generators are integrated at the low voltage level. The major portion is small photovoltaic (PV) plants. Wind turbines and micro hydel plants are also there. The uncertainty associated with these sources poses a big challenge to distribution system management. For maximum utilisation of renewable energy, battery storage systems (BSS) are used. Battery storage systems have the potential to assist with the operation and control of distribution networks in both active and reactive modes. They can support distribution networks by delivering auxiliary services in addition to energy balancing. In this context, BSS can assist in the optimal trade-off between technical and economic goals, such as network voltage deviations, feeders or lines congestion, network losses, and the cost of supplying loads from external grid or local producers. The BSS may support the network by increasing the utilisation of renewable production, but also increases load stochasticity [13]. These BSS units change their roles as load and source during

charging and discharging, which adds to the system dynamics.

### 2.2.2 Dynamic loads (DL)

In the low voltage distribution network, most of the loads are due to domestic consumers or offices. The load variation depends on the nature of the population and climatic conditions. So the load dynamics are not easy to predict accurately. One of the issues is the charging of EVs. Charging an unknown number of EVs with an unknown power and energy consumption provides a challenge in real-time managing the electrical power demand and supply scenario. Furthermore, because of the high charging current and the frequent addition and disconnection of a large number of intermittent EV loads, pose challenges to the efficient operation of the power distribution system [14]. Most of the onboard electric vehicle (EV) chargers are single phase units. For quick charging of batteries, charger capacities are being increased day by day. The stochastic interconnection of single phase EV chargers makes phase balancing difficult to maintain. Also, the expected technologies like Vehicle-to-Grid (V2G) and Vehicle-to-Home (V2H) will change the role of EVs as a source. So the recent developments in low carbon technologies increase the uncertainties at the distribution level.

### 2.2.3 Distribution system losses

The majority of power system losses occur along primary and secondary distribution lines. The losses at this level can be classified as commercial losses and technical losses. Commercial losses are caused by non-technical reasons such as theft, malfunctioning metres, reading errors, un-metered energy consumption, and so on. The technical losses are due to energy dissipated in the conductors, contacts, joints and other equipment such as transformers [15]. Technical losses can be classified as constant or variable. Constant losses are unaffected by load current. These are energy losses that occur as long as the system is powered and are due to magnetization, dielectric leakage, and noise. Variable loss is proportional to the square of the current. Some factors increasing the technical losses are:

- Heating caused by line resistance of long feeders
- Extra losses due to thermal overloading of feeders
- Losses owing to poor workmanship at contact resistance in joints
- Contacts sparking and heating due to insufficient contact pressure

- Losses in non-technically managed transformer bushings, drop-out fuses, isolators, LT switches, and on other components
- The distribution system has a low Power Factor
- Extra transformer losses due to presence of residual and unbalanced flux during unbalanced operation
- High neutral currents due to unequal load distribution among three phases
- Extra losses caused by harmonics

Balancing current along 3 phase lines is one of the simplest ways to reduce distribution system losses. Distribution system phase balancing also helps to balance voltage drops in phase lines, providing a more balanced voltage to 3 phase consumers. Same current magnitudes at the substation do not ensure load balance along the feeder's length. The balance of feeder phases varies during the day and across the seasons. Feeders are often deemed "balanced" when the phase current magnitudes deviate by less than 10 percent. Similarly, balancing load among distribution feeders reduces losses when the conductor resistance is the same.

## 2.3 Power quality issues in low voltage distribution network

The required attributes of public utility power distribution are defined by specific standards [16]. EN 50160 defines the major voltage parameters and their permitted deviation ranges at the customer's common coupling point in low voltage (LV) and medium voltage (MV) energy distribution systems. The EN 50160 and IEC 61000 standards differ in a variety of aspects. The IEC 61000-4 standard specifies measurement methods, measurement formulas, accuracy standards, and aggregation times. This is because the primary goal of this standard is to provide uniform specifications for measurement devices so that analyzers from different manufacturers produce consistent findings. But EN50160 specifies recommended levels for certain power quality criteria, as well as a percentage of time during which the levels should be maintained [17].

Unbalance in phase and harmonics are two significant power quality concerns that are particularly frequent in low voltage power distribution [18]. Unbalanced voltage and voltage variation during peak and off-peak hours are related issues. Transformer

tap changers are often used to control voltage drop along a feeder. Equal load distribution throughout all the 3 phases of the network is one way to address the imbalance issue, but it is not simple to maintain [19, 20]. To meet the increasing power demand,

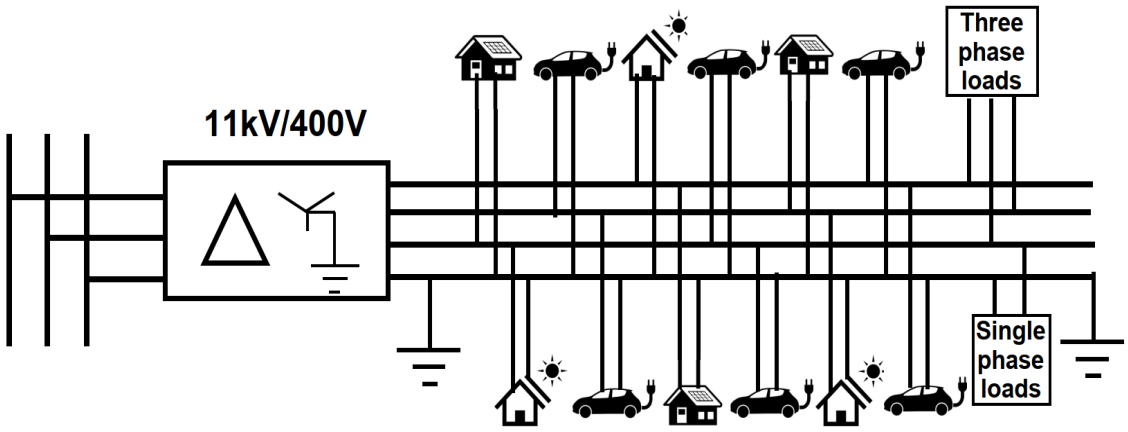


**Figure 2.2:** LV feeder with PVs, EVs and other loads

the modern power system is driving towards renewable energy based Distributed Generator (DG) technology. Rooftop small photovoltaic (PV) units are easier to accommodate and more beneficial for the population and are widely accepted. Reliability and better cost management are other benefits of small PV plants. Such units below 5kW are allowed to interconnect at distribution level [19]. Moreover, the increase in electric vehicles (EVs) also makes the problem difficult to manage as they have intermittent and stochastic characteristics. There are different types of electric vehicle charging systems, and the effects of multiple chargers together are a concern. The level of certain harmonics will be amplified in some situations, while they will be reduced in others [21].

A typical low voltage feeder with single phase loads, PVs, and EVs is shown in Figure 2.2. The PVs and EVs have stochastic and dynamic characteristics, which make it difficult to balance between the phases. Due to the presence of power electronic converters, all of them inject or draw harmonic currents into the system. In phase unbalanced operation, the harmonics affect the system more adversely than in normal balanced operation. The balanced 3 phase loads also draw unbalanced current as the supply voltage is unbalanced. Also, if the voltage at the point of common coupling is distorted, the linear loads also draw non-linear currents. So the problem of unbalance and harmonics have cumulative effects on the system.

### 2.3.1 Phase unbalance

The voltage unbalance can be due to normal reasons, such as the presence of single phase sources and loads, or due to abnormal operation during high impedance faults, poor electrical contacts at switching devices, non-uniform joints, asymmetry in capacitor banks and components etc. The impact of phase unbalance on the power distribution system is elaborated in [22]. The various effects produced by voltage and current unbalances and their interdependence are depicted in the Figure 2.3. The

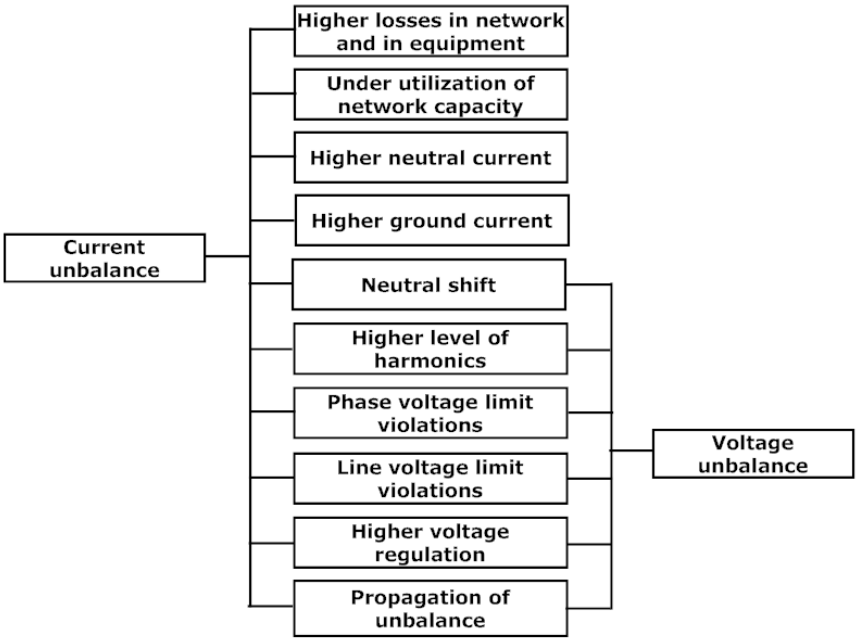


**Figure 2.3:** Consequences of voltage and current unbalances

implications of voltage unbalance on equipment and appliances are wide ranging and potentially catastrophic in nature. A severe unbalance results in a significant reduction in the lifespan of equipment, leading to frequent equipment replacement. Due to increased phase unbalance, the efficiency of 3 phase equipment is reduced, causing higher wastage and a rise in energy consumption. Frequent motor failure is mainly due to unbalance. When a 3 phase motor is driven by a balanced 3 phase voltage with a positive sequence component alone, only positive torque is produced. The negative sequence voltage due to voltage imbalance produces the opposite braking torque and results in motor vibration and noise. An increase in losses due to voltage imbalance causes overheating and eventual failure. Also, the additional heat produced by extra losses due to unbalance raises the winding temperature, causing the insulation to break down. Thus, a voltage imbalance can even result in the complete failure of a motor in extreme circumstances. When a 3 phase voltage with high unbalance is applied to a transformer, the flux in the transformer core becomes asymmetrical.

This asymmetrical flux results in increased core loss, winding temperature, and early failure of the transformer [23]. In a 3 phase, 4 wire system, the zero sequence unbalance increases the neutral current and results in the malfunctioning of the earth fault relay and other equipment.

**Definitions of phase unbalance**

Phase unbalance in a 3 phase system is defined as the deviation of phase voltages or currents from their specified equal magnitudes or a mutual shift of 120 degrees between adjacent phases or both. Different agencies and communities quantify unbalance in different ways. This imparts confusion in analysing the implications of unbalance. Many papers discuss the difference in unbalance definitions [2, 24, 25]. The three definitions of voltage unbalance or imbalance are

1. NEMA (National Equipment Manufacturer's Association) [1]

$$\%LVUR = \frac{\text{Max. voltage deviation from the avg. line voltage}}{\text{Avg. line voltage}} \times 100 \quad (2.3.1)$$

2. IEEE – The phase voltage unbalance rate (PVUR) [26]

$$\%PVUR = \frac{\text{Max. voltage deviation from the avg. phase voltage}}{\text{Avg. phase voltage}} \times 100 \quad (2.3.2)$$

3. True Definition (IEEE Standard 1159-2019) using Fortescue's theorem [27]

$$\%VUF(-\backslash 0) = \frac{\text{Negative or Zero sequence voltage component}}{\text{Positive sequence voltage component}} \times 100 \quad (2.3.3)$$

According to Fortescue's theorem, an unbalanced 3 phase system can be resolved into sum of two sets of balanced sequence components and one set of zero sequence components and as shown in Figure 2.4.

$$\begin{bmatrix} V_a^0 \\ V_a^+ \\ V_a^- \end{bmatrix} = \frac{1}{3} \begin{bmatrix} 1 & 1 & 1 \\ 1 & a & a^2 \\ 1 & a^2 & a \end{bmatrix} \begin{bmatrix} V_a \\ V_b \\ V_c \end{bmatrix} \quad (2.3.4)$$

where $a = 1\angle 120^0$

These definitions have important implications during analysis of effects created by unbalance in various situations or equipment. In the presence and absence of a zero sequence component, the different definitions have significant difference [24]. For 3 phase systems with isolated ground, the different definitions of unbalances do not

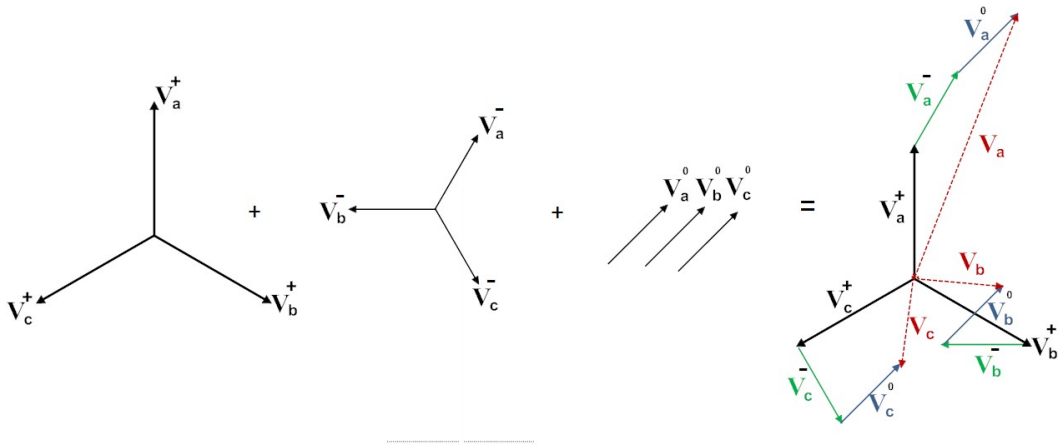


**Figure 2.4:** Sequence components

have a significant difference. But for 3 phase systems with grounding, the presence of zero sequence components may cause errors in unbalance computation by different definitions. Different definitions of voltage unbalance are analysed and compared to find the applicability of definitions in various situations in [25]. The various definitions

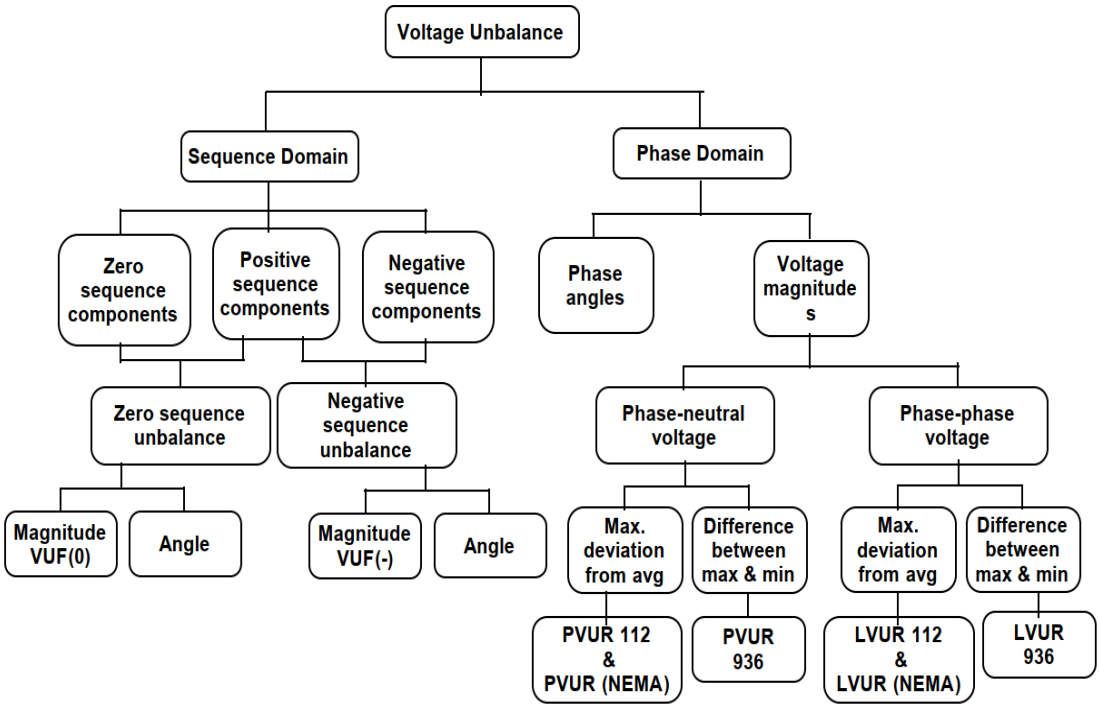


**Figure 2.5:** Various definitions of phase unbalance

and methods used for quantifying unbalance are presented in the form of schematics in Figure 2.5

### Phase unbalance limits

There are different standards and limits set by different agencies for voltage and current unbalance. Though the American National Standards Institute (ANSI) C84.1 limits the maximum voltage unbalance to 3.0 percent at the utility meter, the utilities in the United States restrict voltage unbalance to 2.5 percent. The British Standard European Norm(BS EN) 50160 : 2000 restrict voltage unbalance mostly 2 percent, but occasionally 3 percent. National Equipment Manufacturers Association (NEMA) MG–1, allows only 1 percent of unbalance for motor supply voltage, as it create 6-10 percent current unbalance, violating warranty validity. Unfortunately no standards specify strict limit for current unbalance. However, if the NEMA MG-1 standard is followed, a maximum current unbalance of 30 percent due to 3 percent of voltage unbalance is the limit mentioned. The differences in definitions and limits lead to confusions among the utility, manufacturers, and the end-users. Assessment depends mostly on guidelines of utility and manufacturers.

## 2.3.2 Harmonics

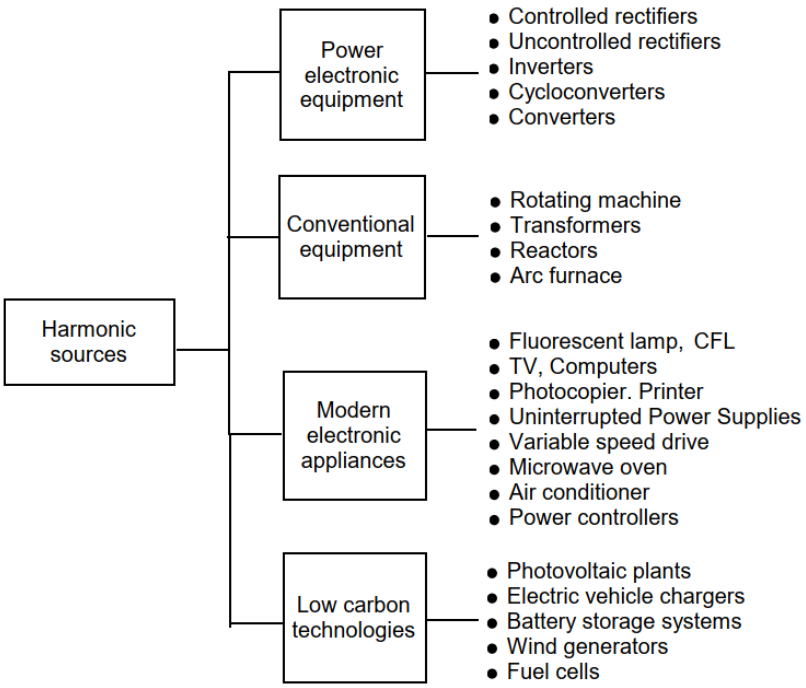


**Figure 2.6:** Harmonic sources

When the current drawn by a load does not have the same waveform as the supply voltage, this is referred to as the nonlinearity of the load. Harmonics are generated

in the power lines mainly by nonlinear sources and loads [6]. Most of the DGs have power electronic based inverters injecting nonlinear currents. Moreover, nonlinear loads connected to the distribution system cause harmonic currents to flow through the system. With the presence of harmonics, current and voltage are distorted and deviate from ideal sinusoidal waveforms, which is undesirable in electrical systems. Harmonics are currents that are multiples of the fundamental line frequency (50 or 60 Hz) [28]. When harmonic currents pass through impedances in a system, voltage harmonics are generated that distort the supply voltage. Harmonics can affect transformers, equipment, and wiring, causing heat and loss. International regulations have made significant strides toward eliminating the issue [7].

Harmonics overload and wear out power transformers. Power transformers are designed to carry current at the frequency of the power grid (50 or 60 Hz). It is the amount of heat generated by a transformer that restricts its power handling capacity. The heat generated by a transformer is caused by the transformer's inherent resistance as well as the current that it is carrying. It follows that if the transformer is carrying significant harmonic currents, its rating must be reduced, otherwise the transformer will overheat and wear out due to insulation degradation, causing it to fail. In contrast to what electrical codes specify, neutral wire with the same capacity as the phase wire (or larger) can be used. But this protects the conductors, but it does not help to protect the transformers. Transformers with a "K" rating of at least 9 should be used in a harmonic environment. These transformers has been specifically designed to withstand the effects of harmonic current [3].

### 2.3.3 Neutral current

Three phase conductors and one neutral conductor are used in the 3 phase, 4 wire system. Single phase loads are connected between the various phase conductors and the neutral conductor. As a result, the neutral conductor serves as the common return for all of the single phase load currents. When each of the 3 phase conductors has a nearly equal load, the neutral current will be nearly zero. This is because each phase current is ideally 120 degrees out of phase with the other. Or in another way, the load currents 'cancel out' when they reach the neutral wire. The cancellation helps in reducing the neutral wire to a smaller size than the phase wires.

In the present scenario, the load balancing is difficult to maintain. Neutral current is primarily due to phase unbalance. Moreover, the higher level harmonic currents generated by non-linear loads have a significant amount of triplen harmonics. Harmonics having an order of multiples of three are called triplen harmonics. Because of the phase properties, triplen harmonic currents add together on the neutral wire

instead of cancelling out each other. The triplen harmonics currents also contribute to higher neutral current [29]. As an example, Figure 2.7 shows the addition of third harmonics at neutral. Consequently, the neutral wire carries much higher currents

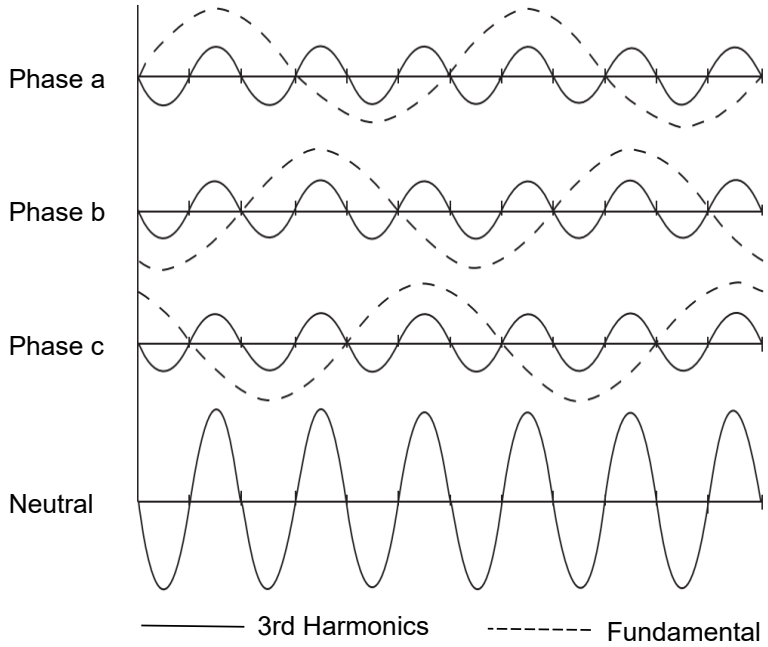


**Figure 2.7:** Addition of third harmonics at neutral

than it was intended to [30,31]. In fact, the harmonic current alone in the neutral wire has the potential to be up to many times larger than the total rated current of the system. Anyway, it is not unusual for the neutral current to reach the phase current value. The use of neutral line undersizing in an unbalanced harmonic environment is therefore absolutely not allowed [7, 32].

## 2.4 Review of modelling of low voltage distribution feeders

To study the impact of low carbon technologies on the distribution network, exact modelling of the system is required [33]. At every consumer interconnection point, the parameters such as voltage regulation, phase unbalance, harmonics, etc. should be within the specified limits. In addition to these considerations, line loading and the possibility of reverse power flow must be analysed when deciding on a DG interconnection request. As a result, it is critical to conduct a distribution system analysis while considering DG interconnection requests. For this purpose, a dependable model of the distribution system is required.

It is much easier and straight-forward to model the transmission line network,

because in transmission systems, the 3 phases are more or less equally loaded, and the lines are transposed at line sections in order to make the line impedances equal. As a result, voltage and current are balanced at the nodes, making power flow analysis simple. The balanced load flow analysis is sufficient for transmission lines. Moreover, on transmission lines, imperfections are not very common. Aside from that, unlike distribution lines, there are loads at either end of the lines only. For studies, only the positive sequence network of the system is required, and parameters computed for one phase can be used for other phases.

The modelling of the distribution system is different, and unbalanced power flow must be performed in order to conduct the analysis. Distribution system lines are loaded asymmetrically and are not transposed. Moreover, the presence of neutral line and neutral current should be taken into account. In addition, distribution feeders are radial in nature and their X/R ratio is lower. As a result, the assumptions that are typically used in transmission system analysis cannot be applied to distribution lines. Instead of the conventional methods used in balanced load flow analysis, forward and backward sweep methods are widely used in distribution system power flow analysis.

The configuration of power distribution networks varies depending on the needs of consumers and the operating scenarios. In addition, the network topology and operating voltages of North American and European style distribution systems are different. So, modelling of a distribution system necessitates more time and effort. There are many distribution system modelling and analysis approaches and methods. However, only a few attempts have been made to model low-voltage distribution systems of European style [10].

The early attempt to model a radial distribution feeder is available in [34, 35]. A Radial Distribution Analysis Program (RDAP) was developed in it for feeder analysis. The motivation for the work was to reduce losses in the feeder by placing capacitor banks and voltage regulators. During the modelling, the spot loads and distributed loads are scaled to match the demands recorded in the substation. The approach was purely a theoretical one to demonstrate the radial analysis program and there was only a low emphasis on the accuracy of the feeder model.

Methods for determining a 3 phase line's sequence impedances and phase frame impedance matrix are discussed in [36]. Though the sequence impedance models and the impedance matrix models give almost the same voltages at nodes, the power losses during balanced and unbalanced operating conditions show differences. This is because the sequence impedance models do not consider the mutual interaction between lines. Moreover, the sequence impedance model has inherent problems during the modelling of two phase and single phase lines. So, for distribution line mod-

elling, the impedance matrix based phase frame method is more suitable. Carson's or modified Carson's equation can be used for forming the matrices of impedance [37,38].

The method for modelling 3 phase, 4 wire line segments for distribution feeders using a mathematical approach is available in literature. The resistance of conductors can be determined directly from the data table. Earlier, impedance calculations of overhead lines were solely dependent on geometry. Skin and proximity effects were further considered. In 1926, Carson proposed a method of assessing the effect of earth return on power lines. It demonstrates that modelling ground returns influences the accuracy of impedances and, hence, the voltage rise and drop. Several formulae for ground return parameters were presented, although Carson's equations for overhead lines are the most extensively used. Carson's equations involve infinite integrals with complex arguments, making them difficult to compute. As a result, converging infinite series were frequently employed. With Carson's equations [39], the self and mutual inductances can be calculated at a given frequency. Carson's equations are useful for calculating the impedance of overhead wires involving earth return paths [36, 37, 39, 40]. For approximating the effect of the earth on conductors, modified Carson's equations are available. In this regard, the modelling of a rural LV feeder presented in [35, 37] is extremely useful. The impedance matrix of overhead line segments calculated using modified Carson's equations is presented in [41].

An attempt was made to model an unbalanced distribution feeder in [42]. To create a balanced decoupled network model from the system data, approximations were made. Single and two-phase buses and branches were removed from the model in order to approximate the actual unbalanced system to a balanced one. In order to compensate for the removed branches, loads were aggregated on the nearest 3 phase upstream bus and represented as unbalanced loads, and the resulting unbalanced loads were replaced with the closest balanced representations. The phase impedance matrix of the transformer delta winding, distribution lines and connected loads are combined. Further approximations were made for the phase decoupled representation and analysis. Transformer and voltage regulator connection types are converted into wye connections and mutual coupling between phases lines is removed and set to zero. All delta or line-to-line connections are represented as equivalent wye connections. The approach is highly non-realistic and optimistic, because of the approximations used for decoupling and balancing of the network. In addition, the level of voltage unbalance is an important piece of information that must be verified in the current situation.

An unbalanced active distribution system with DG modelled in [43] uses three sequence networks. The three networks were used for power flow analysis, similar to the

conventional one positive sequence network representation that was used for balanced network analysis. Each sequence network was subjected to power flow iterations using a forward-backward sweep subroutine in a coupled manner. An entirely decoupled forward backward sweep was performed after the sequence component power flow analysis had reached convergence. However, this method necessitates the repetition of the same power flow algorithm in subroutines for various sequence networks, both coupled and decoupled, in order to achieve the results. Also requires the balanced synchronous machines and electronically coupled unbalanced DGs in their sequence component models. It is difficult to accommodate parameters such as neutral earthing, neutral current, and neutral-to-earth voltage using a decoupled approach as it require additional computations in order to obtain the combined effect of sequence voltages or currents at each line section and node during unbalanced operation.

For the exact feeder modelling in [44], the resistive and reactive parameters of the distribution feeder are obtained by actual measurements of active and reactive power flows at both ends of the feeder. But the solutions to the resulting equations of active and reactive power for different phase lines for both ends of the feeder section are not so easy. So, special solution methods are required for precise computation of feeder parameters.

The Low Voltage distribution network analysis employing smart meters is presented in [45]. Semi-automated LV load flow analysis using real load data is used. The method requires extensive deployment of smart meters and a special algorithm to control them. Modelling of distribution feeders in [46] is based on a reduction criteria. The information gathered from the utility is reduced based on the area of interest within the model. Though the model was validated using short circuit data and field measurement information, the number of line sections, loads, and other system components were reduced conveniently. The representative steady state feeder model developed in [47] was by comparing active power, reactive power, and voltage, utilising data acquisition systems deployed for power quality monitoring.

A feeder modelling approach presented in [48] is exclusively for European style feeders with isolated neutrals. That is, the neutral is grounded at the transformer, and the consumer neutral is isolated from the ground. The impact of the neutral current return route through the neutral conductor is ignored using traditional Kron's reductions [49]. While a 4 wire model provides correct power flow findings and allows for the monitoring of the neutral voltage, it also adds to the computational load.

The modelling of a feeder for studying voltage regulation in a feeder with DGs as the main focus is presented in [50]. But the imperfections in the feeder were not considered during the modelling. In [51] the limit of PV generation allowable in a

low voltage feeder is determined. In this paper, a relationship between the connected load, feeder impedance, and PV generation is established.

The results of theoretical models of distribution systems do not correspond to the actual performance of the system as they are typically ill-conditioned and poorly managed from a technical point of view. Because of improper joints, mismanaged section fuses, and arcing contacts, the line parameters are altered [15]. The theoretical model is unable to account for these imperfections and non-homogeneity. This will result in values for regulation and power loss that are significantly different from the actual values. Compared to theoretical values, actual losses and regulation are significantly different. Based on the results of the theoretical model, incorrect decisions about DG interconnection requests may be made, resulting in violations of the voltage constraints imposed by the supply code.

The papers [47,52] present feeder models based on statistical techniques using large amounts of data. The availability of network parameters is a significant challenge when modelling distribution systems. It is difficult to obtain complete data for all system components, and in some cases, only partial or aggregated parameters are available. For perfect and accurate modelling, further advancements in system data acquisition and management are required. Though smart meters aid in data collection for analysis, they are not yet implemented in all countries. So these methods will not help all DNOs.

In agreement with [53], accurate or realistic representations or models of low voltage networks are difficult to achieve. It is critical to add this level of detail to decide on interconnection requests of DGs at low voltage level. Variation in consumption patterns, as well as the addition of new loads, are common in the distribution system. It is not uncommon for feeder topology to change as a result of modifications, repairs, and the addition of new service connections. It is also difficult to differentiate between the phase lines to which the loads are connected. Because of these considerations, creating an accurate and realistic model of an LV feeder is a difficult task. In order to evaluate the impact of PV penetration, a realistic model of the LV system based on a minimum of data is required. An approximate, but more realistic model using less data, representing the actual feeder condition is preferred.

## 2.5 Review of improving power quality in low voltage distribution feeders

It has been reported that problems such as unbalance, harmonics, and high neutral current can be addressed individually or together. Installation of additional devices or the implementation of special operational strategies are among the approaches taken in order to block or eliminate the neutral current generated, as well as to reduce harmonics and unbalance. Various solutions from different approaches were attempted to address the issue. Many of the solutions are based on power electronics, electro magnetics, or a combination of these technologies. A tabular representation of various solutions proposed for solving these issues individually or together is given for a better presentation. Table 2.1 provides an overview of the solutions in the literature and their short comings.

**Table 2.1:** Review of power quality improvement solutions for LVDN

| **Author, Year** | **Addressed problems** | **Suggested solution and remarks** |
|---|---|---|
| Islam et al., 2019 [54] | Unbalance | Network reconfiguration for phase balancing. It affects 3 phase rotating machines and highly depends on load and renewable energy forecasting. |
| Hashmi et al., 2002 [55] | Unbalance | Phase balancing utilising energy storage facilities. It always demands spare storage, resulting in under-utilisation of storage capacity. |
| Liao & Yang, 2018 [56] | Unbalance | Phase controlled and coordinated charging for electric vehicles. It requires multiple switching of phase lines and EV chargers following a complex algorithm. |

*Continued on next page*

Table 2.1 – Review of power quality improvement solutions for LVDN

| **Author, Year** | **Addressed problems** | **Suggested solution and remarks** |
|---|---|---|
| Kikhavani et al., 2019 [57] | Unbalance | Coordinated charging of EV for load balancing. This can cause delays in EV charging. |
| Das et al., 2018 [58] | Unbalance, Neutral current | Power electronic based Static Var Compensator (SVC) is to be installed at distribution level. |
| Gupta et al., 2014 [59] | Unbalance, Neutral current | Electro magnetic static phase balancer derived from a conventional transformer. It is a bulky and costly solution. |
| Rafi et al., 2020 [60] | Unbalance | Compensation techniques using power electronic converters. To follow network dynamics and restrict high switching losses, a robust controller design is required. |
| Motta & Faundes, 2016 [61] | Harmonics | Conventional active, passive, and hybrid filters. Can eliminate harmonics without addressing other problems. |
| Sun et al., 2015 [62] | Harmonics | An active power filter with a double-resistive network. A separate unit for each order harmonics results in multiple units with an aggregated higher power rating. |
| Pogaku & Green, 2006 [63] | Harmonics | Multiple harmonic impedance elements suggested. The elements have to be installed throughout the network with DG units. |

*Continued on next page*

Table 2.1 – Review of power quality improvement solutions for LVDN

| **Author, Year** | **Addressed problems** | **Suggested solution and remarks** |
|---|---|---|
| Yoshida & Wada, 2015 [64] | Harmonics | Blocking of triplen harmonic current by special control of DG units in a 3 wire system. Other order harmonics are not considered and are not applicable for all configurations. |
| Baghaee et al., 2017 [65] | Harmonics, Unbalance | DGs with virtual impedances of fundamental and harmonic frequency. A special decentralised control strategy is needed. |
| Jedari et al., 2017 [66] | Harmonics | A control strategy was suggested for PVs. Coordinated operation of PVs with active power filters reduce the maximum utilisation of renewable energy. |
| Zeng et al., 2019 [67] | Harmonics | PV acting as a virtual load during harmonic absorption. Active power curtailment of PV is necessory. |
| Fukami et al., 2002 [68] | Neutral current | Special synchronous machines. Synchronous machines may not be necessary in all feeders. |
| Sabir & Javaid, 2019 [69] | Neutral current | Electric springs connected to non-critical loads. The application is limited to microgrids. |
| Singh et al., 2010 [70] | Neutral current | Special electromagnetic equipment dedicated to handling neutral currents. Bulky, additional equipment is needed. |

*Continued on next page*

Table 2.1 – Review of power quality improvement solutions for LVDN

| Author, Year | Addressed problems | Suggested solution and remarks |
|---|---|---|
| Sreenivasarao et al., 2013 [71] | Neutral current | D-STATCOM along with a T-connected transformer and a single phase active power filter (APF). It comprises of many devices. |
| Freitas et al., 2020 [72] | Harmonics, Neutral current | Electromagnetic suppressor. It eliminates zero sequence harmonics only and uses both an electromagnetic blocker and filter. |

Unbalance, harmonics and high neutral current are the main power quality issues in LVDN. They are more or less related to each other and a common solution to this is expected. At the distribution level, equipment with sophisticated controls is not advisable as the life and cost is questionable. It is expected that a robust, low cost, long term solution that addresses these three related issues will be developed.

## 2.6 Review of zero sequence suppression methods

The high neutral current in LVDN is due to the zero sequence components created by unbalance and harmonics. In unbalanced conditions, than the symmetrical control, the unsymmetrical control of individual phase voltages can reduce the voltage unbalance to a greater extent. Though individual phase control can help to reduce the voltage unbalance factor, this control requires additional power ratings of equipment and complex control strategies [73].

Many methods are there for suppressing zero sequence currents. Filters of various configurations are usually preferred. In power electronic converters, switching control based schemes are used in many applications. Power electronic drives of special electric machines require zero sequence suppression to avoid circulating currents [74–78]. Parallel grid-connected converters with common dc and ac buses can effectively contribute to the system power level. But among the voltage source converters working in parallel with a common dc link, if the ac side does not have isolation transformers, a zero sequence current is generated and circulated due to the 3rd order zero sequence

voltage. In [79, 80] an improved space vector modulation scheme is proposed that can effectively achieve zero sequence current suppression. Whereas a hybrid pulse width modulation scheme based on common grid information is followed in [81]. The reduction of zero sequence circulating current suggested in [82] uses coordinated control of neutral potential. All these methods are exclusively for equipment involving power electronic based converters.

The general approach needed for low voltage distribution networks is different. The concept of using zig-zag transformers for generating neutral terminals and handling neutral current harmonics is a well established one [83]. When 3 phase transformer windings are connected in a zig-zag pattern so as to restrict the sequence components having the same phase, it is known as a zig-zag transformer. The schematic of the winding connection and phasor diagram of the zig-zag transformer are given in Figure 2.8.

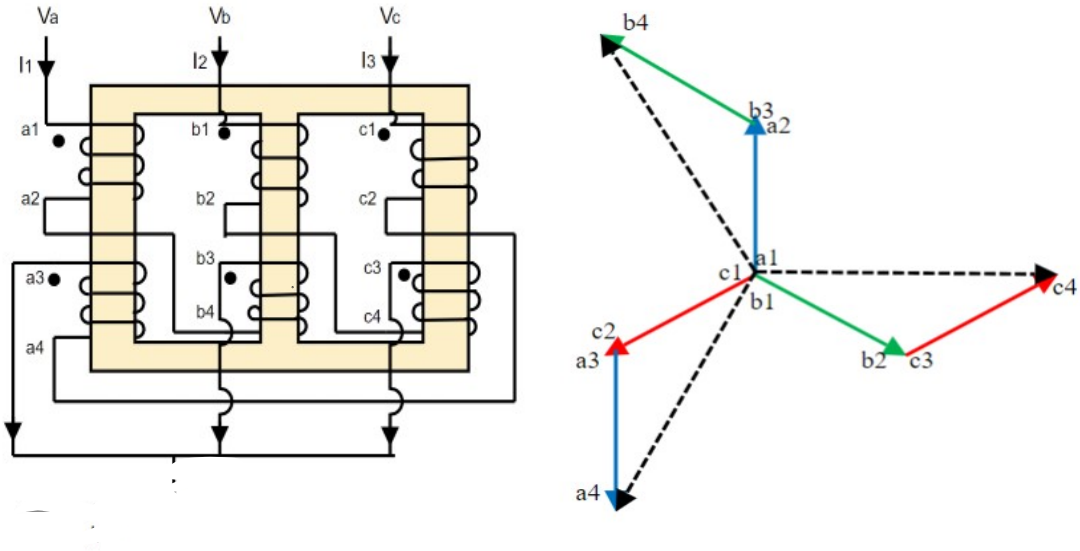


**Figure 2.8:** Connection diagram and phasor diagram of zig-zag transformer

Zig-zag transformers are capable of balancing 3 phase, currents by cancelling zero sequence currents. The total harmonic distortion (THD) and neutral current of a 3 phase, 4 wire distribution system operating under an unbalanced nonlinear load condition can be reduced by installing a zig-zag transformer [84]. Though zig-zag transformers effectively attenuate the neutral current and zero sequence harmonic currents due to load unbalance, the current through the zig-zag transformer and neutral current increase with source side unbalance [30]. The zero sequence blocker (ZSB) suggested as a solution to this problem is a special transformer. The three windings are wound on the same core as other transformers. Ideally, ZSB has zero reactance for positive and negative sequence components, but has three times the self

reactance for zero sequence. The ZSB connected in series with the source provides high zero sequence impedance, while the zig-zag transformer connected in parallel with the load provides low zero sequence impedance. The zero sequence harmonic currents tend to flow through the zig-zag transformer rather than through the source, thereby serving the purpose of harmonic elimination [31].

The zero sequence suppressor (ZSS) also has a similar configuration. It is a combination of two devices: a zero sequence blocker (ZSB) and a zero sequence filter (ZSF). Zero sequence blockers are 3 winding devices connected in series with the load, whereas zero sequence filters are zig-zag transformers connected in parallel with the load [72, 85, 86] and is shown in Figure 5.21. Another category of solution uses

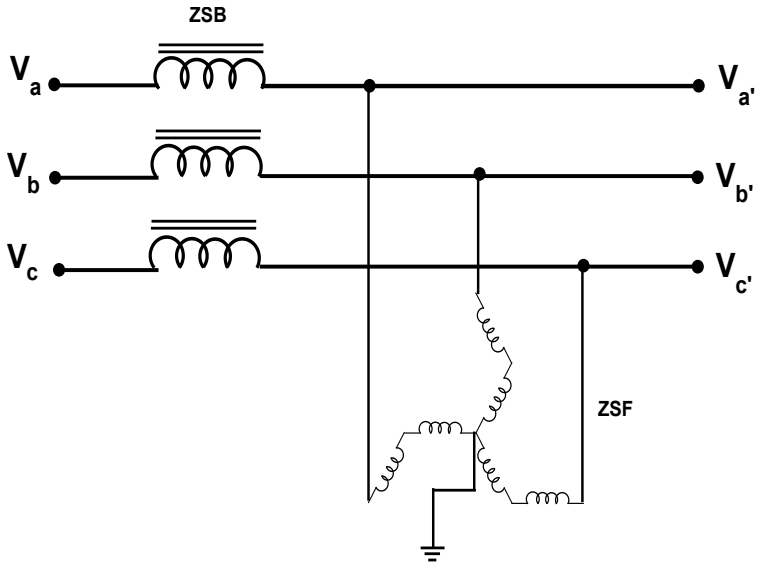


**Figure 2.9:** Circuit diagram of a zero sequence suppressor

a combination of electromagnetic devices along with power electronic devices. Active power filters (APFs) can address the simultaneous challenges of harmonic suppression and reactive power compensation. A 3 phase, 4 wire active filter and a zig-zag transformer suggested in [87] can be used with both three wire and four wire systems. Also, the rating of the required active power filter is reduced due to the presence of the zig-zag transformer. This combination can perform satisfactorily under limited zero sequence utility voltage only. A reduced rating voltage-source converter in conjunction with a zig-zag transformer as a distribution static compensator (DSTATCOM) suggested in [88] can compensate for reactive power, harmonic currents, neutral current, load balancing, and voltage regulation at the common coupling point. In a further modification, a combination of a single phase inverter of reduced rating and a zig-zag transformer is suggested as a hybrid filter for suppressing neutral harmonic currents [89].

A DSTATCOM topology in [90] for improving power quality in a 3 phase 4 wire distribution system has a 3 leg VSC with a zig-zag transformer to compensate for reactive power, voltage regulation, power factor correction, as well as load balancing, harmonic current elimination, and neutral current compensation at the point of common coupling. To reduce the voltage rating of the VSC, a zig-zag transformer is used, and for isolating the power electronics system, a third winding is used additionally.

### 2.6.1 OpenDSS software tool

The software tool to study distribution feeder performance should be able to perform harmonic flow analysis. OpenDSS is a frequency domain simulation tool for general purpose distribution system study. It was developed by the Electric Power Research Institute (EPRI) as a harmonic flow analysis tool and is capable of rapidly solving power flow problems in a wide range of network configurations. OpenDSS can handle both user defined and default harmonic spectra for investigation [91].

OpenDSS employs a nodal admittance circuit model formulation, which is conventionally used in power system analysis. From typical power distribution system data, algorithms in OpenDSS can generate nodal admittance matrices. A primitive admittance matrix, Yprim, is computed for each circuit element in the model. The Yprim matrices are input into the sparse matrix solver. These small nodal admittance matrices are used to build the main system admittance matrix, Ysystem, which connects the circuit model. The structure of the OpenDSS written in Delphi manages the construction and changes of the Yprim matrices for each element in the circuit, as well as the bus lists, collecting of results via meter elements, and execution of control elements.

From an initial guess of the voltages, V, a direct solution of I = YV is obtained. Initially, loads and generators are represented by their linear equivalents that do not include injection currents. All of the phase angles and voltage magnitudes obtained will be in the correct relationship. This is similar to a "flat start" in other power flow algorithms, except that it considers all of the connections in the multi-phase, multi-voltage level system. The generated voltages are relatively close to the final converged solution, even when the nonlinear parts are included. This is significant since the distribution system simulator is intended to solve arbitrary n-phase networks with a wide range of transformer ratios and connections, and thus requires a decent starting approximation of the voltages. The iteration cycle begins by getting the injection currents from all of the power conversion (PC) elements in the system and inserting them into the corresponding slot in the current injection vector shown in Figure 2.10. The sparse matrix is then solved for the next voltage guess. The cycle

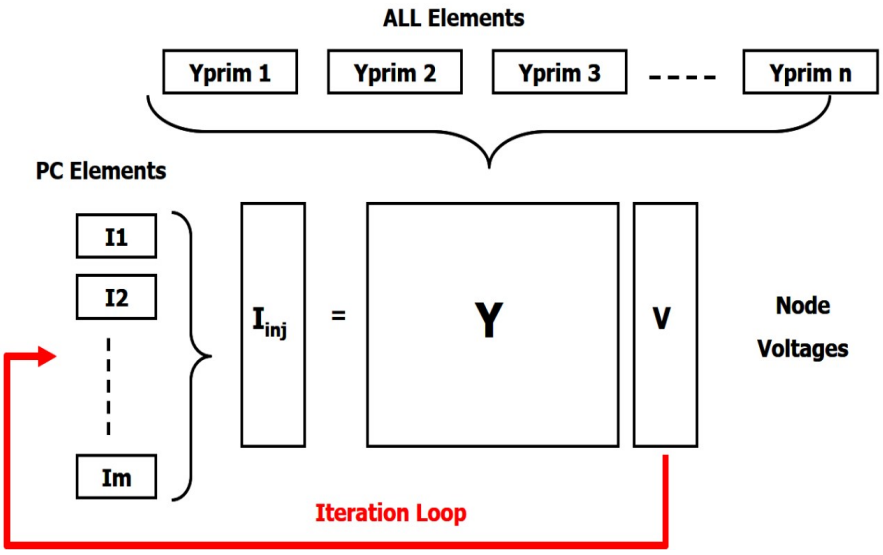


**Figure 2.10:** OpenDSS algorithm

is repeated until the voltages converge to 0.0001 pu.

OpenDSS offers two primary power flow solution types: iterative and direct power flow solutions. Loads and dispersed generators are regarded as injection sources in the iterative power flow mode. For the iterative power flow mode, two power flow algorithms are currently used: the standard current injection mode and the Newton current injection mode. The regular mode is typically faster, while the Newton mode is more robust for difficult-to-solve circuits. The normal mode is a basic fixed-point iterative method that works well for practically all distribution systems. Due to its speed, it is the recommended option for yearly simulations. In the direct solution mode, the loads and generators are incorporated as admittances in the system admittance matrix, which is then solved directly without iteration. Power flow calculations typically utilise an iterative solution with nonlinear load models, whereas fault investigations use a direct solution with linear load models. Following the conclusion of the power flow, the losses, voltages, flows, and other information for the system, each component, and specific designated locations are available. The losses are given as kW losses at each time instant, and energy meter models are used to integrate the power over a time interval [91].

## 2.7 Conclusion

The literature survey on feeder modelling shows that the existing feeder modelling techniques either ignore the realistic condition of the feeder or use excessive data

from field meters. A feeder modelling method that considers actual feeder conditions using minimum data is required for quick analysis of DG integration issues in the low voltage distribution network.

As the end user is directly connected to a low voltage distribution network, power quality at this level is important. Voltage unbalance, harmonic distortion, and high neutral current are the issues that need attention [30]. Devices and methods proposed for addressing one or more of these problems are in the literature. But these solutions need costly equipment or involve complex control strategies, while some solutions need dedicated, bulky electromagnetic devices. A low cost single sustainable solution to alleviate the power quality issues in low voltage distribution systems is being attempted. High neutral current is due to the unbalanced operation of single phase units and harmonics. Zero sequence currents due to unbalance and harmonics add at the neutral conductor to create a high neutral current. The passive and active filters are too costly and less reliable for low voltage levels. The zig-zag transformer and modifications with other equipment are bulky. A robust solution to limit the neutral current and capable of providing some ancillary services is preferred.

# Chapter 3

# Realistic modelling of low voltage feeders and analysis of an actual feeder

## 3.1 Background

The low voltage distribution system, which connects the utility grid to the consumer, is the last and weakest link in the power system. Nowadays, research in this area of power systems is drawing widespread interest. This is due to the new developments in dispersed generation, distribution automation, and smart grid technology. Globally, renewable energy based distributed generators (DGs) are encouraged to accommodate the rising power demand and reduce the carbon footprint. A large number of DGs are photovoltaic (PV) plants as solar irradiation is universal and freely available. Also, to overcome land scarcity, majority of them are installed as rooftop small PV plants integrated into the low voltage distribution network (LVDN) [92,93]. In several countries single phase units up to 5 kWp are allowed to interconnect at low voltage level. But the low voltage distribution system is observed to be inherently unbalanced and poorly managed one. Even without these single phase DGs, the phase balancing and voltage profile of the feeder are difficult to maintain [94]. Also, the identification of phase line to which these sources and loads are connected is difficult to achieve. Moreover, severe power loss is usually recorded at this level as the low voltage feeders are non-technically managed due to frequent repairs and have various imperfections. Being the last link between the supplier and the consumer, any issues at this level directly affect the quality and reliability of the power supply.

Implementing remedial measures, the undesirable effects due to the increased integration of DGs at distribution level can be reduced. The voltage at every consumer connection should be within the range specified by the supply regulation. So the aggregate PV injection has to be limited based on daytime consumption to limit any voltage rise due to local generation [95, 96]. Otherwise, problems like voltage rise, reverse power flow, phase unbalance and increased line loss may occur. Also, the unidirectional nature of the radial feeder may change, and current flow may become

bidirectional. So the extent of DG penetration is to be restricted. Before approving a PV interconnection request, factors like violation of voltage limits, voltage unbalance, line loading, and the possibility of reverse power flow, must all be analysed and reviewed [46, 97, 98]. But, according to renewable energy policy guidelines, distribution network operators (DNOs) must take a decision on PV plant interconnection requests within a certain time frame in which detailed modelling is not easy. So steps in this regard will be helpful for the DNOs.

In distribution systems, there are lot of variation in consumption patterns and load dynamics. Change in feeder condition is frequent due to modifications, repairs, and new service connections. This makes the distribution system non technically managed and ill-conditioned one. Arcing contacts, faulty switches, non-ideal joints, and loose contact in section fuses are common. Figure 3.1 shows a real feeder part in an improper state. Mathematical models can be used for analysing the performance of the feeders. But the imperfections and non-homogeneity are not accommodated in a theoretical model [99]. So such models give values for regulation and power loss that are far from true values [100]. The rise in voltage due to PV integration has close connection with feeder parameters [19]. As the theoretical feeder models predict unrealistic results, a model that is more accurate to actual feeder conditions will be beneficial. Also to investigate the effects of PV penetration in the distribution system, a realistic model of the LV feeder is necessary for analysis and decision making. But a perfect and accurate modelling of an LV feeder is difficult to achieve. Though smart metering aid in the collection of data for modelling, it is not yet available in all developing nations [101]. As a result, the solution based on data collection through smart meters cannot be possible for all distribution network operators (DNOs). Many available approaches necessitates extensive data collection using data loggers or phasor measurement units and its processing [102].

A realistic model of LV feeder using minimum data is proposed in this work. Modelling of LV feeder is done by theoretical method, and modification using limited data is proposed to approximate it close to real conditions. The model ensures more close results to real performance. In order to prove the efficacy of the method, a feeder under Kerala State Electricity Board Ltd. (KSEB) is modelled, analysed and validated. Open Distribution System Simulator (OpenDSS), a tool developed by Electric Power Research Institute (EPRI) [103] is used for the analysis. In this chapter the modelling of the low voltage feeder in the theoretical manner is given in Section 3.2 and the proposed low voltage realistic feeder model is presented in Section 3.3. The validation of the realistic model and comparison of results from the two models are given in Section 3.4, whereas Section 3.5 gives the analysis for issues of PV penetration

in a Kerala low voltage feeder using the realistic feeder model. The summary of the findings are provided in Section 3.6

**Figure 3.1:** Non-technically managed low voltage distribution feeder

## 3.2 Theoretical modelling of low voltage feeders

Unlike transmission lines, distribution lines are not transposed to equalise reactance due to mutual inductance between lines [10]. In a distribution feeder the loads are distributed along the length of the feeder, and phase currents through the lines are unbalanced due to the presence of single-phase sources and loads. Therefore, distribution lines are inherently unbalanced [104], and their analysis requires unbalanced power flow solutions different from transmission line analysis. Additionally, for single-phase loads, the neutral line and the effect of earth should be explicitly considered. So the modelling of the low voltage feeder requires a different approach than transmission lines.

The voltage profile of a feeder is determined by the load distribution along its length and the impedance of the line. Figure 3.2 illustrates a simple radial feeder with branches. Feeder head or branch head is a conductor section at the begining of a feeder or a lateral branch. In radial topology, the feeder head current and branch head currents are more as loads are interconnected at intervals along the length of the feeder. Feeder tail or branch tail is a conductor section at the end of the feeder or branch. The voltage profile along the feeder will be unevenly reduced towards the tail end due to the interconnection of consumer loads at different locations. So, normally, without any DG, at the fag end or tail end of the feeder, voltages and currents are low compared to the head ends.

The analysis of a low voltage distribution network requires solving unbalanced power

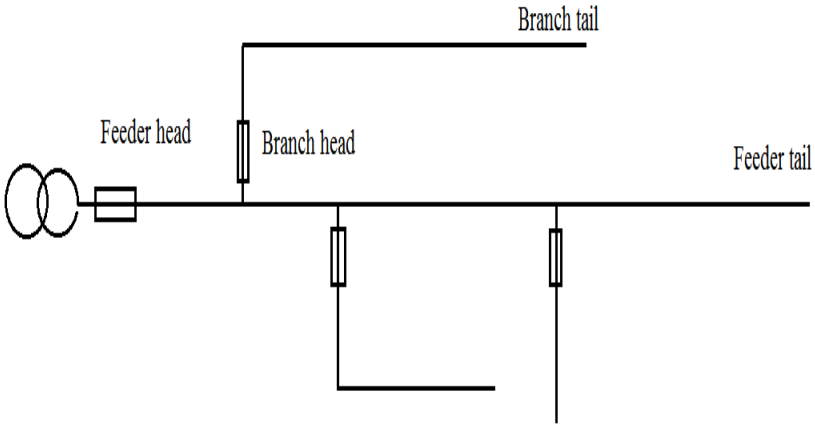


**Figure 3.2:** Simple radial feeder topology

flow equations. An unbalanced system can be analysed either by sequence component method or by phase frame method. As sequence component method involves three sequence component networks and their solutions, the phase frame method is widely adopted, also in OpenDSS. For modelling a feeder section, Carson's equations can be used. Carson's equations are helpful for determining the self and mutual impedances of conductors located above ground [38, 105]. Figure 3.3 depicts a line section of a 3 phase, 4 wire system with a grounded neutral line. The conductor voltage drop can be calculated using the impedance matrix using equation (3.2.1). The resistance of the conductor used for each line, the spacing between lines, and the earth resistance are all required to form the impedance matrix using Carson's equations [38, 104].

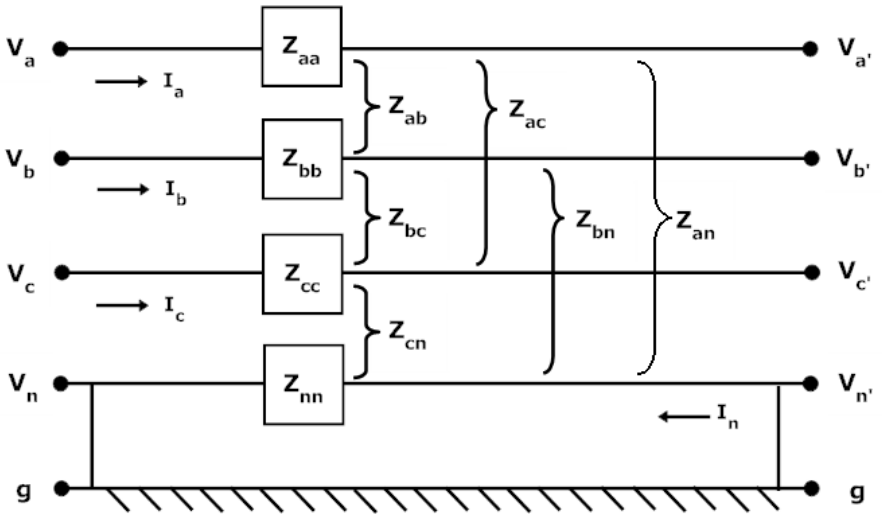


**Figure 3.3:** A 3 phase, 4 wire line section.

$$\begin{bmatrix} V_{ag} - V_{a'g} \\ V_{bg} - V_{b'g} \\ V_{cg} - V_{c'g} \\ V_{ng} - V_{n'g} \end{bmatrix} = \begin{bmatrix} Z_{aa} & Z_{ab} & Z_{ac} & Z_{an} \\ Z_{ba} & Z_{bb} & Z_{bc} & Z_{bn} \\ Z_{ca} & Z_{cb} & Z_{cc} & Z_{cn} \\ Z_{na} & Z_{nb} & Z_{nc} & Z_{nn} \end{bmatrix} \begin{bmatrix} I_a \\ I_b \\ I_c \\ I_n \end{bmatrix} \tag{3.2.1}$$

Where,

$V_{ag}, V_{bg}, V_{cg}, V_{ng}$ and $V_{a'g}, V_{b'g}, V_{c'g}, V_{n'g}-$ voltages at either end of the line sections

$I_a, I_b, I_c-$ phase currents

$I_n-$ neutral current,

$Z_{aa} = R_{aa} + jX_{aa}-$ self impedance of phase 'a' line,

$Z_{ab} = R_{ab} + jX_{ab}-$ mutual impedance between phase 'a' line and phase 'b' line,

All other terms have similar definitions.

The impedance matrix is predefined in equation (3.2.2)

$$\begin{bmatrix} Z_{aa} & Z_{ab} & Z_{ac} & Z_{an} \\ Z_{ba} & Z_{bb} & Z_{bc} & Z_{bn} \\ Z_{ca} & Z_{cb} & Z_{cc} & Z_{cn} \\ Z_{na} & Z_{nb} & Z_{nc} & Z_{nn} \end{bmatrix} = \begin{bmatrix} R_{aa} & R_{ab} & R_{ac} & R_{an} \\ R_{ba} & R_{bb} & R_{bc} & R_{bn} \\ R_{ca} & R_{cb} & R_{cc} & R_{cn} \\ R_{na} & R_{nb} & R_{nc} & R_{nn} \end{bmatrix} + j \begin{bmatrix} X_{aa} & X_{ab} & X_{ac} & X_{an} \\ X_{ba} & X_{bb} & X_{bc} & X_{bn} \\ X_{ca} & X_{cb} & X_{cc} & X_{cn} \\ X_{na} & X_{nb} & X_{nc} & X_{nn} \end{bmatrix} \tag{3.2.2}$$

Where,

$R_{aa}-$ self resistance of phase 'a' line,

$X_{aa}-$ self reactance of phase 'a' line,

$R_{ab}-$ mutual resistance of phase 'a' line and phase 'b' line due to proximity effect,

$X_{ab}-$ mutual reactance of phase 'a' line and phase 'b' line due to coupling of magnetic fields,

All other terms have similar definitions.

The voltage drop equation can be used to model each section of the entire feeder.

### 3.2.1 Theoretical modelling of an actual low voltage feeder

An actual low voltage feeder near Kerala State Housing Board, Thiruvananthapuram under the urban circle in the southern region of Kerala State Electricity Board (KSEB) was selected for modelling. In Kerala, the HT to LT ratio is low, and each low voltage feeder serves hundreds of consumers, resulting in higher distribution losses. Table 3.1 shows the technical specification of the transformer that supplies the feeder [106]. The feeder serves domestic and business consumers in Gandhari Amman Kovil Street

**Table 3.1:** Transformer data

| | |
|---|---|
| Type | Dyn11 |
| Rating | 250 kVA |
| High voltage | 11 kV |
| Low voltage | 433 V |
| Percentage impedance | 4.58 |
| Frequency | 50 Hz |

(Line 1) and Santhi Nagar Area (Line 2) through overhead lines. Figure 3.4 depicts the pole layout and consumer distribution along the feeder length. Poles PN1 to PN3 are in the feeder head sections, which connect the transformer to the branches. Line 1 is made up of poles PN3 to PN26, whereas Line 2 is made up of poles PN27 to PN47. Even though around 150 consumers are served by the lines, there are only a few three-phase connections among them. Line 1 carries more load and is around 0.3 kilometres long, while Line 2 carries a lower load and is around 0.4 kilometres. The consumer loads are distributed along the length of the feeder. The 3 phase lines and neutral are constituted by the same conductor and the spacing is similar to IEEE spacing ID500 [107]. ACSR conductor is used at the feeder sections and conductor data is given in Table 3.2. The earth resistivity is considered as $100\Omega m$, a standard value [37].

Average consumer consumption is computed from the energy meter readings. The

**Table 3.2:** Details of the ACSR conductor

| | |
|---|---|
| Code Name | Rabbit |
| Voltage rating | 433V |
| Diameter of conductor | 10.05 mm |
| Gross area of cross section of Aluminium | 52.95 Sq.mm |
| Resistance at $20°C$ | $0.54\Omega/km$ |
| Current Rating | 148A |

daytime average load in the feeder is derived using the consumption pattern and load factor, based on the information available [106]. The average connected load during the day time was calculated as 53.1kW. Line 1 has a connected load of 30.8kW, while Line 2 has a connected load of 22.3kW. A proper distribution of consumer load along the feeder was done as shown in the pole layout diagram presented in Figure 3.4. Using the conductor resistance ($R_T$) the line parameters of the theoretical feeder model were calculated, and the resistance (R) and reactance (X) of the impedance matrix (Z) are presented in equations (3.2.3) and in (3.2.4) respectively. Here ratio

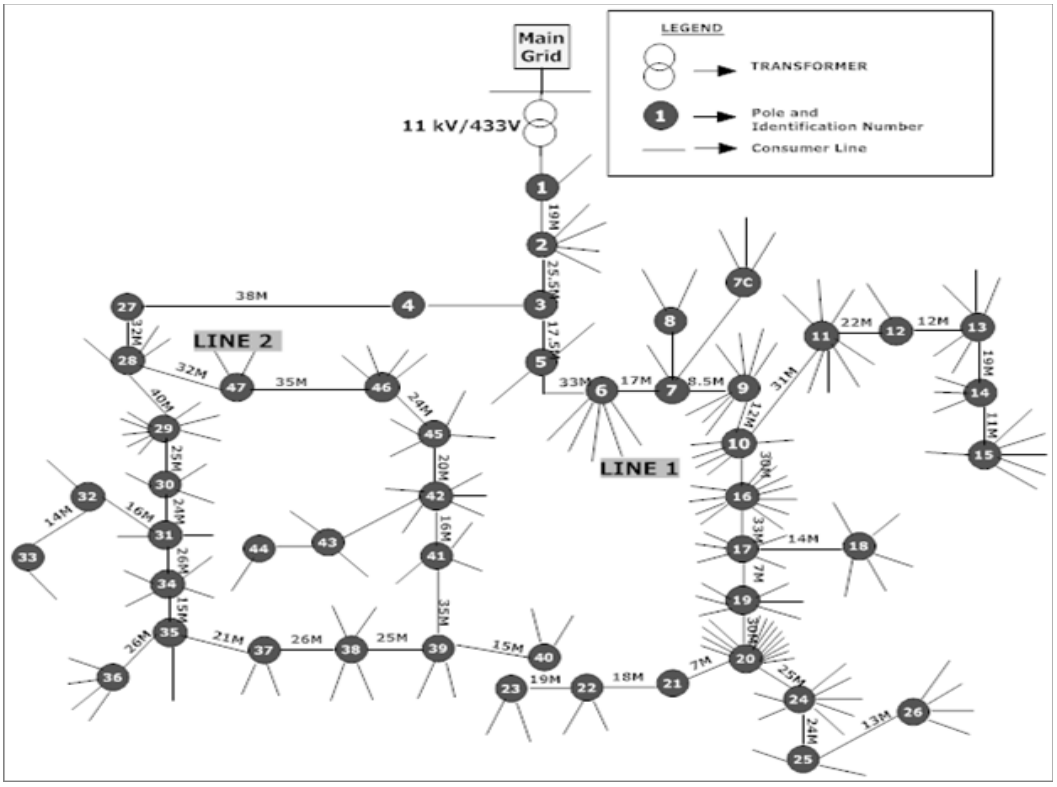


**Figure 3.4:** Pole layout and consumer distribution of the KSEB feeder

of R and X is small. But for a practical distribution system it is not.

$$R = \begin{bmatrix} 0.588756 & 0.0486036 & 0.0486035 & 0.0486561 \\ 0.0486036 & 0.588756 & 0.0486035 & 0.0486562 \\ 0.0486035 & 0.0486035 & 0.588756 & 0.0486562 \\ 0.0486561 & 0.0486562 & 0.0486562 & 0.588861 \end{bmatrix} \Omega/km \tag{3.2.3}$$

$$X = \begin{bmatrix} 0.928166 & 0.440815 & 0.387578 & 0.40091 \\ 0.440815 & 0.928166 & 0.42274 & 0.420781 \\ 0.387578 & 0.42274 & 0.928166 & 0.408665 \\ 0.40091 & 0.420781 & 0.408665 & 0.928059 \end{bmatrix} \Omega/km \tag{3.2.4}$$

The line losses and voltage drops dependent on the feeder parameters. Voltage regulation at the tail end and line loss in the feeder are obtained from analysis using the theoretical feeder model. The comparison of computed values and the actual reported values from the field study [106] are presented in Table 3.3. The values obtained from the analysis and from actual field study vary significantly, showing that the theoretical model could not represent the actual condition of the feeder indicating the requirement for a better modelling method.

**Table 3.3:** Comparison of voltage regulation and line loss in an actual feeder

| **Method used** | **Regulation** | **Line loss** |
|---|---|---|
| Theoretical model | 2.72% | 1.56% |
| From actual study report | 10.64% | 4.40% |

## 3.3 Proposed realistic modelling of low voltage feeders

As the parameters in the theoretical feeder model are computed using the conductor data alone, it gives results that deviate far away from reality. The additional resistance contributed by improper joints, mismanaged section fuses, arcing contacts, and other non-ideal factors are not considered in theoretical model. To obtain more realistic results, the feeder parameters should be approximated to values close to actual feeder conditions. So a method to modify the feeder parameters considering the imperfections using minimum field measurement is proposed. The procedure followed for the parameter approximation are:

1. Sample field measurements were taken to examine the actual feeder head current and corresponding head and tail end voltages.

2. The average value of actual feeder head current ($I_A$) and the corresponding actual voltage regulation ($V_{rA}$) at the tail end was computed from the measured data.

3. The feeder parameter matrix ($Z$) for the theoretical model was calculated using the information of conductor resistance ($R_T$) and spacial configuration of lines. The details of consumer load along the length was also incorporated in the model.

4. Using OpenDSS, an unbalanced power flow was performed in the theoretical model to find the currents and corresponding voltages at nodes to compute the regulations.

5. For better approximation, the load factor in the theoretical model was adjusted to make the theoretical model feeder head current ($I_T$) comparable or equal to the actual average feeder head current, and the average theoretical regulation at tail end ($V_{rT}$) was determined.

6. Using the above data, the conductor resistance ($R_T$) is modified using the equation (3.3.1). The feeder parameters were recalculated using the realistic conductor resistance ($R_R$).

7. The realistic model of the feeder was formed using new realistic parameters ($Z'$) and the developed model was validated using published line loss information.

In the above procedure an assumption considered was that the high resistance caused by imperfections is distributed uniformly along the length of the feeder. Also, all voltage regulations were calculated based on the feeder head voltages. Due to the common occurrence of phase unbalance in LV feeders, the average of phase currents and the worst value of regulation were taken into account wherever necessary.
The equation proposed for modifying the conductor resistance is,

$$R_R = R_T \times \left[\frac{V_{rA}}{V_{rT}}\right] \times \left[\frac{I_T}{I_A}\right] \tag{3.3.1}$$

Where,
$R_R$ - realistic resistance computed by approximation
$R_T$ - theoretical resistance as per conductor data
$V_{rA}$- regulation at feeder tail end by actual measurement
$V_{rT}$- regulation at feeder tail end by theoretical model
$I_A$ - feeder head current by actual measurement
$I_T$ - feeder head current by theoretical model

For a given conductor resistance, X/R ratio of power distribution systems is low compared to transmission systems. Value of X is mainly decided by spatial configuration of conductors [12, 35]. Most of the imperfections like section fuses and joints in distribution systems mainly contribute to resistance [44]. So parameter approximation was extended to conductor resistance and not in reactance. The R and X matrices were computed using modified Carson's equations with the help of OpenDSS software.

A real feeder under Kerala State Electricity Board was modelled using the two methods. The realistic model was validated using the data of the field study conducted by Energy Management Centre (EMC), Kerala and Bureau of Energy Efficiency (BEE), Govt. of India. Performance of the two feeder models were analysed and results compared to establish the difference. The modified conductor resistance was calculated using equation (3.3.1). The average actual voltage regulation from field measurement($V_{rA}$) was found to be 10.638 percent. By appropriately changing the load factor in the theoretical model, the average feeder head current in the theoret-

ical model was adjusted to the actual measured feeder head current and the current ratio was made unity. Thus the average voltage regulation from theoretical feeder model ($V_{rT}$) was obtained as 2.72 percent. From these values, the realistic conductor resistance($R_R$) was obtained as 2.112 Ω/km. Then the line parameters of the realistic feeder model was recalculated using the modified conductor resistance($R_R$). The resistance matrix ($R'$) and reactance matrix ($X'$) of the realistic feeder parameter ($Z'$) are given in equations (3.3.2) and (3.3.3).

$$R' = \begin{bmatrix} 2.15864 & 0.0486036 & 0.0486035 & 0.0486561 \\ 0.0486036 & 2.15864 & 0.0486035 & 0.0486562 \\ 0.0486035 & 0.0486035 & 2.15864 & 0.0486562 \\ 0.0486561 & 0.0486562 & 0.0486562 & 2.15864 \end{bmatrix} \Omega/km \tag{3.3.2}$$

$$X' = \begin{bmatrix} 0.928166 & 0.440815 & 0.387578 & 0.40091 \\ 0.440815 & 0.928166 & 0.42274 & 0.420781 \\ 0.387578 & 0.42274 & 0.928166 & 0.408665 \\ 0.40091 & 0.420781 & 0.408665 & 0.928059 \end{bmatrix} \Omega/km \tag{3.3.3}$$

The realistic model parameters have slight changes reflected in the impedance matrices and are slightly higher compared to the theoretical model parameters.

## 3.4 Model validation and analysis of an actual low voltage feeder

Validation of the realistic feeder model was done by comparing the results with data from a field study conducted by the national agencies [106]. Moreover, results from the two models were also compared to establish the difference.

### 3.4.1 Validation of the proposed realistic feeder model

The line losses and voltage drops depend on the feeder parameters. The results of voltage regulations and line losses from Theoretical model, Realistic model and actual study are presented in Table 3.4 for comparison. Voltage regulation calculated using the realistic feeder model was 9.26 percent, while the reported value after field study conducted is 10.64 percent [106]. But the percentage regulation calculated using theoretical model was only 2.72 percent faraway from the two. Considering the line loss, the realistic model predicts a 5.5 percent loss while the actual reported value

**Table 3.4:** Comparison of results from Theoretical model and Realistic model with results from actual study

| Method used | Regulation | Line loss |
|---|---|---|
| Realistic model | 9.26% | 5.51% |
| From actual study report | 10.64% | 4.40% |
| Theoretical model | 2.72% | 1.56% |

is slightly less, that is 4.4 percent, whereas the theoretical model shows only 1.56 percent. There is a significant difference between the reported values and those given by the theoretical model. However the results from the realistic model are more close to the reported values, making it trustworthy.

Though the voltage regulation obtained from the realistic model is slightly less than the actual value, the line loss predicted is slightly more. But this is due to the fact that the line voltage drop aggravated by line joints and imperfections are approximated as resistive voltage drops due to additional resistances during parameter approximation. As the X/R ratio of distribution line is low, it is justifiable. Since all additional voltage drops are approximated as resistive voltage drops during parameter approximation, the ohmic line loss in the realistic model naturally shows slight increase.

### 3.4.2 Comparison of feeder models without PV integration

Performance of a real feeder in KSEB was evaluated using both theoretical and realistic models. The amount of energy supplied and consumed by consumers were available from installed energy meters. The average connected load during the day time was calculated as 53.1kW. Line 1 has a connected load of 30.8kW, while Line 2 has a connected load of 22.3kW. The average current through the feeder head was 83.27A. Even though the loads were distributed evenly among the 3 phases to achieve the best possible balance a current unbalance of 16.75 percent was at the feeder head. For analysis, the voltage regulation tolerance is set to ±5 percent of the feeder head voltage. An unbalanced power flow analysis using the OpenDSS software tool was conducted to compute voltages and currents at each line section of the feeder.

The voltage profiles plotted using the theoretical and realistic feeder models are shown in Figure 3.5. The initial voltage drop at the feeder head is caused by the impedance of the distribution transformer. The theoretical model shows a worst voltage regulation of 2.95 percent at the tail end of the lines, whereas the the realistic model gives a rather high regulation of 8.53 percent. The maximum voltage unbal-

ance using the theoretical model and realistic model are 0.82 percent and 1.85 percent respectively. For both models the worst maximum voltage regulation and unbalance are observed at the tail end of the lines. The values obtained using the theoretical model are significantly low and too optimistic. The proposed realistic feeder model developed using the suggested parameter approximation gives a more accurate representation of the feeder and gives results close to actual reported values.

### 3.4.3 Comparison of feeder models with PV integration

With the integration of DGs, the voltage profile of the feeder will change, and voltage regulation and unbalance at the sections cannot be predicted. For the thorough analysis of the feeder, a dynamic analysis considering the variation in load and local generation may be conducted. However, a simple steady state power flow will be easy and useful to determine the DG integration limit and to predict the unbalance levels. To analyse the impact of DG integration, single phase PV units were connected uniformly among the 3 phases. This is to ensure that only minimum unbalance was contributed by these sources. single phase PV plants each of 5kW capacity were connected at various nodes along the feeder to investigate the variation in voltage profile. A total capacity of 60kW PV was included in the feeder with 30kW in each line. The connected load in Line 1 was 30.8kW and the level of PV penetration is 97.4 percent, that is less than the connected load. While in Line 2 the connected load was 22.3kW only, and the PV penetration is 135 percent which is more than the connected load. The PV interconnection higher than the connected load results in a reverse power flow in the line sections.

The voltage profiles of the feeder with PV integration is analysed using both the models and are presented in Figure 3.6. The voltage profiles obtained from the two models show significant differences. The voltage profiles of Line 1 and Line 2 obtained from the theoretical model are almost flat. Even though the PV generation is less than 100 percent in Line 1, and more than 100 percent in Line 2, the voltage profiles are well within the acceptable limit. This is because of the fact that the theoretical model does not consider imperfections in the feeder and gives optimistic results.

But from the realistic model, for Line 1 in which the load and PV generation are nearly the same, the voltage profile is almost flat. While in lightly loaded Line 2, where PV generation is greater than the connected load, the voltage profile shows a rise and exceeds 5 percent at the tail end. The greater rise in voltage profile indicates the reversal of power flow in the line sections.

Voltage profiles from the two feeder models vary significantly, predicting more voltage rise and unbalance by the realistic model. So, the realistic feeder model is useful to

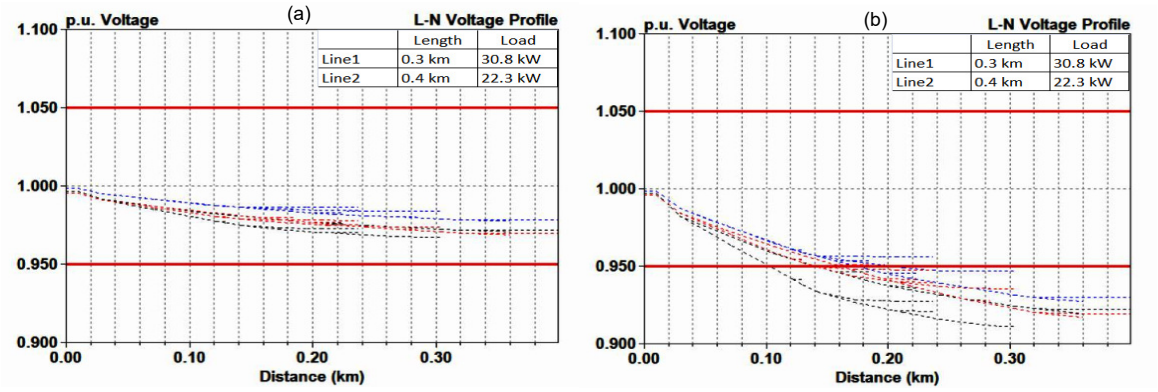


**Figure 3.5:** Profiles of phase voltages of the LV feeder using a) Theoretical feeder model b) Realistic feeder model

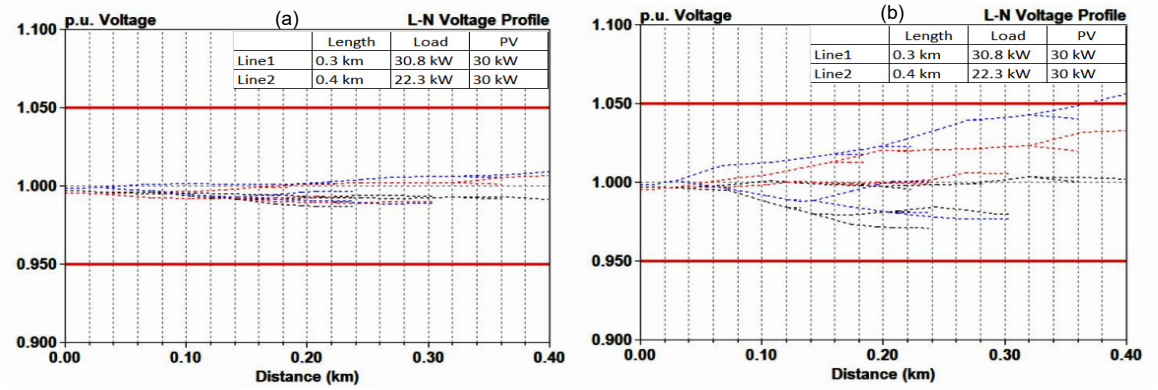


**Figure 3.6:** Profiles of phase voltages of the LV feeder with PV integration using a) Theoretical feeder model b) Realistic feeder model

determine the allowable maximum level of PV penetration. Also, it is important to reduce imperfections in the feeder that cause high resistance to bare minimum, so as to reduce voltage drop and voltage rise.

## 3.5 Performance analysis of an actual LV feeder using realistic feeder model

The realistic model is more reliable for analysis since it accounts the improper state of the feeder and gives results more close to actual performance. So further analysis were carried out using the realistic feeder alone and inferences were drawn.

### 3.5.1 Analysis of voltage spread with PV integration

To analyse the voltage spread along the feeder at various levels of PV penetration, PV units of 5kW capacity each were placed uniformly along the length and increased their number so as to achieve PV penetration of 0 to 225 percent. The voltage variation in

Lines 1 and 2 are shown in Figure 3.7 as a three-dimensional plot.

With zero PV integration, the voltages at the tail ends of the lines are less than the feeder head voltage indicating poor voltage regulation at those sections. As the connected load in Line 1 is greater, the voltage profile of Line 1 is slightly lower than that of Line 2. So a voltage support at the tail end is necessary. As the percentage of PV penetration increases, the voltage profile improves. Around 100 percent of PV penetration results in a nearly flat voltage profile, indicating that local generation is serving the local load. When PV penetration is more than 100 percent, the tail end voltage rises above the feeder head voltage. This is due to the reverse power flow in the line sections. The tail end of lightly loaded branch, Line 2 shows the highest voltage rise.

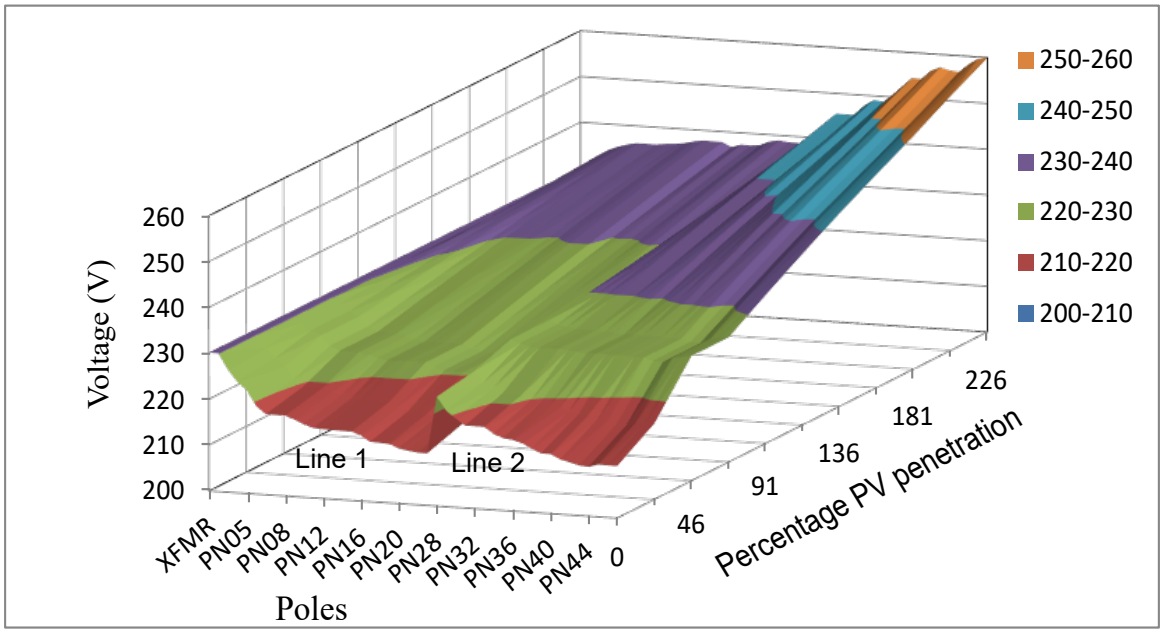


**Figure 3.7:** Voltage spread in the LV feeder with PV integration

Even though PV penetration was made uniform along the length of the feeder, voltage rise is greater at the tail end. This is due to the fact that there are only fewer number of loads present at the tail line sections and the local generation cause a reverse power flow. Without PV penetration the tail end voltage is the lowest, but at the same time, with higher PV penetration the tail end voltage is the highest. So with and without local generation, that is during day and night hours, the tail end consumers experiences the highest voltage variation and regulating voltage at these sections is challenging. So it is better to encourage PV integration near the feeder head for avoiding power flow reversal with in the feeder. Obviously this will reduce the feeder tail end voltage variation, making voltage regulation more easy to manage.

### 3.5.2 Analysis of phase unbalance and line loss with PV integration

The variation of phase unbalance and line loss in the feeder due to PV penetration was also analysed. The unbalance was computed as per the IEEE definition. To analyse the effect on phase unbalance, three cases were considered. Other than no PV integration, the status on aggregate PV penetration less than the connected load and more than the connected load are illustrated in Figure 3.8.a. Without any PV integration, maximum voltage unbalance due to the loads in Line 1 was 4.5 percent and in Line 2 was 3.5 percent. With a balanced PV penetration of 90 percent, the maximum voltage unbalance increases to 4.7 percent and 4.0 percent respectively for Line 1 and Line 2. The unbalance increases with the level of PV integration and at 226 percent of PV penetration the maximum voltage unbalance in Line 1 is 5.1 percent and in Line 2 it is 4.6 percent.

During the analysis the greatest unbalance was observed at the tail end of the feeder. The consumers at the tail end of the feeder is found to be affected more. In all levels of balanced local generation, the voltage unbalance along the feeder increases. This shows the critical requirement of load balancing prior to PV integration. For

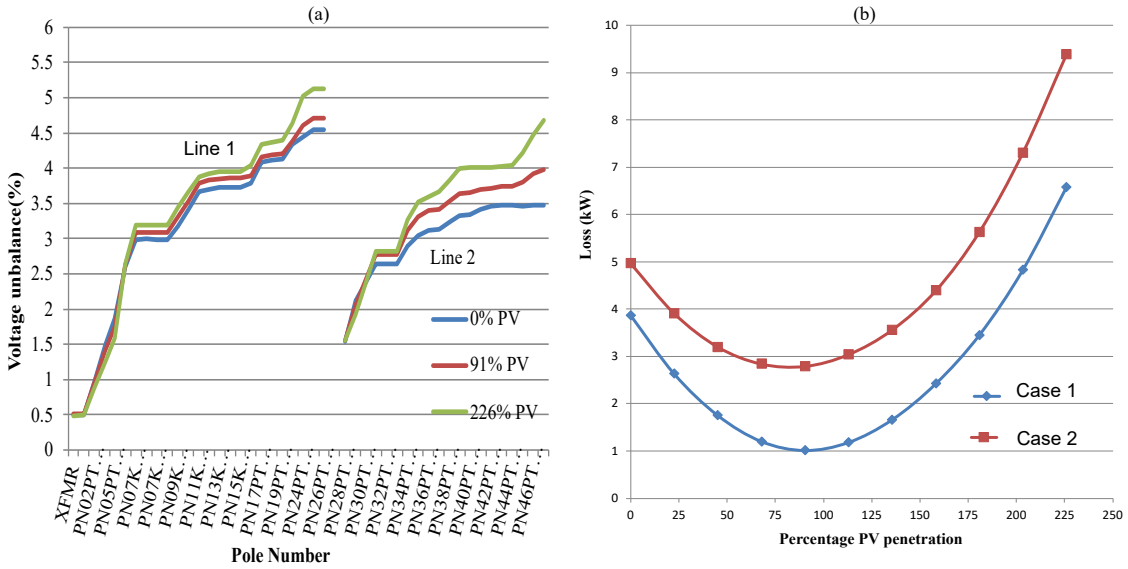


**Figure 3.8:** Variation of a) voltage unbalance and b) line loss in the LV feeder with PV integration

analysing the variation of line loss with current unbalance and PV penetration level, two cases were considered. For both cases current unbalance at some line sections were high due to single phase laterals. So maximum current unbalance at feeder head section was considered as reference. By load balancing along the feeder, the

maximum current unbalance at feeder head without any PV connection was made 5.82 percent. The current unbalance at line sections are shown in Figure 3.9.a. This was considered as Case 1. After shifting load among phases, the maximum current unbalance at feeder head was increased to 44.46 percent without PV penetration and was considered as Case 2. The current unbalances at line sections of Case 2 are shown in Figure 3.9.b. The variation of line loss for the two cases with increasing PV penetration is illustrated in Figure 3.8.b. The variation shows that when current unbalance is more, the line loss is greater irrespective of the level of PV penetration. This indicates the necessity of better load balancing for better efficiency.

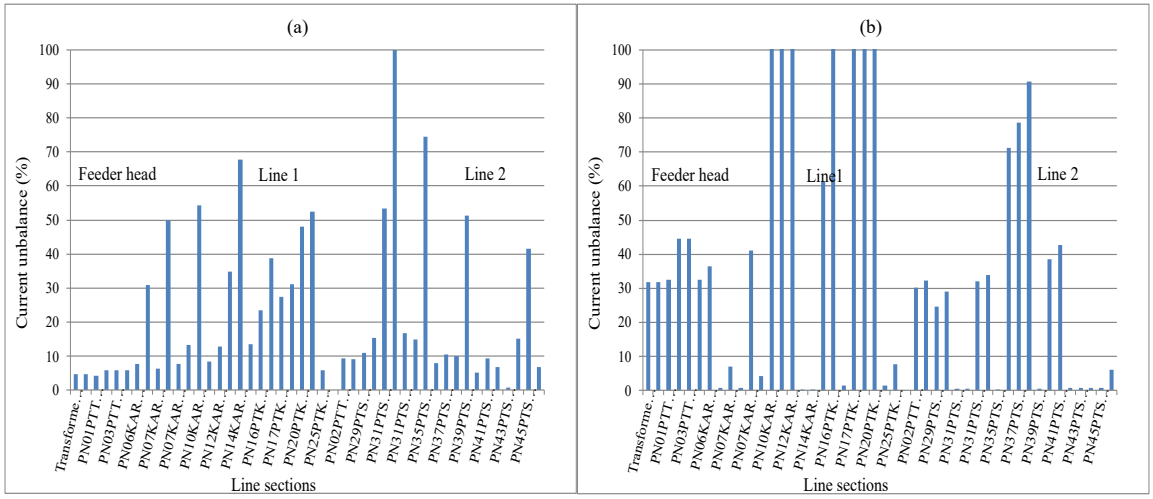


**Figure 3.9:** Current unbalance at line sections prior to PV integration a) Case 1 and b) Case 2

Another factor is that the line loss decreases with increase in PV generation and reaches a minimum when the local generation is almost equal to the connected load. But further PV generation causes increase in line loss due to the reverse power flow. This is because when the local generation is less, additional power is drawn from the transformer through feeder head creating line loss. However, when the PV generation is sufficient to meet the connected load, power flow through feeder head is less, so is the line loss. As PV generation rises above connected load, the analysis shows that power flows in the reverse direction through the lines causing a higher line loss. In a line loss density plot, magnitude of line loss is represented by the thickness of the feeder line. A line loss density plot of the feeder is shown in Figure 3.10. Without photovoltaic generation, total load is supplied by the transformer, resulting in an increased line loss at the feeder head. It indicates the necessity of thick conductors near the feeder head as illustrated in Figure 3.10.a. However, when 90 percent of load in the feeder is met by the local photovoltaic generation during the day time, the line loss is reduced and more evenly distributed as shown in Figure 3.10.b. So it is ideal

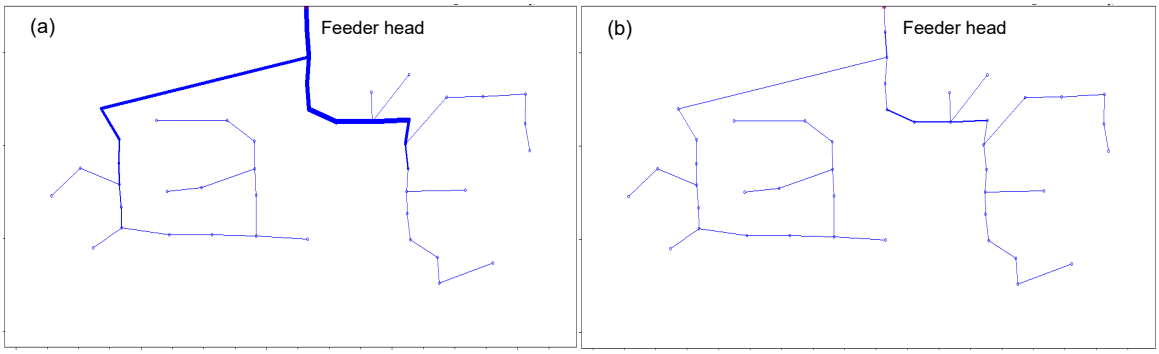


**Figure 3.10:** Line loss density plot of the LV feeder with a) 0% PV integration and b) 90% PV integration

to limit the PV generation at 100 percent or below 100 percent of the connected load to avoid line overloading and to minimize line loss.

## 3.6 Summary

A reliable feeder model is required to study the impact of photovoltaic penetration. But the theoretical model cannot account for the imperfections in the feeder. So a realistic feeder model using minimum data is proposed. The proposed model is validated using line loss information. The comparison of results from the two models shows significant variation. Since the theoretical model gives optimistic results that may lead to wrong conclusions, the developed realistic model is helpful for deciding on PV or DG interconnection requests.

The analysis using the realistic feeder shows that the voltage variation is more towards the tail end of the feeder. When PV generation is more than the connected load, the voltage rise occurs resulting in reverse power flow. Consumers at the tail end are most affected by voltage drop and rise. Moreover, even with balanced PV penetration the voltage unbalance in the feeder increases if there exists a load unbalance. Also, at all levels of PV penetration the line loss is higher if the current unbalance in the feeder is higher. So the line loss can be minimised by phase balancing the feeder loads and keeping local generation equal to the connected load. So phase balancing is extremely important to reduce some of the adverse effects of PV penetration.

# Chapter 4

# Improving the power quality in a low voltage distribution feeder

## 4.1 Introduction

Increased harmonics, unbalance, and high neutral current are some of the issues in low voltage distribution network (LVDN) due to the higher integration of low carbon technologies [108]. Small photovoltaic (PV) plants and electric vehicle (EV) chargers are single phase and non-linear units that are connected at the distribution level in a random fashion [109, 110]. The majority of these single phase sources and loads have dynamic and intermittent nature, and their precise division among the phases is not easy. Lines are not transposed in the distribution system, and line impedances are not equal. As a result, the line voltage drops are not equal. Due to the unbalanced voltages at the point of common coupling, the balanced loads also draw unequal currents and generate a higher neutral current. A load imbalance among the phases is the primary source of neutral current. It has grown in recent years [111]. Harmonics are produced by almost all recent home appliances [112, 113]. At the neutral, zero sequence harmonic currents add and augment the neutral current [114].

To save money, the neutral conductor was previously chosen with half the cross section of phase conductors. However, in the current situation, the neutral current has significantly increased and frequently exceeds phase currents. [8]. So the neutral conductor size reduction is no longer permitted and the importance of the neutral line cannot be ignored.

The neutral-to-earth voltage (NEV) is a concern in systems with large neutral currents. When the NEV exceeds the allowable value, it results in safety hazards and equipment failure. Harmonics, unbalance, and high neutral current affect power delivery equipment like transformers, causing derated operation and premature ageing [115]. Problems with the low voltage distribution system directly affect the customers as it is their connecting link with the power system [116]. The propagation of these power quality issues through distribution feeders should be restricted to min-

imise their impact.

Harmonics, imbalances, and high neutral current are issues that can be addressed separately or collectively. Earlier solutions managed to stop or reduce neutral current by incorporating additional devices or implementing special operating procedures. Solutions involve power electronic devices, electromagnetic equipment, or a combination of both. Because of the stochastically fluctuating nature of the distribution system, power electronic based solutions require robust control algorithms, while electromagnetic equipment is bulky. To solve the issues at LVDN, new devices are added, PVs and EVs are controlled or coordinated, or active reactive power exchange is regulated. The aim of this work is to propose a single, low cost solution to reduce the power quality issues at LVDN.

A method for improving the power quality of 3 phase, 4 wire distribution feeders without the installation of extra equipment is proposed in this study. An idea of using neutral current as a power quality enhancer is suggested and a novel neutral line grounding strategy is proposed. The effect of neutral current on unbalance and harmonic propagation is investigated considering the electromagnetic coupling between the lines. The IEEE European low voltage test feeder was modelled and analysed to verify the performance of the proposed strategy. OpenDSS, an open-source distribution system simulation tool by EPRI, was used for the analysis.

The remainder of the chapter is divided into the following sections. Section 4.2 describes the mathematical modelling of a four wire distribution feeder. Section 4.3 presents existing and proposed neutral grounding practices. Section 4.4 explains the analysis and the results are discussed in section 4.5. A chapter summary is included as the last section.

## 4.2 Modelling of a 3 phase, 4 wire distribution feeder

Modelling of a 3 phase, 4 wire segment, explicitly including the neutral line and the ground, is required to study an unbalanced distribution system. Modelling a distribution feeder precisely considering the presence of the earth is difficult and different techniques and estimates are provided in a number of publications. In this section, the steps for modelling a LV feeder to analyse the influence of neutral current in the spread of power quality problems are explained.

In a 3 phase, 4 wire system, equation (4.2.1) displays the relationship between phase and neutral currents. If the feeder currents are unbalanced, currents in phase

conductors do not aggregate to zero and $I_n \neq 0$ as shown in equation (4.2.2).

$$I_a + I_b + I_c + I_n = 0 \tag{4.2.1}$$

$$I_a + I_b + I_c \neq 0 \tag{4.2.2}$$

Where

$I_a$– Phase 'a' current

$I_b$– Phase 'b' current

$I_c$– Phase 'c' current

$I_n$– Neutral current

The fully grounded neutral (FGN) distribution feeder is widely adopted. Figure 4.1 depicts a feeder line section in which current in the neutral wire is routed to the ground in the line section itself.

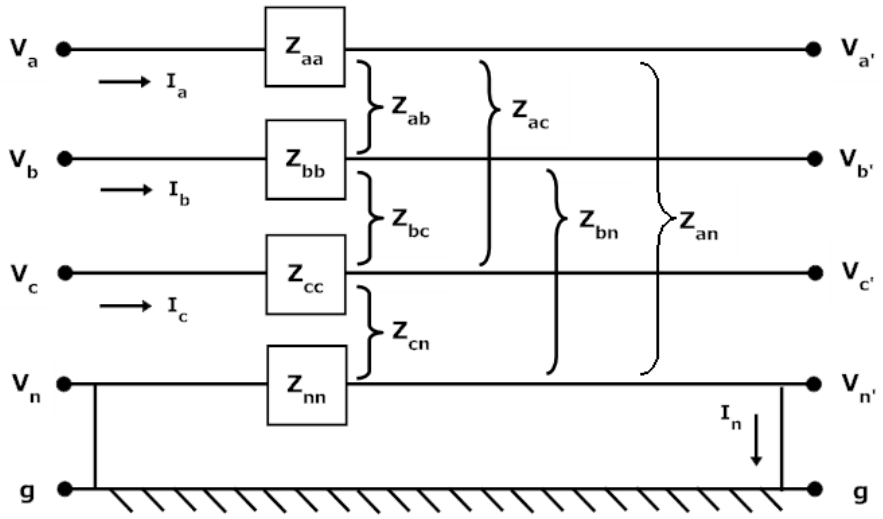


**Figure 4.1:** Fully Grounded Neutral line segment

Usually to simplify analysis, the effect due to the neutral current is ignored or combined with phase lines using Kron's reduction [117, 118]. But neutral is explicitly considered in this analysis to maintain the generality. A 4x4 matrix was used for the generic expression for line voltage drop, which is given in equation (4.2.3).

$$\begin{bmatrix} V_{ag} - V_{a'g} \\ V_{bg} - V_{b'g} \\ V_{cg} - V_{c'g} \\ V_{ng} - V_{n'g} \end{bmatrix} = \begin{bmatrix} Z_{aa} & Z_{ab} & Z_{ac} & Z_{an} \\ Z_{ba} & Z_{bb} & Z_{bc} & Z_{bn} \\ Z_{ca} & Z_{cb} & Z_{cc} & Z_{cn} \\ Z_{na} & Z_{nb} & Z_{nc} & Z_{nn} \end{bmatrix} \begin{bmatrix} I_a \\ I_b \\ I_c \\ I_n \end{bmatrix} \tag{4.2.3}$$

Where

$Z_{aa} = R_{aa} + jX_{aa}$, self impedance of phase 'a' line,
$R_{aa}$ = resistance of phase 'a' line, and
$X_{aa}$ = reactance due to self inductance of phase 'a' line,
$Z_{ab} = R_{ab} + jX_{ab}$, mutual impedance between phase 'a' and 'b' lines,
$R_{ab}$ = mutual resistance between phase 'a' and 'b' lines,
$X_{ab}$ = reactance due to mutual inductance between phase 'a' and 'b' lines,
All the other parameters, such as $Z_{bb}, Z_{cc}, Z_{nn}$, and so on, have similar definitions.

For a distribution system, the capacitance between the lines is minimal and of the order of nanoFarad.
The voltage drop for phase 'a' can be expressed as in equation (4.2.4).

$$V_{ag} - V_{a'g} = Z_{aa}I_a + Z_{ab}I_b + Z_{ac}I_c + Z_{an}I_n \tag{4.2.4}$$

The neutral line of the FGN system is grounded at all poles, therefore it only carries a little current. So the influence of neutral conductor current in line voltage drop is not significant. Hence equation (4.2.3) can be transformed into equation (4.2.5).

$$\begin{bmatrix} V_{ag} - V_{a'g} \\ V_{bg} - V_{b'g} \\ V_{cg} - V_{c'g} \\ V_{ng} - V_{n'g} \end{bmatrix} = \begin{bmatrix} Z_{aa} & Z_{ab} & Z_{ac} \\ Z_{ba} & Z_{bb} & Z_{bc} \\ Z_{ca} & Z_{cb} & Z_{cc} \\ Z_{na} & Z_{nb} & Z_{nc} \end{bmatrix} \begin{bmatrix} I_a \\ I_b \\ I_c \end{bmatrix} \tag{4.2.5}$$

The line voltage drop is caused by line resistance and inductive reactance.

## 4.3 Proposed neutral line grounding strategy to improve power quality

In 3 phase, 4 wire systems, a fully grounded neutral line (FGN) is the most prevalent. Neutral current is bypassed to ground at several locations in the distribution feeder [119]. As a result, the current through the neutral line is reduced and the conductor size may be reduced during normal operation. A fully grounded neutral line (FGN) is commonly used for economic reasons. Due to the fact that the neutral current is routed to earth at numerous grounding locations along the FGN line system, so during unbalanced operation total conductor currents in a line section does not sum to zero, as illustrated in equation (4.2.2). The electromagnetic interaction due to

the mutual inductance of the current carrying conductors is unbalanced [120]. If the electromagnetic interaction is made balanced, beneficial consequences are expected.

The inclusion of neutral current in the line segment can help maintain electromagnetic balance, as the current in line segment add to zero, as illustrated in equation (4.2.1). If the neutral line is grounded selectively or the neutral point of transformer alone is grounded, more current flows back through the neutral wire. In such cases, the sum of conductor currents in the line section is zero, resulting in a more balanced electromagnetic interaction between the lines.

The voltage drop in phase 'a' is shown in equations (4.3.1) and (4.3.2). A compensatory effect is shown by the existence of terms with a negative sign.

$$V_{ag} - V_{a'g} = Z_{aa}I_a + Z_{ab}I_b + Z_{ac}I_c - Z_{an}(I_a + I_b + I_c) \tag{4.3.1}$$

$$V_{ag} - V_{a'g} = (Z_{aa} - Z_{an})I_a + (Z_{ab} - Z_{an})I_b + (Z_{ac} - Z_{an})I_c \tag{4.3.2}$$

To take advantage of this, a new strategy for neutral line grounding is proposed. For short feeders, the neutral line is grounded exclusively at the transformer star point; for longer feeders, the neutral line is grounded at appropriate positions. The number and position of grounding points can be decided by the length of the feeder and the location of the load centres. Due to the presence of neutral current, enhanced current balance at feeder sections is ensured. It is referred to as a single or selectively grounded neutral (SGN) line system.

As seen in Figure 4.2, the SGN line system may lack explicit grounding in the line segments, implying that Kron's reduction is not applicable. Due to imbalance and harmonics, the neutral conductor carries current from sources and loads distributed throughout the line segment. Equation (4.3.3) can be used to calculate the voltage drop in the line, assuming perfect current balance in the line section.

$$\begin{bmatrix} V_{ag} - V_{a'g} \\ V_{bg} - V_{b'g} \\ V_{cg} - V_{c'g} \\ V_{ng} - V_{n'g} \end{bmatrix} = \begin{bmatrix} (Z_{aa} - Z_{an}) & (Z_{ab} - Z_{an}) & (Z_{ac} - Z_{an}) \\ (Z_{ba} - Z_{bn}) & (Z_{bb} - Z_{bn}) & (Z_{bc} - Z_{bn}) \\ (Z_{ca} - Z_{cn}) & (Z_{cb} - Z_{cn}) & (Z_{cc} - Z_{cn}) \\ (Z_{na} - Z_{nn}) & (Z_{nb} - Z_{nn}) & (Z_{nc} - Z_{nn}) \end{bmatrix} \begin{bmatrix} I_a \\ I_b \\ I_c \end{bmatrix} \tag{4.3.3}$$

As a result of the electromagnetic coupling of neutral and phase currents, the line voltage drop in SGN is less than that in FGN, as established by equations (4.2.5) and (4.3.3).

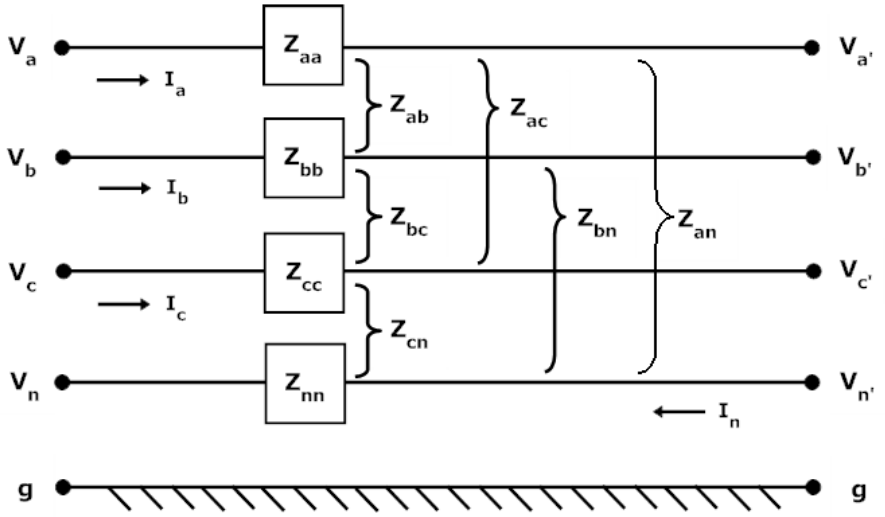


**Figure 4.2:** Single or Selectively Grounded Neutral line segment.

## 4.4 Analysis and comparison of neutral line grounding strategies

Traditional power flow analysis techniques were developed for 3 phase balanced systems and are used to analyse medium and high voltage networks. Distribution system analysis requires unbalanced power flow solutions since the lines are not transposed and have an asymmetrical admittance matrix. Their high resistance to reactance ratio mandates the employment of specialised computer techniques that are not achievable using balanced power flow methods [121]. When analysing the performance characteristics of a distribution feeder, both the explicit neutral line and the presence of the earth must be considered. The proposed grounding approach is implemented and analysed using OpenDSS, an open source distribution modelling tool, on the IEEE European low voltage test feeder. The test feeder details and software package are described below.

### 4.4.1 The IEEE European low voltage test feeder

The majority of test feeders prepared by the Test Feeder Working Group (TFWG) are designed primarily for the purpose of analysing the North American supply system. In European distribution systems, long, low-voltage feeders serve a broader region. The IEEE European low voltage test feeder is the first one based on the 50Hz frequency for testing systems outside of America, and was released only in 2015 [122]. While it has a number of shortcomings that must be addressed, it provides a common framework for analysing power distribution systems in other regions of the world. It is an under-

ground radial low voltage feeder operating at 416V in the United Kingdom, identical to any normal unbalanced feeder found throughout Europe. The single-phase and three-phase loads are linked directly to the 240V and 416V power supplies, respectively. It begins with an 800kVA delta-wye transformer rated at 11kV/416V. This transformer is connected to 55 single-phase residential loads distributed among 906 buses. The load distribution between phases is slightly unequal. Phases 'a' and 'b' are each connected to twenty houses, while phase 'c' is connected to fifteen. The transformer is loaded at a very low level of 6.88 percent. Figure 4.3 shows a schematic representation of the feeder layout with loads. The harmonic sources included for analysis purpose is also there. The IEEE European Low Voltage Test Feeder was

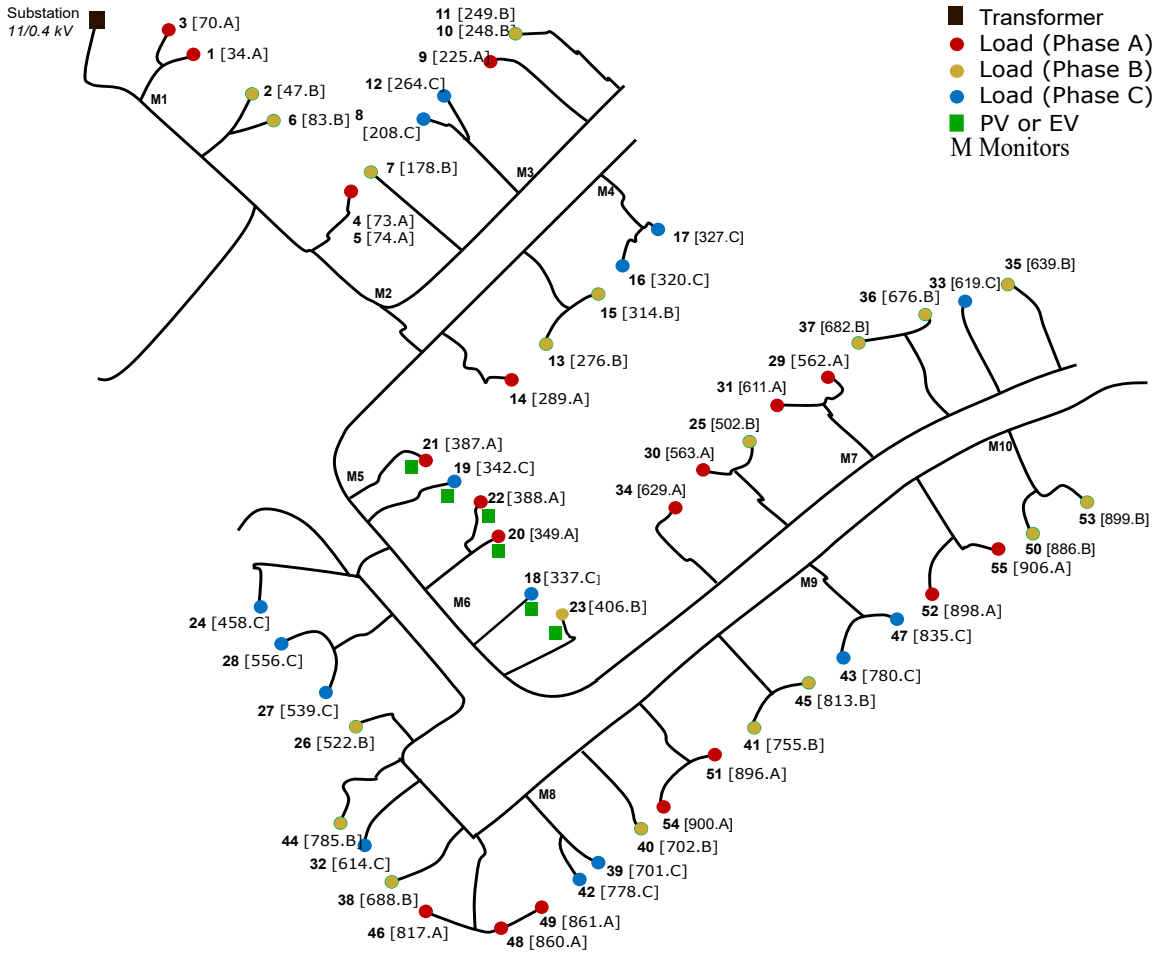


**Figure 4.3:** IEEE European LV Test feeder

used to analyse the proposed neutral line grounding approach.

### 4.4.2 Analysis using the test feeder

The basic IEEE European LV test feeder was slightly modified for the purpose of analysing neutral line grounding methods. The underground cables were substituted

with ACSR overhead conductors, while the rest of the architecture remained unchanged. IEEE spacing ID500 was used to configure the line spacings [107] and is shown in Figure 4.4.

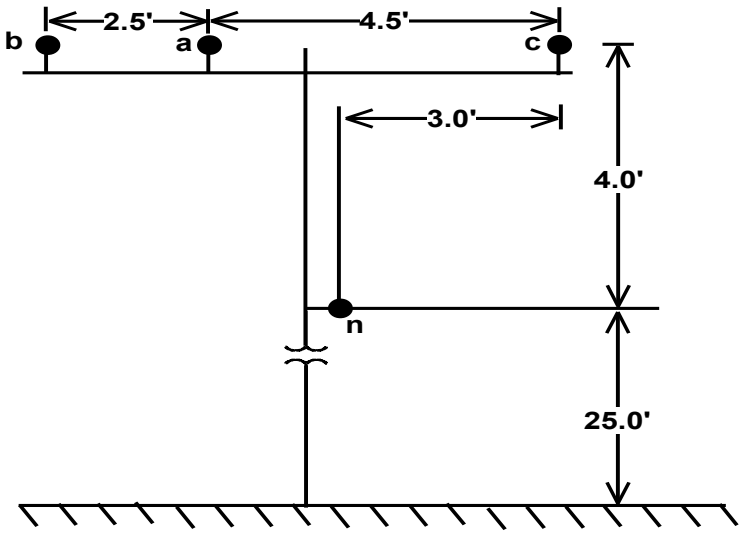


**Figure 4.4:** Conductor configuration in ID500

The load unbalance in the test feeder was enough to analyse the propagation of unbalance. To account for the nonlinear nature of PVs and EVs, a harmonic spectrum was introduced to the middle of the feeder as shown in Figure 4.3. The resistivity of the Earth was taken as $100\Omega m$, and line constants of the test system were calculated using Carson's equations. The capacitance parameters of distribution system are negligibly small and can be ignored. Inductive reactance and resistance per kilometre were calculated and are given in equations (4.4.1) and (4.4.2) respectively.

$$R = \begin{bmatrix} 0.588756 & 0.048603 & 0.048603 & 0.048656 \\ 0.048603 & 0.588756 & 0.048656 & 0.048656 \\ 0.048603 & 0.048656 & 0.58875 & 0.048656 \\ 0.048656 & 0.048656 & 0.048656 & 0.588861 \end{bmatrix} \Omega/km \tag{4.4.1}$$

$$X = \begin{bmatrix} 0.928166 & 0.440815 & 0.387578 & 0.40091 \\ 0.440815 & 0.928166 & 0.42274 & 0.420781 \\ 0.387578 & 0.42274 & 0.928166 & 0.408665 \\ 0.40091 & 0.420781 & 0.408665 & 0.928059 \end{bmatrix} \Omega/km \tag{4.4.2}$$

The self reactance of the lines is given by the diagonal terms of matrix (4.4.2), while

the off-diagonal terms represent the electromagnetic interaction caused by mutual inductance among lines, and their value depends on the degree of mutual coupling. The matrix is symmetrical but the off diagonal elements are not equal because the couplings between the lines are not the same due to the unequal spacing between the lines.

The modified IEEE test feeder was modelled for testing both SGN and FGN systems. To capture various voltage and current parameters, ten monitors were placed at different locations in the feeder. Steady state and dynamic analysis were done. For steady state analysis, a constant load was used. A time varying daily load pattern was used for dynamic analysis. Fault current analysis was also performed. The voltages and currents at the monitoring points were recorded. Harmonic sources were integrated near the feeder centre and harmonic propagation towards head and tail was investigated by conducting a harmonic power flow analysis. Both neutral line grounding systems were modelled and analysed in a similar manner. Variations were consistent across phases, and results from phase 'a' are provided for comparison wherever applicable.

## 4.5 Results and discussion

### 4.5.1 Comparison of voltage regulation and unbalance

Variation of voltage regulation of phase 'a' at the monitoring points of the two neutral line grounding methods is shown in Figure 4.5.a. In comparison to FGN, the SGN system has less voltage regulation, which results in a better voltage level at the feeder's tail end. Likewise, similar results were achieved for the subsequent phases. The voltage drop is a consequence of the wires resistance and inductance. Due to mutual coupling, the neutral current injects voltages into phase lines, hence lowering the inductive line drop in the SGN. Examining equations (4.3.3) and (4.2.5) reveals that voltage drop in SGN is less because of the presence of negative terms in impedance matrix. The negative terms are introduced by the involvement of neutral current. This helps to improve feeder voltage profile as a whole compared to FGN. Voltage unbalance variation along the feeder is given in Figure 4.5.b. According to data from the test feeder, the maximum current unbalance in the test feeder is only 10.36 percent. No changes to the load distribution were made to raise the unbalance because the actual level of unbalance was enough to examine the spread of unbalance. The voltages at ten monitoring points were measured after performing an unbalanced power flow analysis on the feeder. Voltage

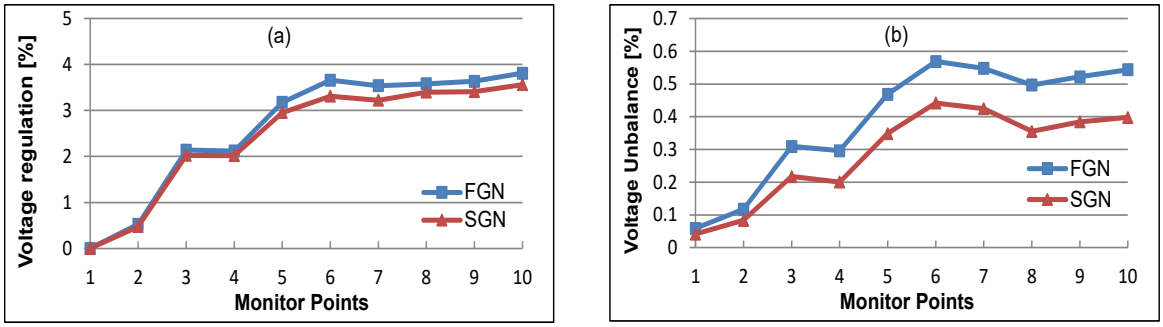


**Figure 4.5:** Variation of a) voltage regulation and b) voltage unbalance

unbalance was calculated as the ratio of negative sequence component to positive sequence component. The transformer balances the voltage at the feeder head. Due to the relatively small current unbalance present in the feeder, a small voltage unbalance occurred near the feeder head and increased toward the tail end. However, in the SGN system, it is less. The influence will be more noticeable in systems with significant unbalance. It demonstrates that the proposed strategy improves the voltage profile without worsening phase balancing. On the other hand, onload tap changers and reactive power compensators improve voltages of all phases uniformly, which may result in an undesirable increase in voltage unbalance.

### 4.5.2 Comparison of dynamic behaviour with load variation

The load pattern and local generation in distribution feeders vary and are decided by a variety of external factors. As a result, system's behaviour to the stochastic power variation is to be investigated. Dispersed generating units were treated as negative loads. Loads connected to each node were assigned with various daily load shapes according to consumer behaviour. The resulting variation in load in each phase is

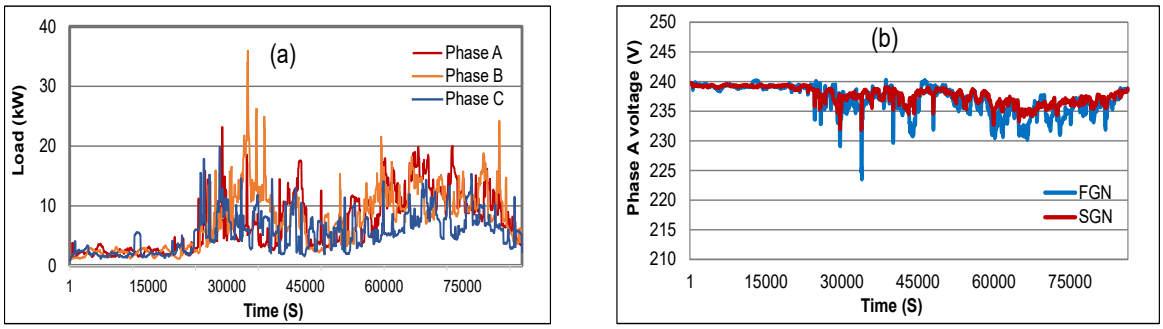


**Figure 4.6:** a) Daily load variation in the feeder and b) voltage variation at a monitoring point

depicted in Figure 4.6.a. Both systems were simulated as time series over a day with a one minute step size. Voltage variation at monitoring points caused by load variation

was recorded. Figure 4.6.b illustrates the voltage change in both systems in phase 'a' at the fifth monitoring point. Both systems exhibit identical voltage changes, but with a small difference in magnitudes. This is because of the resultant variation in line parameters. The results show that the suggested SGN system has no adverse effect on the stochastic load variation.

### 4.5.3 Comparison of harmonic propagation along the feeder

To investigate the harmonic spread caused by non linear sources and loads, a harmonics spectrum was included near the 6th monitor at buses 337, 342, 349, 387, 388, and 406, in the test feeder shown in Figure 4.3. Table 4.1 provides information of magnitude and phase of each harmonic in the spectrum. The harmonic sources were modelled by including the spectrum with the load model of openDSS.

**Table 4.1:** Harmonic spectrum added

| **Order of harmonics** | **1** | **3** | **5** | **7** | **9** | **11** | **13** | **15** |
|---|---|---|---|---|---|---|---|---|
| Percentage amplitude | 100 | 9.2 | 62.2 | 41.8 | 1.48 | 7.08 | 3.12 | 0.48 |
| Phase angle ($^o$) | 305 | 120 | 255 | 332 | 357 | 358 | 284 | 69 |

A harmonic analysis was conducted and harmonics at ten monitors along the feeder were recorded. The results are plotted and presented for analysis. The harmonic frequencies decides the self and mutual reactance of lines during harmonic power flow. The harmonic power flow is decided by the magnitude and phase angle of harmonics and their power factors. It is also necessary to consider the spatial configuration of phase and neutral lines. As a result, harmonic voltage variation seems paradoxical. However, it demonstrates certain linkages based on their order and sequence effects. Table 4.2 illustrates the sequence effect of each harmonic order, which helps in explaining the harmonic voltage variation.

**Table 4.2:** Sequence effects produced by harmonics

| **Order of harmonics** | **1, 7, 13** | **5, 11** | **3, 9, 15** |
|---|---|---|---|
| Effect produced | Positive sequence | Negative sequence | Zero sequence |

Currents with zero sequence effect are generated by harmonics of the third, ninth, and fifteenth orders. They all have the same phase relationship. Harmonic currents

with a zero phase relation collect in the neutral wire and flow through it. Figure 4.7.a illustrates the variation of the third harmonics and Figure 4.7.b illustrates the variation of the ninth harmonics. Zero sequence harmonics have nearly flat profiles in both

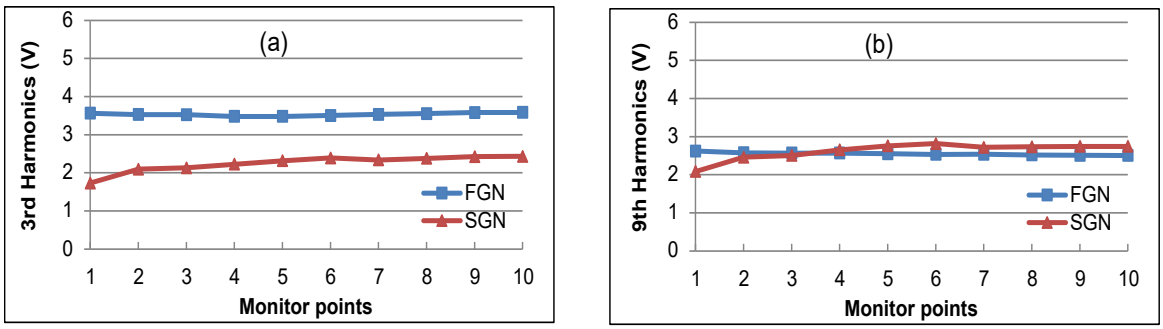


**Figure 4.7:** Propagation of zero sequence harmonics a) 3rd harmonics b) 9th harmonics

systems. The SGN system exhibits a noticeable uniform damping of the prominent third order harmonic. Other order zero sequence harmonics do not exhibit that much damping. This is due to their low magnitudes and lack of strong coupling between the lines. Negative sequence harmonics generate a revolving magnetic field that gen-

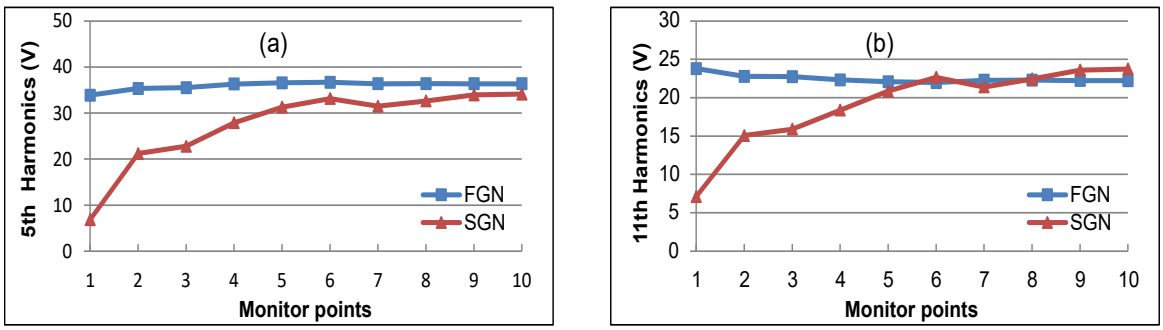


**Figure 4.8:** Propagation of negative sequence harmonics a) 5th harmonics b) 11th harmonics

erates braking torque in machines. This category contains the fifth and eleventh order harmonics. Figure 4.8.a and b illustrate the magnitudes of these harmonics. In SGN, these harmonics propagate very little toward the source end, whereas in FGN, they propagate uniformly. Harmonics of order seven and thirteen are positive sequence harmonics, generating a forward revolving magnetic field at their own frequencies. Figure 4.9.a and 4.9.b depict the effect on these harmonics. Due to the higher damping in SGN to the seventh harmonic, the magnitude drops from 16.03V to 13.95V at the tail end, whereas the feeder head exhibits a sharp drop from 15.11V to 1.47V. At the tail end, the thirteenth harmonics drops from 21.23 to 18.59V, while at the feeder head, it drops from 17.81 to 4.78V.

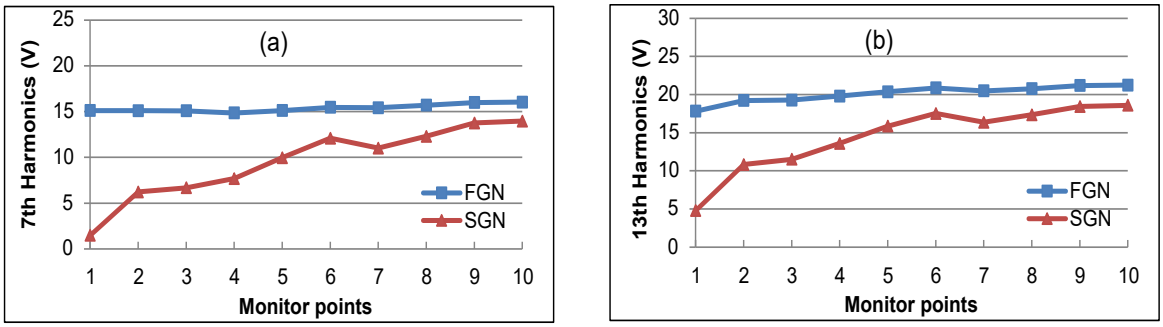


**Figure 4.9:** Propagation of positive sequence harmonics a) 7th harmonics b) 13th harmonics

These plots demonstrates that harmonics are well damped in SGN in comparison to FGN. SGN exhibits a considerable suppression of larger magnitude harmonics. For FGN, all harmonics have a constant profile across the feeder, revealing that they propagate uniformly. However, in SGN, zero sequence harmonics are suppressed uniformly, while other harmonics are suppressed and propagate very less towards the source end. Positive and negative sequence harmonics are more dampened as they approach the feeder head, due to the magnitude of the neutral current being greater in this region. It is evident that the electromagnetic interaction of lines have significant effects in the propagation of harmonics through the feeder. The effect of neutral current is directly observable when the results of SGN and FGN configurations are compared. Variation in harmonic voltages along the feeder is caused by electromagnetic interaction of neutral current.

### 4.5.4 Comparison of current TDD and voltage THD

The current harmonics in the system due to the presence of harmonic sources were examined. It is not very well damped in SGN due to the decreased effective line reactance. All order harmonic currents have a slightly higher value in the SGN system than in the FGN system. To quantify the effect, the Total Demand Distortion (TDD) of current at each monitoring point is shown in Figure 4.10.a. The average TDD in SGN is 25.32 percent, slightly greater than 21.06 percent in FGN. Total harmonic distortion (THD) of voltage was computed at each of the 10 monitoring nodes to examine the harmonic spread, and the findings are shown in Figure 4.10.b. THD at the feeder head, where the neutral current is higher is clearly reduced in SGN. The THD in SGN is only 4.82 percent compared to 22.98 percent in FGN. The THD is lowered from 25.27 to 24.85 percent at the tail end. It is less for SGN than FGN at all monitoring points along the feeder. Despite the fact that the average TDD in SGN

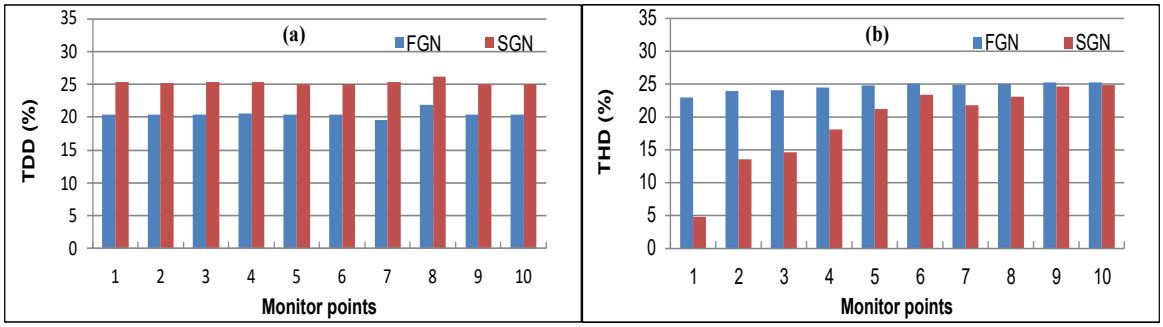


**Figure 4.10:** Variation of a) TDD and b) THD at the monitoring points

is slightly greater, the resulting THD at monitoring points is lower due to the lower line reactances in SGN. This achieves minimal supply voltage distortion at PCCs. So the proposed neutral line grounding strategy can efficiently suppress the harmonic propagation, especially towards the source.

### 4.5.5 Comparison of neutral-to-earth voltage and fault current

The neutral wire and the earth share the current due to unbalance and harmonics, which eventually returns to the source neutral. The amount of current shared is proportional to the earth's resistivity and the number of points grounded. Earth resistance changes with soil conditions and is not quite as low as it seems. Conduction of current to earth is determined by its resistivity [123]. When the neutral current was low, the neutral-to-earth voltage of a completely grounded neutral system was considered as zero. This is not true in the present circumstances of higher neutral currents and many issues were reported [124, 125]. When neutral current is high, the neutral-to-earth voltage (NEV) may rise, posing a risk. The issue of ground current poses risk to human and animal life. Saving money is one of the motivation of using multi-grounded or fully grounded neutral line system.

A high frequency power flow analysis was conducted to study the difference in NEV in both systems using OpenDSS. The earth resistivity was set to $100\Omega m$, a standard value, and the Deri earth model was used [126, 127]. Figure 4.11.a shows comparison of Neutral-to-earth voltage (NEV) in SGN and FGN systems. SGN can significantly reduce NEV during unbalanced harmonic operation. This is because the earth plays a minor role in carrying the neutral return current.

Distribution systems are susceptible to a variety of faults, the most common of which are Single Line to Ground (SLG) faults. The loop impedance of the ground fault current path determines the fault current and fault level [125]. In addition to the ground fault current, neutral current also traverses through the earth in FGN.

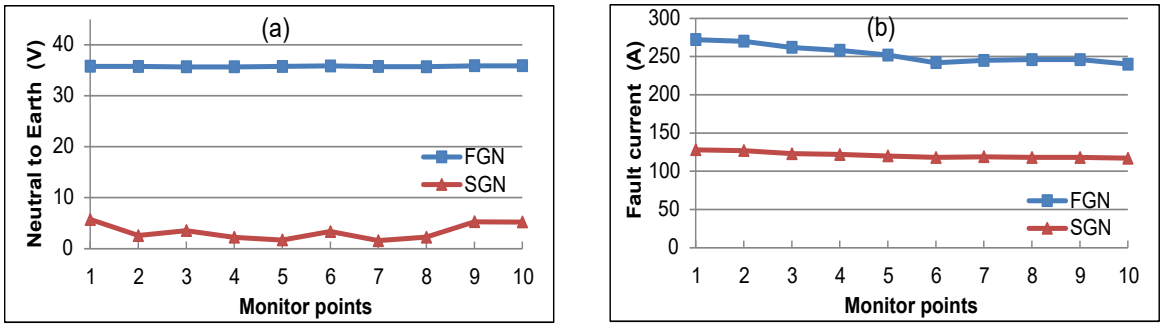


**Figure 4.11:** Comparison of a) neutral-to-earth voltage and b) single line to ground fault current

The protection device's discrimination between the two components of currents is a challenge, and configuring it is difficult [128]. However, as there are only less number of grounding points in SGN, the earth return current accounts for a significant portion of the fault current.

To determine the capability of the two systems to limit the fault current, a fault current analysis is performed. In both systems, a short circuit current setting of 1000A was used. For a SLG fault, SGN shows a significant current limiting capability compared to FGN, as illustrated in Figure 4.11.b. This is due to the fact that SGN has a higher loop impedance. In both systems the fault level near the feeder head increases as the loop impedance is less. Ground fault protection is easy to configure in SGN, and the fault level is significantly reduced.

### 4.5.6 Comparison of line loss

In SGN, the neutral return current flowing from the load centre to the grounding point flows through the neutral line, increasing the line loss. The total loss in the line of both systems were calculated and compared. As illustrated in Table 4.3, SGN has 0.12 percent higher line loss. Thus, the benefits of SGN are achieved with a slight increase in line loss.

**Table 4.3:** Line loss analysis

| Neutral line grounding | **FGN** | **SGN** |
|---|---|---|
| Total line loss(kW) | 1.10 | 1.20 |
| Percentage line loss | 2.08 | 2.20 |

## 4.6 Summary

A novel neutral line grounding procedure is recommended for a 3 phase, 4 wire distribution system during unbalanced harmonic operating condition. Currently available harmonics and unbalance mitigation solutions require additional devices or regulation of low carbon technology. Normally, the neutral current is compensated or bypassed. It is a novel idea to utilise neutral current for improving power quality by restricting spread of disturbances. Furthermore, the attempt to examine the influence of neutral current in limiting power quality issues, accounting the electromagnetic interaction between lines is new. The following are the outcomes of the analysis.

- Without implementing any additional compensation scheme, voltage regulation is diminished to enhance the voltage level all along feeder.
- Without regulating the operation of EVs and PVs and limiting their active power, the voltage unbalance is reduced. Reconfiguration of the network and usage of storage is also avoided.
- Without any filtering scheme or complex control of DGs, harmonic propagation towards the feeder head is significantly reduced, regardless of the harmonic order.
- Because the majority of unbalanced and harmonic currents pass through the neutral line itself, the problem with ground current is eliminated and voltage between neutral and earth is reduced.
- Level of the earth fault and rating of protection equipment are reduced as the high loop impedance of the path limits earth fault current. Configuring the earth fault relay is made easier as the fault current is easy to differentiate.

The proposed method accomplishes these benefits without the addition of any equipment, but at the expense of a slight increase in line loss. Dynamic analysis results ensure that the technique is robust and unaffected by random load variations in the system. The approach can be applied to any structure with some level of mutual inductance between phase and neutral lines. The solution is robust, sustainable and low cost.

# Chapter 5

# A new custom power device - Mutual Compensator Extractor (MuCE)

## 5.1 Introduction

Phase balancing in low voltage distribution systems is difficult to manage due to the presence of unequal line impedances and a large number of single phase loads. In a 3 phase, 4 wire system, the zero sequence currents produced by phase unbalance and harmonics create a significantly higher neutral current [129]. It was discovered in the field that the zero sequence components of current and voltage are not as insignificant as previously thought. They cannot be ignored in the calculation of unbalance. Also, as discovered and reported, current unbalance is relatively difficult to attenuate by the electrical networks themselves. According to studies, when current and voltage imbalances propagate through a network, lines provide little attenuation to the unbalances [130]. So, dedicated additional equipment is necessary to handle zero sequence unbalance.

In conventional configurations, shunt connected zig-zag transformers are commonly used for filtering zero sequence components because active filters are an expensive solution [131]. If the utility voltage is unbalanced, the zig-zag transformers draw a significant amount of neutral current. Neutral reactors are not a suitable solution as it result in a potentially hazardous rise in neutral voltage [30]. Another option is to use a series connected electromagnetic suppressor in conjunction with a shunt connected zig-zag transformer. The combined size of the two electromagnetic devices are quite large [132]. Furthermore, additional capacitor banks are required to provide reactive power support in order to maintain power factor.

## 5.2 Sequence components and unbalance

A 3 phase unbalanced voltages or currents can be resolved and expressed as the sum of positive, negative, and zero sequence components by the well known Fortescue

theorem [133], and is illustrated in Figure 5.1. The positive and negative sequence

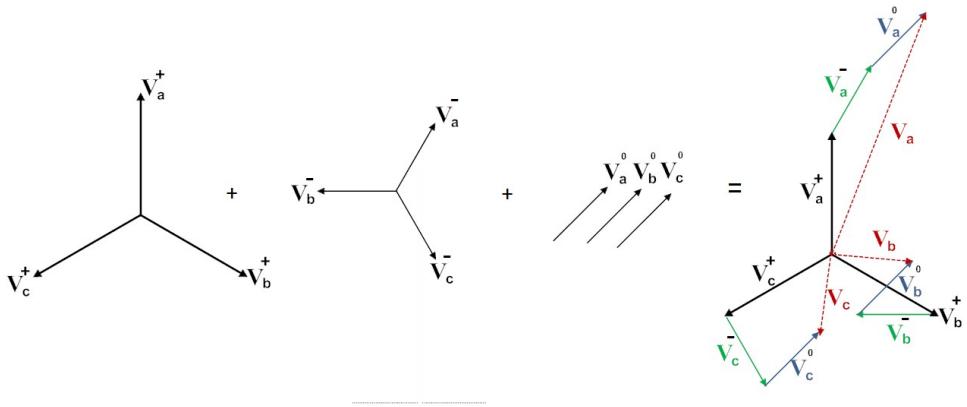


**Figure 5.1:** Sequence components

components are 120 degree phase shifted among each other and balance themselves, while the zero sequence components are unidirectional with zero phase shift. Since they are unidirectional, they add up instead of cancelling each other. Equation (5.2.1) specifies the sequence components of phase 'a' voltage. The three zero sequence currents add to the residual current and flow through the neutral, whereas the zero sequence voltages cause neutral shift. A new custom power device which is designed to reduce zero sequence unbalance and is also capable of providing reactive power support is discussed here. The experimental results and additional benefits are presented.

$$\begin{bmatrix} V_{a^0} \\ V_{a^+} \\ V_{a^-} \end{bmatrix} = \frac{1}{3} \begin{bmatrix} 1 & 1 & 1 \\ 1 & \boldsymbol{a} & \boldsymbol{a^2} \\ 1 & \boldsymbol{a^2} & \boldsymbol{a} \end{bmatrix} \begin{bmatrix} V_a \\ V_b \\ V_c \end{bmatrix} \tag{5.2.1}$$

Where '**a**' is an operator that shifts the phasor by 120 degrees in the anticlockwise direction.

As per true definition, unbalance levels are defined using the sequence components [134] and are given in equations (5.2.2) and (5.2.3).

Negative sequence voltage unbalance factor,

$$VUF(-) = \frac{V_{a^-}}{V_{a^+}} \times 100 \tag{5.2.2}$$

Zero sequence voltage unbalance factor,

$$VUF(0) = \frac{V_{a^0}}{V_{a^+}} \times 100 \tag{5.2.3}$$

## 5.3 New custom power device - Mutual Compensator Extractor (MuCE)

The Mutual Compensator Extractor (MuCE) has a set of mutually coupled coils and star connected capacitors as shown in Figure 5.2. MuCE has a fourth compensating coil in addition to the 3 phase coils. The fourth compensating coil is in equal tight coupling with the 3 phase coils and is identical to them. In order to adjust current and voltage in the fourth compensator coil variable resistors may be employed as shown in the circuit.

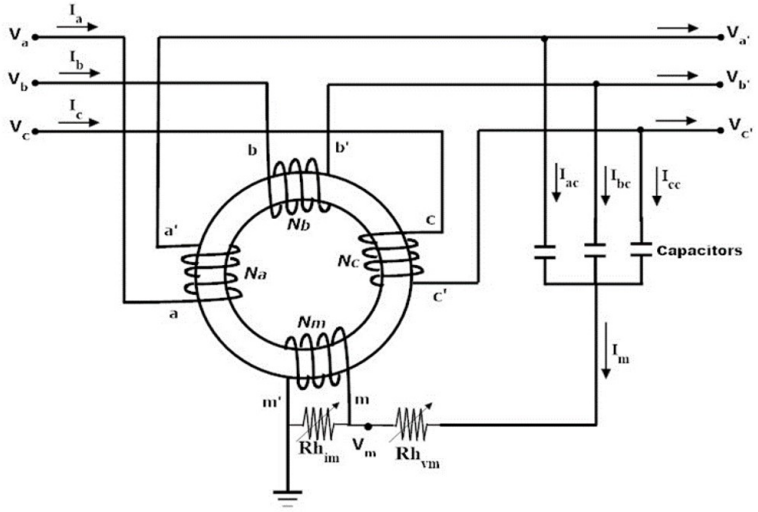


**Figure 5.2:** Connection diagram of the Mutual Compensator Extractor (MuCE)

### 5.3.1 Mutually coupled coils of MuCE

Four identical coils are wound on a common toroidal core for equal and tight coupling between them as shown in Figure 5.3. Loads are connected through the 3 phase coils to the source as shown in Figure 5.4, while the fourth one is used as a compensator coil. The equation (5.3.1) gives total Ampere-Turns (AT) by the phase coils. The flux in the core during balanced loading is zero. As the residual flux in the core is zero, the voltage, $V_m$ across the fourth coil is zero.

$$\begin{aligned} I_a + I_b + I_c &= I_{res} = 0 \\ N_a I_a + N_b I_b + N_c I_c &= 0 \end{aligned} \tag{5.3.1}$$

So $\Phi = 0$, and $V_m = 0$.
Where,

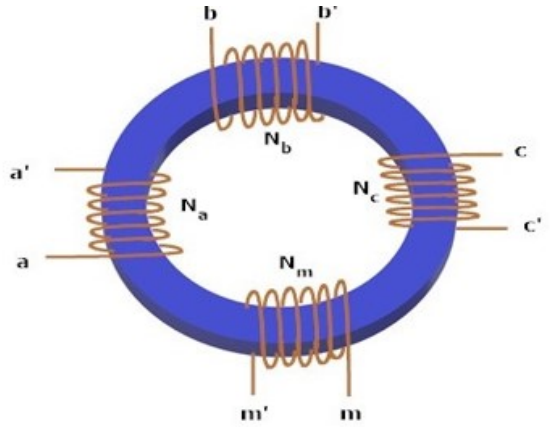


**Figure 5.3:** Mutually coupled coils of MuCE in a toroid core

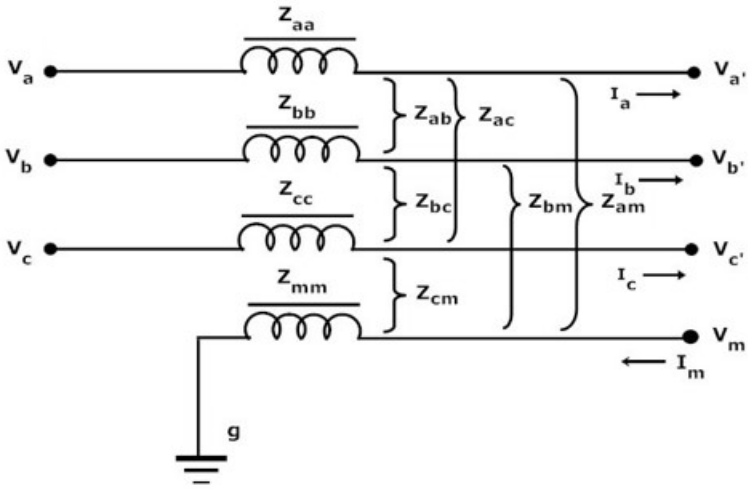


**Figure 5.4:** Mutual impedance of coupled coils in MuCE

$I_a, I_b, I_c-$ are the load currents in the phase coils,
$N_a, N_b, N_c-$ are the number of turns of the phase coils,
$\Phi-$ magnetic flux in the toroid core
$V_m-$ voltage in the fourth coil

During current unbalance, the Ampere-Turns (AT) of the phase coils do not sum to zero as given by equation (5.3.2). As the non-zero Ampere-Turns produce a residual flux in the core, a voltage $V_m$, proportional to the residual current is induced in the fourth coil. The magnitude and phase angle of voltage, $V_m$, is decided by the magnitudes and phase angles of load currents. So, analysis of $V_m$ is helpful for detecting any abnormal conditions, such as unsymmetrical faults or reverse power flow due to higher integration of renewable energy sources.

$$\begin{aligned} I_a + I_b + I_c &= I_{res} \neq 0 \\ N_a I_a + N_b I_b + N_c I_c &\neq 0 \end{aligned} \tag{5.3.2}$$

So $\Phi \neq 0$ and $V_m \neq 0$

If the compensator coil is short circuited, a current $I_m$ flows through the coil. According to Lenz's law and Ampere-Turns balancing [135] as given in equation (5.3.3), the residual flux is cancelled. Thus a short circuited compensator coil is capable of arresting any transients propagated through the phase lines by Ampere-Turn balancing.

$$N_a I_a + N_b I_b + N_c I_c \ = N_m I_m \tag{5.3.3}$$

By adjusting the current $I_m$ in the fourth coil, the flux in the toroid core can be varied. This can be used to vary the effective inductance of the coils and to avoid any possibility of resonance or to customise the device for an application. Above all, if an external current is passed through the fourth coil, a flux can be set up in the core. The flux thus created can inject a voltage into phase coils similar to a series injection transformer. The behaviour of the mutually coupled coils can be analysed using sequence components approach or a phase frame approach.

The impedance of the 3 phase coils can be written as

$$\left[Z_{abc}\right] = \begin{bmatrix} Z_{aa} & Z_{ab} & Z_{ac} \\ Z_{ba} & Z_{bb} & Z_{bc} \\ Z_{ca} & Z_{cb} & Z_{cc} \end{bmatrix} \tag{5.3.4}$$

Where,

$Z_{aa}$−Self impedance of phase 'a' coil,

$Z_{ab}$−Mutual impedance between phase 'a' and 'b' coils,

Other terms have similar definitions.

Transforming into sequence impedances [36]

$$\left[Z_{012}\right] = \left[A\right]^{-1} \left[Z_{abc}\right] \left[A\right] \tag{5.3.5}$$

$$\left[Z_{012}\right] = \begin{bmatrix} Z_p + 2Z_m & 0 & 0 \\ 0 & Z_p - Z_m & 0 \\ 0 & 0 & Z_p - Z_m \end{bmatrix} \tag{5.3.6}$$

where,

$[A]-$ sequence component transformation matrix
Self impedance $Z_{aa} = Z_{bb} = Z_{cc} = Z_p$
Mutual impedance $Z_{ab} = Z_{bc} = Z_{ac} = Z_m$

As per equation (5.3.6), the coupled coils offer high zero sequence impedance, whereas the positive and negative sequence impedance are less. Neglecting the coil resistance using the corresponding reactances we have,

$$j\left[X_{012}\right] = j\begin{bmatrix} X_p + 2X_m & 0 & 0 \\ 0 & X_p - X_m & 0 \\ 0 & 0 & X_p - X_m \end{bmatrix} \tag{5.3.7}$$

Assuming tight coupling between coils, then $X_p = X_m$

$$\left[jX_{012}\right] = j\begin{bmatrix} 3X_p & 0 & 0 \\ 0 & 0 & 0 \\ 0 & 0 & 0 \end{bmatrix} \tag{5.3.8}$$

For ideal coupling with unit coefficient of coupling, the reactance offered to positive and negative sequence components are zero, while the zero sequence reactance is three times the phase coil reactance. The phase frame representation is useful for analysis, including the fourth compensating coil. The voltages across the coils can be written in equation (5.3.9) neglecting the resistance of the coils.

$$\begin{bmatrix} V_{aa'} \\ V_{bb'} \\ V_{cc'} \\ V_m \end{bmatrix} = \begin{bmatrix} X_{aa} & X_{ab} & X_{ac} & X_{am} \\ X_{ba} & X_{bb} & X_{bc} & X_{bm} \\ X_{ca} & X_{cb} & X_{cc} & X_{cm} \\ X_{ma} & X_{mb} & X_{mc} & X_{mm} \end{bmatrix} \begin{bmatrix} I_a \\ I_b \\ I_c \\ I_m \end{bmatrix} \tag{5.3.9}$$

Where,

$V_{aa'}, V_{bb'}, V_{cc'}-$ are the voltages across the phase coils,

$I_a, I_b, I_c-$ are the current through the phase coils,

$V_m$,$I_m-$ are the voltage and current in the compensating coil,

$X_{aa}-$Reactance due to self-inductance of phase 'a' coil,

$X_{ab}-$Reactance due to mutual inductance between phase 'a' and 'b' coils,

$X_{am}-$Reactance due to mutual inductance between phase 'a' and device coils.

All other terms have similar definitions.

Assuming all coils are identical and assuming ideal coupling between them, the

reactances are

$X_{aa} = X_{bb} = X_{cc} = X_{ab} = X_{bc} = X_{ac} = X_{mm} = X_p$

The compensating coil is also identical and has the same coupling with phase coils. So,

$X_{ma} = X_{mb} = X_{mc} = X_{am} = ... = X_{pm} = X_{mp}$

If there is a current $I_m$ in the compensating coil, then voltage $V_m$ is given by equation (5.3.10)

$$\begin{aligned} V_m &= jX_{ma}I_a + jX_{mb}I_b + jX_{mc}I_c + jX_{mm}I_m \\ &= jX_{mp}(I_a + I_b + I_c) + jX_{mm}I_m \\ &= jX_{mp}(I_{res}) + jX_{mm}I_m \end{aligned} \tag{5.3.10}$$

### 5.3.2 Star connected capacitors of MuCE

Three equal capacitors are connected in a star configuration. Conventionally the star point of the capacitor is directly connected to neutral. But in MuCE it is connected through the compensator coil as shown in Figure 5.5. If the voltages at the point of common coupling (PCC) are balanced, the net capacitor current and the voltage at the star point are zero. During phase unbalance, the resultant capacitor current is proportional to the residual voltage at PCC. Also, a voltage applied at the star point of the capacitor bank can regulate reactive power injection into phases and adjust the phase voltages. If $V_m$ is the voltage at the star point, then the current, $I_m$ is given by equation (5.3.11)

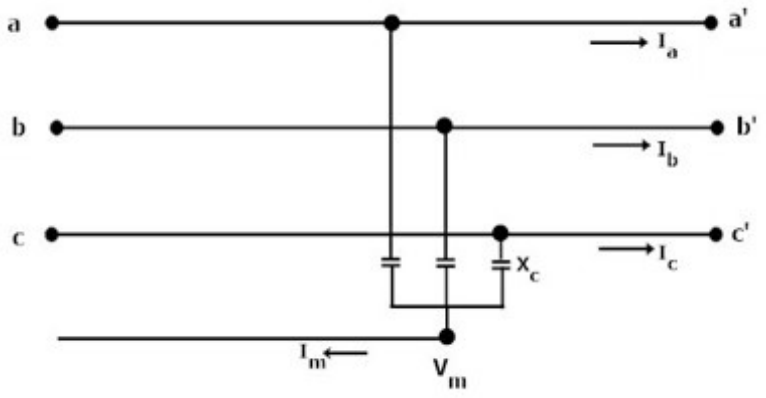


**Figure 5.5:** Star connected capacitors for MuCE

$$
\begin{aligned}
I_m &= \frac{V_{a'} - V_m}{-jX_c} + \frac{V_{b'} - V_m}{-jX_c} + \frac{V_{c'} - V_m}{-jX_c} \\
&= \frac{V_{a'} + V_{b'} + V_{c'}}{-jX_c} - \frac{3V_m}{-jX_c} \\
&= \frac{V_{res}}{-jX_c} - \frac{3V_m}{-jX_c}
\end{aligned} \tag{5.3.11}
$$

### 5.3.3 Working principle of MuCE

The mutually coupled coils and star connected capacitors are interconnected as shown in Figure 5.6 to form a new device called the Mutual Compensator Extractor (MuCE). Using equation (5.3.10) for $V_m$,

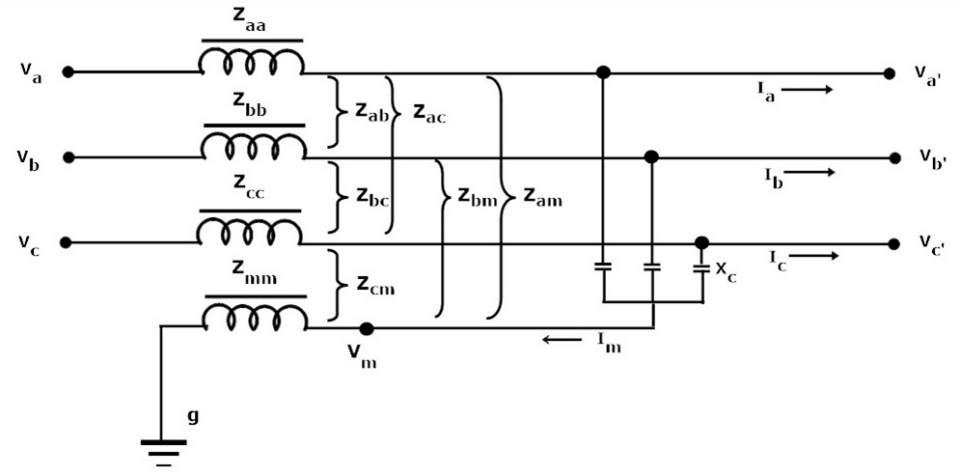


**Figure 5.6:** Circuit diagram of the proposed MuCE

$$
\begin{aligned}
I_m &= \frac{V_{res}}{-jX_c} - \frac{3(jX_{mp}I_{res} + jX_{mm}I_m)}{-jX_c} \\
I_m + \frac{3(jX_{mm}I_m)}{-jX_c} &= \frac{V_{res}}{-jX_c} - \frac{3(jX_{mp}I_{res})}{-jX_c} \\
\frac{-jX_cI_m + 3(jX_{mm}I_m)}{-jX_c} &= \frac{V_{res}}{-jX_c} - \frac{3(jX_{mp}I_{res})}{-jX_c} \\
I_m &= \frac{V_{res}}{3jX_{mm} - jX_c} - \frac{3jX_{mp}I_{res}}{3jX_{mm} - jX_c}
\end{aligned} \tag{5.3.12}
$$

When the compensator coil is open, $I_m = 0$, and

$$
\frac{V_{res}}{I_{res}} = 3jX_{mp} \tag{5.3.13}
$$

For ideal coupling,
the zero sequence reactance,

$$
X_0 = \frac{V_0}{I_0} = 3jX_p \tag{5.3.14}
$$

$V_m$ is the voltage proportional to zero sequence load currents, while $I_m$ is the current proportional to zero sequence voltage at PCC. From equations (5.3.10) and (5.3.11), $I_m$ can be written as in (5.3.15).

$$\begin{aligned} I_m &= \frac{(V_{res})}{-jX_c} - \frac{3(jX_{mp}I_{res} + jX_{mm}I_m)}{-jX_c} \\ &= \frac{V_{res}}{-jX_c + 3jX_{mm}} - \frac{3jX_{mp}I_{res}}{-jX_c + 3jX_{mm}} \end{aligned} \tag{5.3.15}$$

The voltage across phase 'a' coil is given by

$$\begin{aligned} V_{aa'} &= jX_{aa}I_a + jX_{ab}I_b + jX_{ac}I_c + jX_{am}I_m \\ &= jX_pI_{res} + jX_{mp}I_m \end{aligned} \tag{5.3.16}$$

Substituting $V_{res} = 3V_0$, and $I_{res} = 3I_0$, in terms of zero sequence components defined in equation (5.2.1) and also for $I_m$ from equation (5.3.15),

$$\begin{aligned} V_{aa'} =& jX_p(3I_0) - \left(\frac{3jX_{mp}jX_{mp}}{-jX_c + 3jX_{mm}}\right)(3I_0) \\ &+ \left(\frac{jX_{mp}}{-jX_c + 3jX_{mm}}\right)(3V_0) \end{aligned} \tag{5.3.17}$$

Other phase coils also have similar voltage equations. The left hand side of the equation (5.3.17) has zero sequence current and voltage, indicating that the coils and capacitors together can compensate for zero sequence components. From equations (5.3.15) and (5.3.16), it is explicit that the voltage, $V_m$ regulates the reactive power to each phase, whereas the current, $I_m$ decides the series compensating voltage injected. As long as the operation is balanced, the capacitors provide equal voltage support to all phases, and only a resistive drop exists across the coils. During such an operation the voltage and current in the compensator coil are zero.

## 5.4 Design of MuCE

The series coils are designed mainly for injecting compensating voltages. As per regulation, the allowed maximum deviation of supply voltage is ± 6%. For 230 V supply the maximum deviation permitted is $2 \times 13.8 = 27.6V$ among phases. Considering this as a zero sequence component in most adverse cases and with possible 180 degree phase turning of zero sequence components the extreme voltage to be compensated is $2 \times 27.6 = 55.2V$. The equivalent winding reactance required for injecting the voltage with a 10A load current is 5.52Ω. Since the conductor thickness should be suitable to wind on the toroid core, the current rating is restricted to 10A. The required induc-

tance of each coil is 17.58 mH at 50Hz frequency.
The inductance, L of a toroid coil is given by

$$L = \frac{\mu NNA}{2\pi r} \tag{5.4.1}$$

Where,

$N-$ number of turns of the coil,

$A-$ cross sectional area of the core,

$r-$ average radius of the core,

$\mu-$ permeability of the material of the core.

For an available toroid core of 11 cm average radius and 6.9 cm average coil radius shown in Figure 5.7, 60 turns give an inductance of 19.58mH if relative permeability of silicon steel is considered as 200 at 2 Tesla flux density.

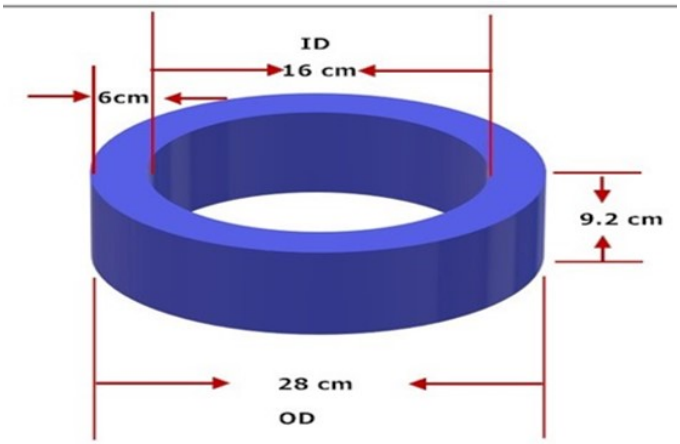


**Figure 5.7:** Dimensions of the toroid core

**Table 5.1:** Design parameters of mutually coupled coils

| Coil | Self inductance (mH) | Coils | Mutual inductance (mH) |
|---|---|---|---|
| Phase a | $L_{aa}$=19 | Coils a and m | $L_{am}$=18.4 |
| Phase b | $L_{bb}$=19 | Coils b and m | $L_{bm}$=18.2 |
| Phase c | $L_{cc}$=19 | Coils c and m | $L_{cm}$=18.5 |
| Compensator | $L_{mm}$=19 | Coils a and b | $L_{ab}$=18.3 |
| | | Coils b and c | $L_{bc}$=18.5 |
| | | Coils c and a | $L_{ca}$=18.4 |

**Table 5.2:** Specification of MuCE

| Rating of MuCE | |
|---|---|
| kVAr | 1.5 kVAr |
| Series voltage injection | 58V, 10A |
| Voltage between the coils | 500V |

The balanced and unbalanced supply for conducting the experiment was directly derived from a 415V, 50Hz, 3 phase utility supply. An R L series load was used for unbalance compensation tests. A resistive load with a step variation of 850W (62Ω) was used to create unbalance in the load. A coil having a 100mH inductance was used in series with the resistive load to form an R L load. For harmonic analysis, a 3 phase uncontrolled rectifier was used as a nonlinear load.

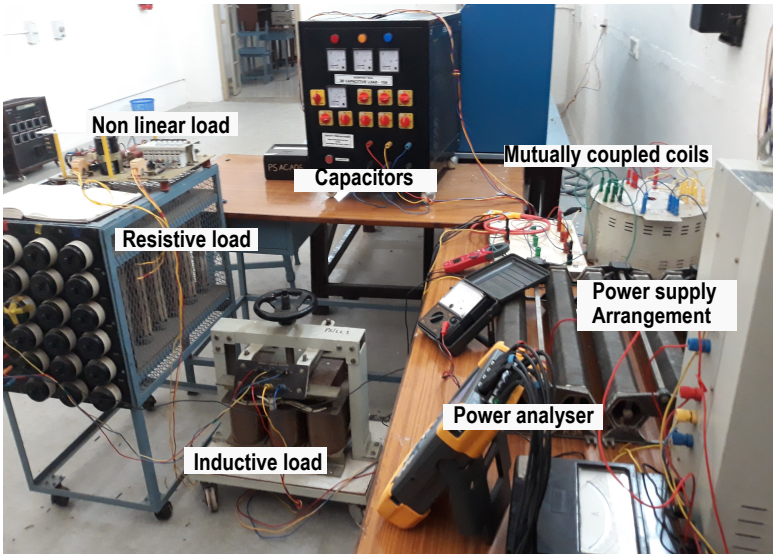


**Figure 5.8:** Experimental setup for MuCE testing

## 5.5 Experimental analysis and comparison of MuCE with capacitor bank

To validate the concept, a prototype of MuCE was designed and tested in the laboratory. The performance and capabilities are analysed and compared with conventional capacitor bank having the same capacity.

### 5.5.1 Zero sequence compensation

Zero sequence current is the main contributor to neutral current. Other than the current due to unbalance and harmonics, during parallel operation of inverter based DGs without isolation transformers, the common mode zero sequence currents circulates in the network. Performance of the device to mitigate zero sequence unbalance was analysed. The comparison with a capacitor bank that can supply same reactive power was done. The results of two test cases considered are presented.

### 5.5.2 Case 1. Unbalanced supply and balanced R L load

A balanced RL series load having 62Ω and 100mH in each phase was connected to the unbalanced supply. As the supply voltage was unbalanced, the balanced load also drew unbalanced currents. The details of voltages, currents, and unbalance are shown in Figure 5.9.a. With 1.5kVAr reactive power supply by conventional star connected capacitors, the prevailing 3.0 percent zero sequence voltage unbalance at the load terminals increases to 3.3 percent as shown in Figure 5.9.b. Due to the capacitor bank addition, the zero sequence current unbalance increased from 3.3 percent to 4.2 percent. Whereas Figure 5.9.c indicates that the presence of 1.5kVAr MuCE gives better zero sequence compensation as the zero sequence voltage and current unbalances are significantly reduced to 0.9 percent and 1.0 percent respectively, indicating the load is getting a more balanced supply. The zero sequence voltage unbalance, VUF(0) and zero sequence current unbalance, IUF(0) along with the corresponding neutral currents for the test case are shown in Table 5.3. It reveals that the neutral current created by the supply voltage unbalance is reduced by the compensation provided by MuCE. With MuCE device, the zero sequence unbalance on the load side is considerably reduced and the load gets a better balanced supply along with reactive power support to the system.

**Table 5.3:** Comparison of zero sequence unbalances and neutral current for Case 1

| System status | VUF(0) | IUF(0) | $I_n(A)$ |
|---|---|---|---|
| Load alone | 3.0% | 3.3% | 0.3 |
| With PF capacitors | 3.3% | 4.2% | 0.4 |
| With MuCE | 0.9% | 1.0% | 0.1 |

The supply voltage unbalance is shown in Figure 5.10.a where phase 'b' voltage is low compared to other phases. The conventional reactive power compensation with

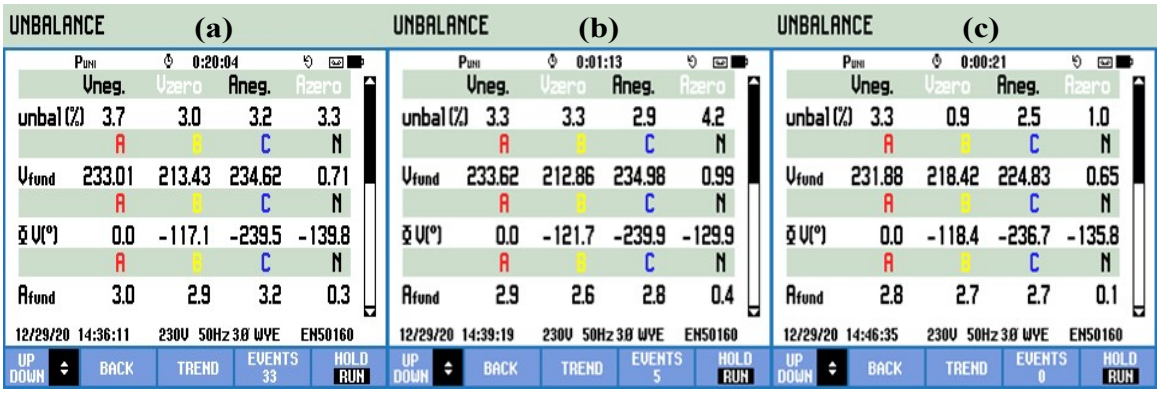


**Figure 5.9:** Case 1. Unbalance on load terminals (a) when balanced load is connected to an unbalanced supply (b) with 1.5kVAr PF capacitors (c) with 1.5kVAr MuCE

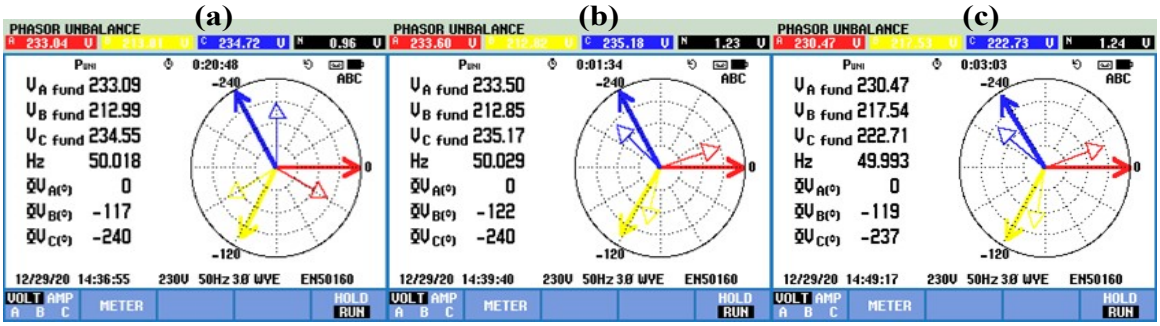


**Figure 5.10:** Case 1. Load voltage phasors (a) when balanced load connected to an unbalanced supply (b) with 1.5kVAr PF capacitors (c) with 1.5kVAr MuCE

capacitor bank does not have much positive influence on the system status, whereas the MuCE helps to boost the voltage of the weak phase and improves system status reducing the zero sequence unbalance as shown in Figure 5.10.c.

Due to the unbalance in the supply voltage, load currents are also unbalanced as shown in Figure 5.11.a. The currents lag behind the voltage as the load is inductive. The reactive power supply by capacitors improves the power factor to leading, but unbalance in the current is not compensated. Figure 5.11.c shows that the MuCE makes the load currents more balanced though there is unbalance in supply voltage.

### 5.5.3 Case 2. Balanced supply and unbalanced R L load

Both phases 'a' and 'b' were connected with 62Ω and 100mH in series, and phase 'c' with 31Ω and 100mH to form an unbalanced load supplied from a balanced source. The unbalanced load draws unbalanced currents at different power factors and the system status is shown in Figure 5.12.a. Reactive power supply with 1.5kVAr capacitors increases the zero sequence unbalance at PCC and is in Figure 5.12.b, while the MuCE device with the same capacitors restrict the zero sequences and give reactive

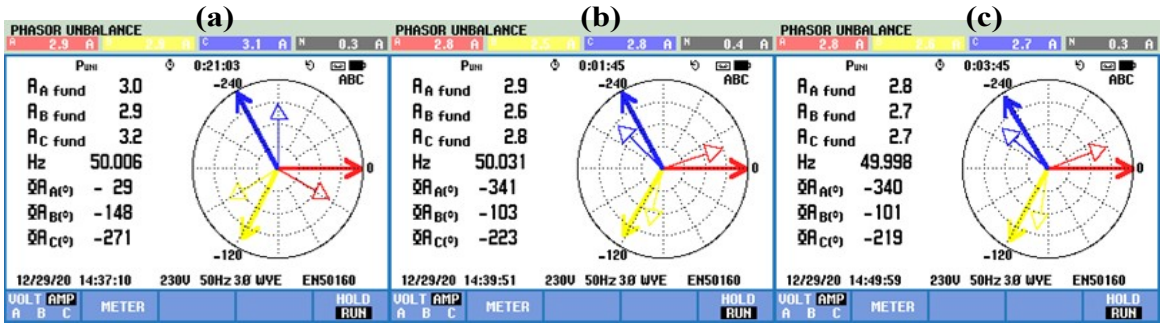


**Figure 5.11:** Case 1. Load current phasors (a) when balanced load connected to an unbalanced supply (b) with 1.5kVAr PF capacitors (c) with 1.5kVAr MuCE

power support as per Figure 5.12.c. The different unbalances and neutral currents for each condition is tabulated in Table 5.4. It shows that the MuCE device can restrict the load zero sequence unbalance while supplying the required reactive power without increasing the neutral current.

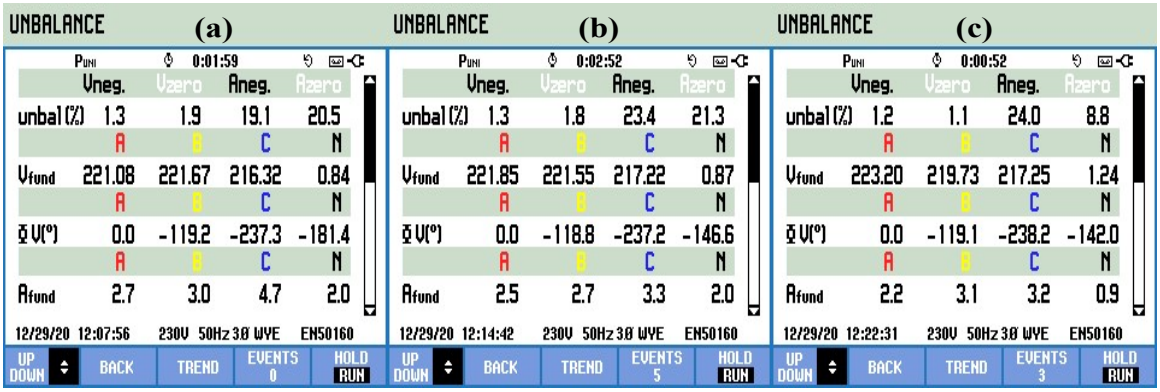


**Figure 5.12:** Case 2. Unbalance on supply side (a) when unbalanced load is connected to a balanced supply (b) with 1.5kVAr PF capacitors (c) with 1.5kVAr MuCE

**Table 5.4:** Comparison of zero sequence unbalances and neutral current for Case 2

| System status | VUF(0) | IUF(0) | $I_n(A)$ |
|---|---|---|---|
| Load alone | 1.9% | 20.5% | 2.0 |
| With PF capacitors | 1.8% | 21.3% | 2.0 |
| With MuCE | 1.1% | 8.8% | 0.9 |

As a custom power device, MuCE can restrict zero sequence unbalance either on the source side or on the load side itself, providing a better balanced condition on the other side. Thus, balanced sources and loads can be relieved from adverse effects due to zero sequence unbalance on the other side.

## 5.6 Ancillary services by MuCE

Other than zero sequence compensation, MuCE can provide some additional functions that can enhance the system performance. Some of them are presented for verification.

### 5.6.1 Case 3. Prevention of voltage and current harmonic spread

The harmonic mitigation ability of the device is analysed using a 3 phase uncontrolled rectifier as a nonlinear load. The voltage wave forms at the PCC due to the non linear load without any compensation is given in Figure 5.13.a. The non linear voltage at the load terminals after connecting MuCE is shown in Figure 5.13.b, whereas after connecting MuCE voltage at source is illustrated in Figure 5.13.c. It is evident that after inclusion of the MuCE, the distortion on source side is considerably reduced and the waveform distortion is restricted on load side itself. In order to quantify the level

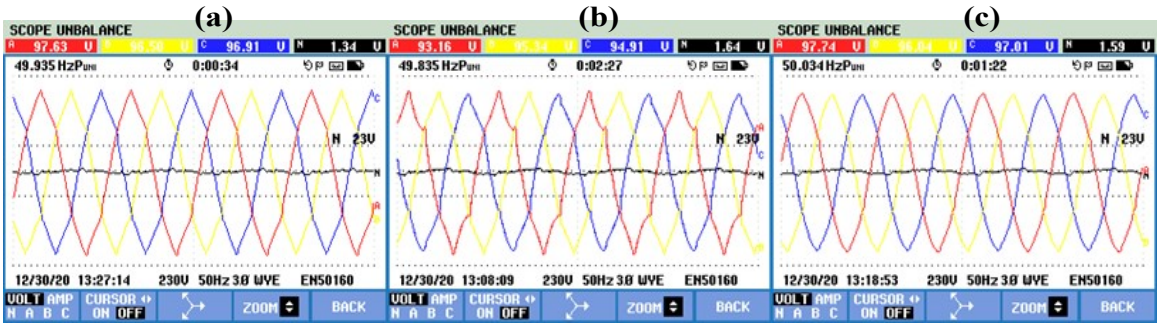


**Figure 5.13:** Voltage distortion due to non-linear load (a) without MuCE (b) on load side of MuCE (c) on source side of MuCE

of distortion in each case, voltage THDs are shown in Figure 5.14. It clearly indicates that, MuCE restricts the waveform distortion due to load on the load side itself. So on the source side, the voltage THD is less when MuCE is present. At the same time, current harmonics are also significantly reduced by the presence of MuCE and it is presented in Figure 5.15. The K factor of the system was initially 12.4 due to the presence of harmonics, but has been reduced to 7.2 by the introduction of MuCE. So MuCE can mitigate harmonics in the system along with zero sequence compensation.

### 5.6.2 Case 4. Reduction of neutral voltage and current

The current waveforms during the phase unbalanced state are shown in Figure 5.17.a. The neutral voltage is 1.84V and the current is 2.4A. With 1.5kVAr reactive power

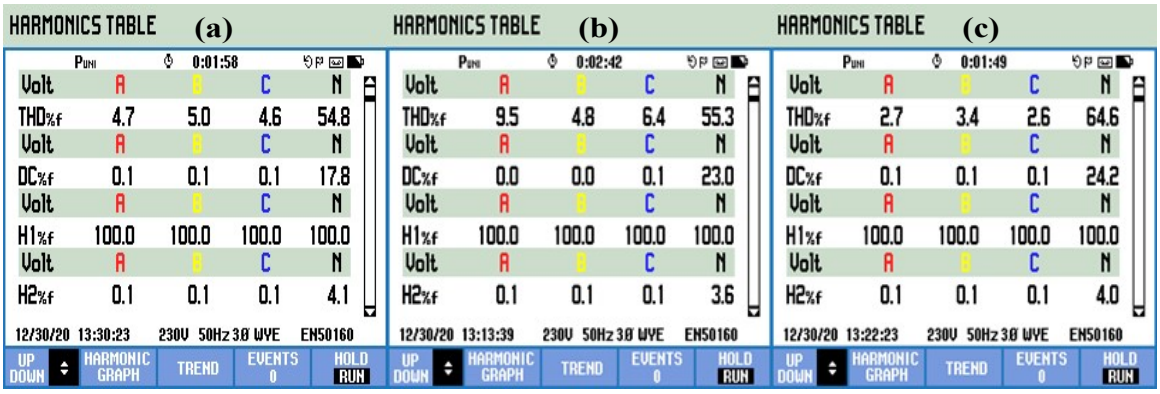


**Figure 5.14:** Voltage harmonics ($THD_V$) due to non linear load (a) without MuCE (b) on load side of MuCE (c) on source side of MuCE

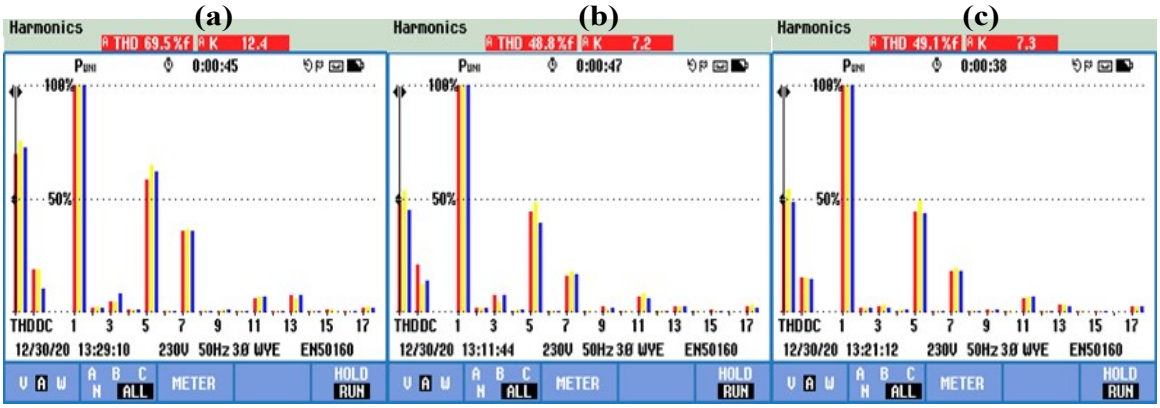


**Figure 5.15:** Current harmonics due to non-linear load (a) without MuCE (b) on load currents with MuCE (c) on source currents with MuCE

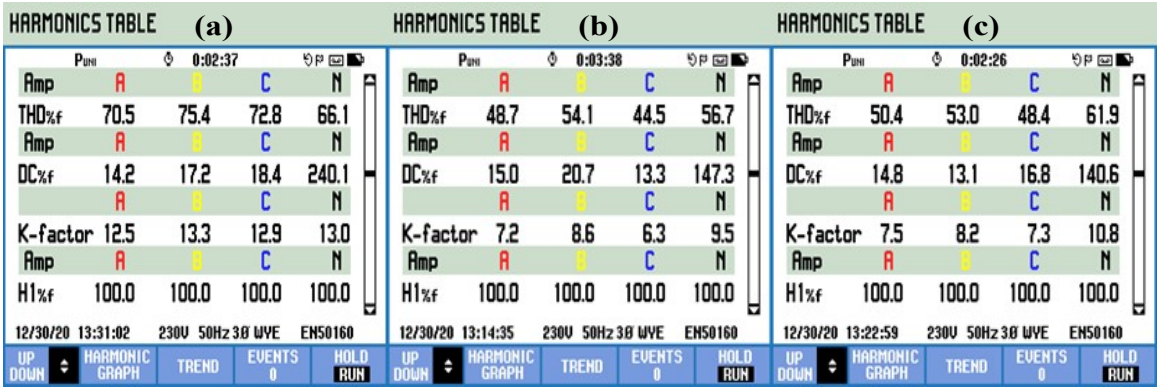


**Figure 5.16:** Current harmonics ($THD_I$) due to non linear load (a) without MuCE (b) on load currents with MuCE (c) on source currents with MuCE

supply using power factor improving capacitors, the neutral voltage increases to 2.01V and the current rises to 2.5A, and the distortion on neutral is shown in Figure 5.17.b. However, the introduction of 1.5kVAr MuCE reduces the neutral voltage and current to 1.4V and 1.0A respectively. Also, the distortion in neutral voltage and current is reduced as per Figure 5.17.c and Table 5.5.

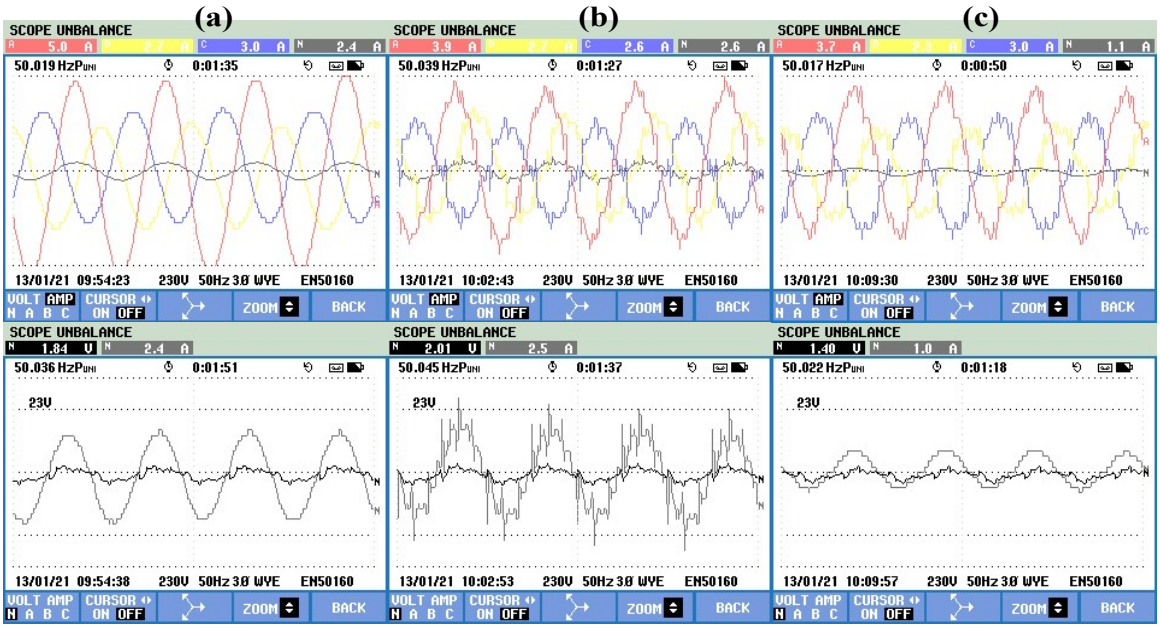


**Figure 5.17:** Comparison of phase currents, neutral voltage and neutral current (a) when an unbalanced R L load is connected to a balanced supply (b) with 1.5kVAr PF capacitors (c) with 1.5kVAr MuCE

**Table 5.5:** Comparison of neutral voltage and current for Case 4

| System status | Neutral voltage | Neutral current |
|---|---|---|
| Unbalanced R L load alone | 1.84V | 2.4A |
| With PF capacitors | 2.01V | 2.5A |
| With MuCE | 1.4V | 1.0A |

### 5.6.3 Case 5. Adaptive power factor correction

Usually, the power factor at the load end is kept at a higher value to reduce system losses. During unbalanced system operation, the conventional compensation schemes inject reactive power irrespective of unbalance, resulting in an inefficient power factor correction. MuCE helps to inject reactive power more efficiently to phases considering the zero sequence unbalance, so that overall system power factor increases with the same reactive power supply. Figure 5.18 and Table 5.6 illustrates the role of MuCE in adaptive power factor correction. The power factor was lagging due to the inductive load. Using 1.5kVAr capcitor bank, the power factor improves to 0.90 leading while MuCE having the same rating effectively improves the power factor to 0.94.

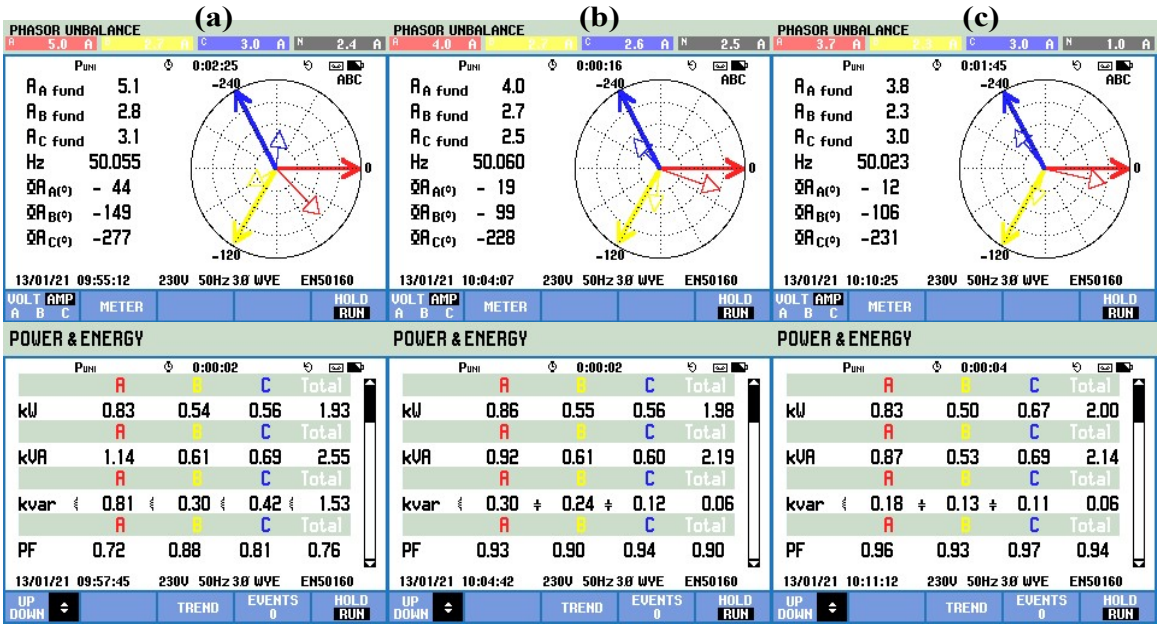


**Figure 5.18:** Comparison of phase currents, active, reactive powers, and power factors (a) when an unbalanced R L load is connected to a balanced supply (b) with 1.5kVAr PF capacitors (c) with 1.5kVAr MuCE

**Table 5.6:** Comparison of power factor and reactive power for Case 5

| System status | Power Factor | Reactive power |
|---|---|---|
| Unbalanced R L load alone | 0.76(lagging) | 1.53kVAr(Inductive) |
| With PF capacitors | 0.90(leading) | 0.06kVAr(Capacitive) |
| With MuCE | 0.94(leading) | 0.06kVAr(Capacitive) |

### 5.6.4 Case 6. Capacitor life enhancement

While power factor capacitors are installed in the power system, if voltage harmonics are present in the system, they can increase the harmonic problems and potentially damage capacitors. This is due to the high frequency currents through the low reactance path created by shunt capacitors [136]. Thus high frequency harmonics have a significant impact on the life of power factor improving capacitors. Capacitors provide a low impedance path for the higher order harmonics, causing higher losses and overheating. The high frequency current increases the dielectric stress in capacitors, resulting in their early failure [137]. So the life expectancy of capacitors is reduced in a high frequency environment. The high frequency ripple on the R L load current is very small as shown in Figure 5.19.a. But when a capacitor bank is included for power factor improvement, the high frequency ripples in the supply current increase and are shown in Figure 5.19.b. This is due to the low reactance path provided for the high frequency components of current by the shunt capacitors. The capacitor currents

shown in Figure 5.19.d illustrates this. The current wave forms after the inclusion of MuCE is shown in Figure 5.19.c and 5.19.e, clearly show that the presence of MuCE decreases the high frequency ripples. The reduction of high frequency harmonics in the capacitor current helps to enhance the capacitor life. Figures 5.19.f and 5.19.g show the effect of MuCE on the magnitude and phase angle of capacitor currents. MuCE adjusts the magnitude and phase angle of capacitor currents according to zero sequence unbalance of the system.

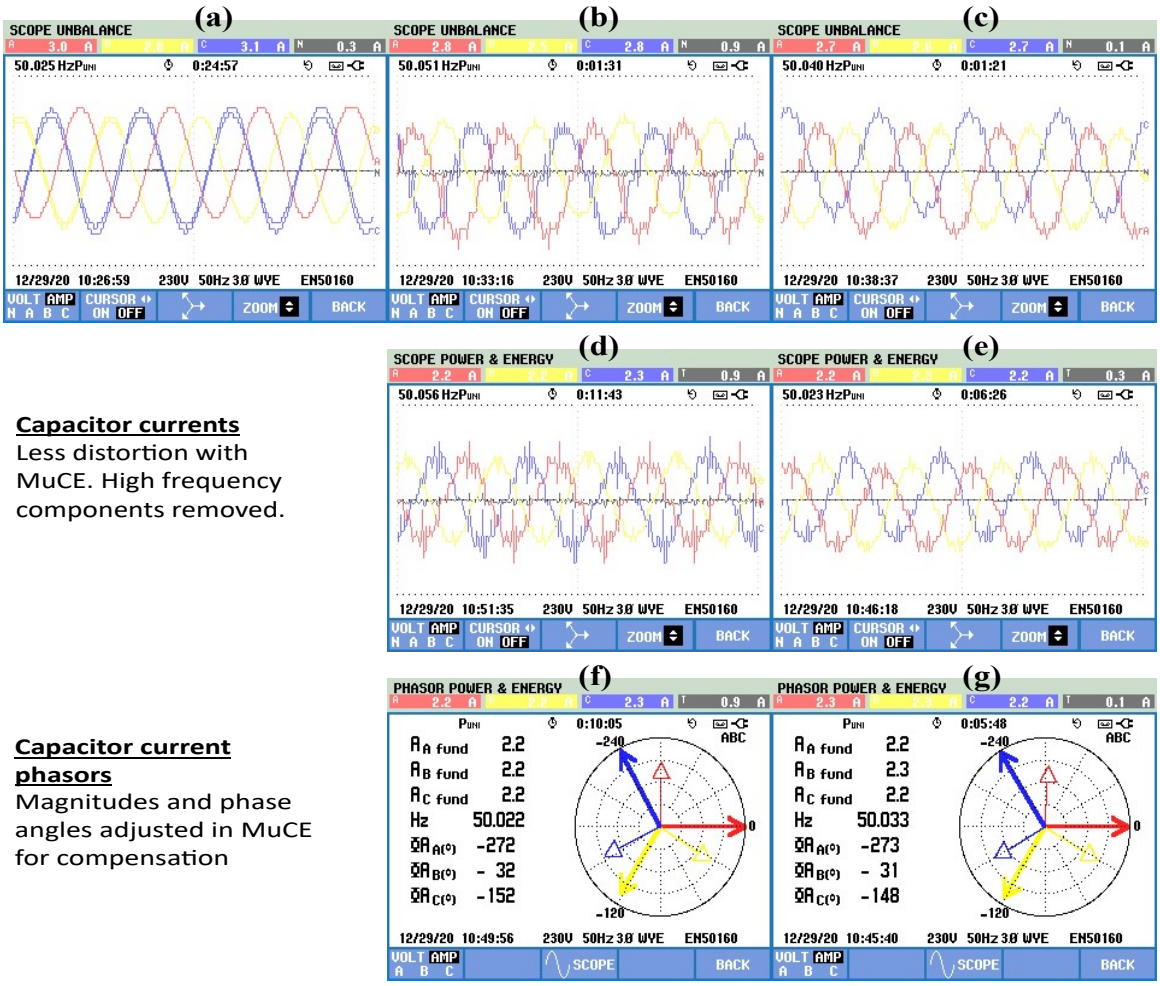


**Figure 5.19:** (a) Phase currents when an unbalanced R L load connected to a balanced supply (b) phase currents with 1.5kVAr PF capacitors (c) phase currents with 1.5kVAr MuCE (d) currents through PF capacitors (e) current through MuCE capacitors (f) current phasor of PF capacitors (g) current phasor of MuCE capacitors

### 5.6.5 Case 7. Unbalance variation with capacitor addition

To demonstrate the role of MuCE and effect of unbalance with capacitor varation, the reactive power injection is varied in steps by including different values of capacitors. The source was kept unbalanced and a balanced resistive load of 62 $\omega$ per phase was

connected. The results are shown in Figrure 5.20. In Figure 5.20.(a) the unbalance at load terminal without any other device is shown. Without MuCE, capacitors were directly connected to inject reactive power and the unbalance level at load terminal was found to be increasing as per Figure 5.20.(b). With the addition of capacitors, the reactive power injection increases, reflecting it in the increasing leading current. The results illustrates that the zero sequence components are reduced by the mutual compensation by the series coils and shunt capacitors, while capacitors alone increases the system unbalance.

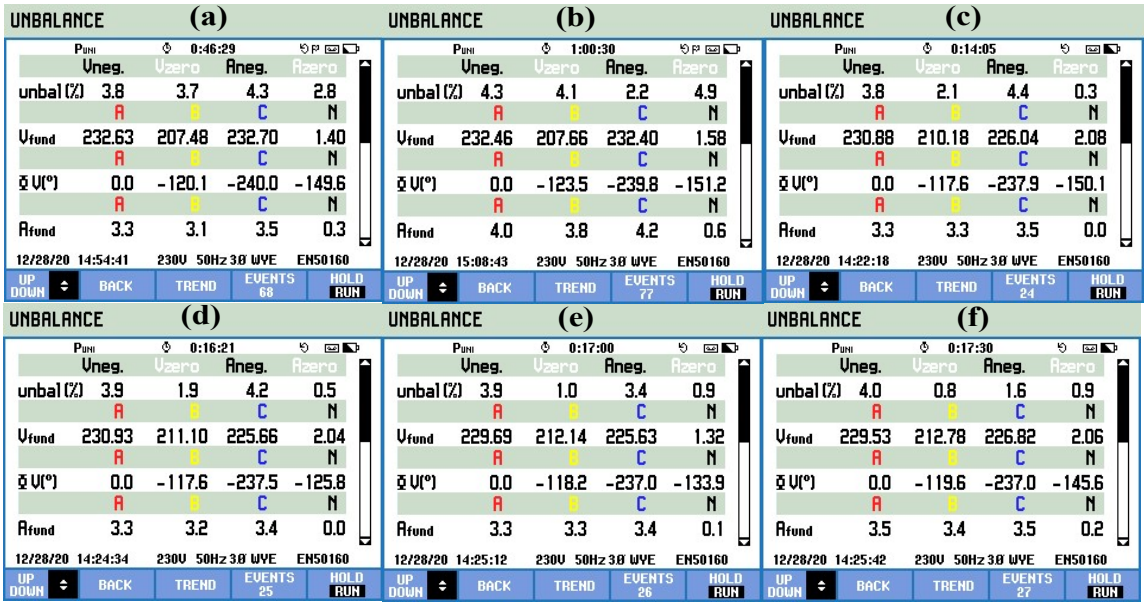


**Figure 5.20:** (a) Source and load alone (b) With $33\mu F$ capacitors (c) With MuCE of $0\mu F$ capacitors per phase (d) With MuCE of $2\mu F$ capacitors (e) With MuCE of $8\mu F$ capacitors (f) With MuCE of $18\mu F$ capacitors

**Table 5.7:** Variation of zero sequence unbalance with capacitor addition

| System status | VUF(0)% | IUF(0)% |
|---|---|---|
| Source and balanced load alone | 3.7 | 2.8 |
| With $33\mu F$ capacitors | 4.1 | 4.9 |
| MuCE with $0\mu F$ capacitors | 2.1 | 0.3 |
| MuCE with $2\mu F$ capacitors | 1.9 | 0.5 |
| MuCE with $8\mu F$ capacitors | 1.0 | 0.9 |
| MuCE with $18\mu F$ capacitors | 0.8 | 0.9 |

## 5.7 Comparison with similar devices

The features of MuCE can only be compared with devices having similar capabilities. The additional benefits and performance comparison of MuCE with equal rated conventional capacitor bank were presented in earlier sections. Though not exact, zero sequence suppressor and Distribution Static Compensator (DSTATCOM) may fulfil some functions of MuCE.

### 5.7.1 Comparison with zero sequence suppressor

Zero Sequence Suppressor (ZSS) is a combined arrangement of a Zero Sequence Blocker (ZSB) and a Zero Sequence Filter (ZSF). The zero sequence blocker is a three winding device connected in series with the load, while the zero sequence filter is a zig-zag transformer connected in parallel [72, 85, 86]. A combination of these two devices can simultaneously block zero sequence components on source and load sides. Though the device can reduce zero sequence components to some extent, the presence of two electromagnetic devices dedicated to a single purpose makes the solution a bulky one. Since the fourth compensating winding is absent in ZSB, the configuration cannot provide any series voltage injection for additional compensation. Also, ZSS is not at all capable of supplying any reactive power, but only makes the circuit more inductive.

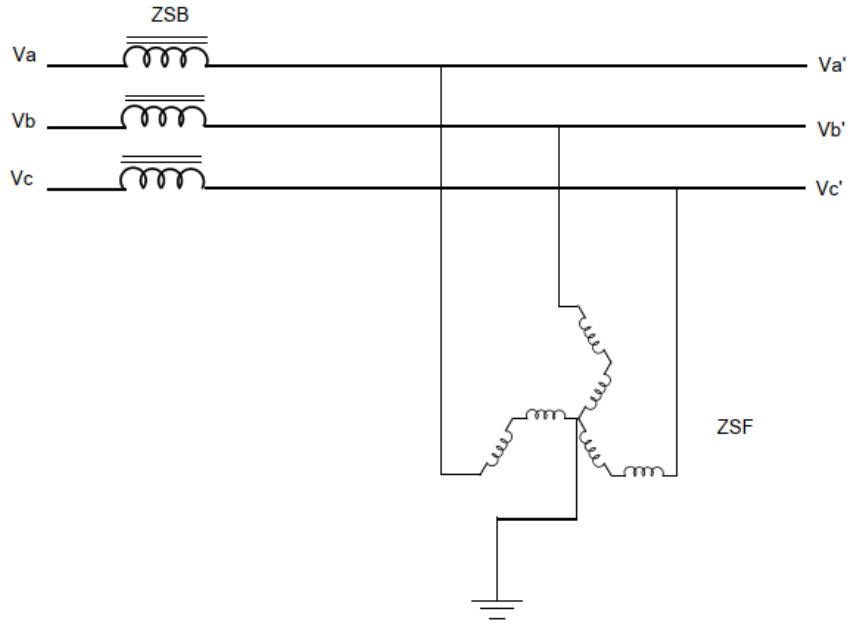


**Figure 5.21:** Circuit diagram of a zero sequence suppressor

### 5.7.2 Comparison with DSTATCOM

Another device that may perform some functions of MuCE is DSTATCOM. It is a shunt connected power electronic based solution, primarily intended for reactive power compensation and voltage regulation. With special control strategies DSTATCOM may be used for unbalance and harmonic mitigation [138]. During the dynamic load variation in different phases and resulting phase unbalance variation, DSTATCOM needs a special fast responding control algorithm [139]. So it is very difficult to incorporate all the functionalities of MuCE, such as unbalance compensation, adaptive power factor correction, and harmonics mitigation in a DSTATCOM. Moreover, in robustness, the DSTATCOM is not at all comparable with MuCE, as MuCE is an electromagnetic unit without any switching devices or controller. The overall requirements to meet all the functionalities of MuCE will make the DSTATCOM a costly and complex device. A 1.5kVAR DSTATCOM is costlier and is less reliable than MuCE.

## 5.8 Summary

The experimental results show that the proposed custom power device is capable of compensating for the zero sequence unbalances from the source and load sides. As a custom power device, MuCE can restrict zero sequence unbalance on the source side or on the load side itself, providing a better balanced condition on the other side. Thus, balanced sources and loads can be relieved from adverse effects due to zero sequence unbalance on the other side. This is helpful for enhancing the life of 3 phase induction motors, transformers, etc. Also, it is expected to help in synchronising 3 phase inverters to the grid during unbalanced grid conditions and to avoid zero sequence circulating current during multiple DG interconnection without isolation transformer.

The conventionally connected power factor improving capacitors worsen the zero sequence unbalance, while the proposed MuCE device reduces it and supplies reactive power more fruitfully. In this proposed configuration, the usage of dedicated zig-zag transformers can be avoided and the already installed capacitor banks can be effectively utilized for the purpose. The device is capable of reducing harmonics in capacitor currents which is helpful for extending capacitor life. The electromagnetic solutions are popular for their low cost, ease of installation, and less requirement of maintenance.

# Chapter 6

# Conclusion

## 6.1 Conclusions

A reliable feeder model is required to study the impact of DG penetration in a low voltage distribution network. But the theoretical model cannot account for the imperfections in a feeder. Solutions utilising large data from smart meters and data loggers are not suitable for all DSOs. So a realistic feeder model using minimum data is proposed. Analysis was done with a theoretical model and the proposed realistic model, and the proposed model was validated using line loss information. The comparison of results from the two models shows significant variation. The theoretical model gives results far away from real values that may lead to wrong conclusions. The developed realistic model gives results near to actual performance and is helpful for deciding on DG interconnection requests.

The analysis using the realistic feeder model shows that the voltage drop is more towards the tail end of the feeder when there is no power generation from PV units. When the power generation from PV is higher than the connected load, a voltage rise occurs, indicating reverse power flow, and the voltage rise is also more prominent at the tail end of the feeder. So, consumers at the tail end of the feeder are most affected by the voltage drop and rise. This can be minimised by encouraging more DG integration near the feeder head. Moreover, if there is a load unbalance, even with balanced PV penetration, the voltage unbalance in the feeder increases. At all levels of PV penetration, the line loss is higher if the current unbalance in the feeder is higher. The line loss can be minimised by maintaining a better phase balancing of loads and keeping local generation equal to the connected load. So phase balancing is extremely important while allowing PV penetration.

A novel neutral line grounding procedure is recommended for a 3 phase, 4 wire distribution system operating in an unbalanced harmonic condition. Currently, available harmonics and unbalance reduction solutions demand installation of additional equipment with special strategies or regulated interconnection of low carbon technologies. Normally, the neutral current generated is suppressed or bypassed. It is

a novel idea to use the neutral current in line sections as a power quality enhancer to limit the propagation of disturbances. Furthermore, a novel attempt was made to investigate the role of neutral current in the proliferation of power quality issues, taking electromagnetic coupling of lines into account. The following are the positive outcomes of the test feeder analysis.

- Without any additional compensation scheme, voltage regulation is lowered to enhance the voltage profile along the feeder.
- Without coordinating the operation of EVs and PVs or limiting their active power, the voltage unbalance is reduced. Reconfiguration of the network and storage use is also avoided.
- Without any additional filter units or complex DG control, harmonic propagation towards the feeder head is significantly reduced, regardless of the harmonic order.
- As the majority of unbalance and harmonic current returns through the neutral line itself, the neutral-to-earth voltage is reduced and the problem due to ground current is minimised.
- The high loop impedance in the path of earth fault current helps to limit the magnitude of fault current, and to reduce the fault level of protection device required. Configuring the earth fault relay is easier, since the fault current can be easily differentiated.

In this aspect, the method is sustainable and promising as it achieves the benefits without the use of any additional equipment. According to the dynamic analysis, the approach is robust and is unaffected by stochastic load variations in the distribution system. The method is applicable to any 3 phase, 4 wire configuration having some degree of mutual coupling between phase and neutral lines. The only drawback noticed is a slight increase in line loss.

A new neutral line grounding practice is proposed for a 3 phase, 4 wire distribution system, operating in an unbalanced harmonic condition. The existing methods of harmonics and unbalance reduction involve the installation of additional equipment with specific strategies. Otherwise, regulated or coordinated interconnection of low carbon technologies is suggested. Conventionally, the neutral current produced is suppressed or bypassed. Utilizing the neutral current in the line sections as a power quality enhancer for restricting the propagation of disturbances is a novel idea. Furthermore, investigating the role of neutral current in the propagation of power quality issues considering electromagnetic coupling is a new attempt.

The proposed new custom power device is capable of compensating for the zero sequence unbalances from the source and load sides. MuCE, as a custom power device, can prevent zero sequence unbalance on the source and load side, resulting in a more balanced situation on the other side. Thus, balanced sources and loads can be spared from the negative impacts of zero sequence imbalance on the other side. This is beneficial for extending the life of 3 phase induction motors, transformers, and similar devices. Additionally, it can assist in synchronising 3 phase inverters to the grid during unbalanced grid situations and prevent zero sequence circulation current during multiple DG interconnection without isolation transformers.

Experimental results show that the conventionally connected power factor improving capacitors worsen the zero sequence unbalance, while the proposed MuCE reduces it and supplies reactive power in a better manner. In this proposed configuration, the usage of dedicated zig-zag transformers is avoided and the already installed capacitor banks can be effectively utilized for zero sequence compensation. The device can reduce neutral current and neutral voltage distortion. Additionally, the MuCE is capable of reducing high frequency harmonics in capacitor current, which helps in extending capacitor life.

## 6.2 Major contributions

The major contributions from the research work are:

- Proposed a parameter approximation method for the realistic modelling of a low voltage distribution feeder using minimum data. The proposed model can accommodate the imperfections present in the feeder. The proposed realistic model is useful for analysing the feeder performance for distribution system operators having no smart meters and data loggers installed. The findings and suggestions to reduce issues due to higher level DG interconnection are also presented.

- Proposed a sustainable solution to improve power quality in a 3 phase, 4 wire distribution feeder without installing any additional devices. In the novel neutral grounding strategy suggested, the neutral current itself is utilised as a power quality enhancer. Analysing the role of neutral current, emphasising the electromagnetic coupling between lines in the propagation of power quality disturbances, is a novel attempt. The method is robust against dynamic load variation.

- A new custom power device capable of mitigating zero sequence unbalance and

reducing neutral current is proposed. The device can reduce zero sequence unbalance due to source and load. The device is robust and low cost. It can deliver ancillary services like reactive power support, harmonic reduction, and adaptive power factor correction.

## 6.3 Scope of future work

The realistic feeder model proposed in this work to analyse the impact of DG interconnection requires only minimum measured data. As an extension, the accuracy of the model can be enhanced by modelling each phase line and each line section separately. Application of parameter estimation methods can also be attempted during realistic feeder modelling.

In the proposed neutral grounding strategy for improving power quality, the neutral line is single or selectively grounded. As a further step, application of optimization techniques can be used to select the number and location of neutral grounding points. Unbalance, harmonics, line loss, and neutral-to-earth voltage are to be considered for optimising the number and location of neutral grounding points. The electromagnetic interference of the proposed system with communication cables is expected to be less compared to fully grounded neutral line system. This can also be investigated and compared for verification in future work.

The features of the novel custom power device proposed for zero sequence suppression are extendable to various other purposes. Reverse power flow, unsymmetrical faults, and loss of phase lines etc can be detected by analysing the voltage and current in the fourth compensator coil of the device. It can be further used for subsequent isolation of line sections. The ability of the device to limit unsymmetrical fault currents and to arrest transients by ampere turn balancing is under consideration. Extending the role of fourth winding to avoid resonance by varying inductance through flux regulation is another possibility that can be investigated. Devices having other configurations based on the same concept may be considered for increasing the lifespan of capacitor banks. Modification of the device for addressing the negative sequence components can also be considered as a future extension.

# Bibliography


[1] NEMA, MG, "Mg 1-2011 motors and generators," *NEMA Publishes*, 2011.

[2] P. Pillay and M. Manyage, "Definitions of voltage unbalance," *IEEE Power Engineering Review*, vol. 21, no. 5, pp. 50–51, 2001.

[3] J. Faiz, B. M. Ebrahimi, and M. Ghofrani, "Mixed derating of distribution transformers under unbalanced supply voltage and nonlinear load conditions using tsfem," *IEEE Transactions on Power Delivery*, vol. 25, no. 2, pp. 780–789, 2010.

[4] ANERT (Agency for new and renewable energy research and technology) Department of Power, Government of Kerala Thiruvananthapuram, Kerala – 695 033, "Technical specifications of on-grid solar pv power plants."

[5] K. Ma, L. Fang, and W. Kong, "Review of distribution network phase unbalance: Scale, causes, consequences, solutions, and future research directions," *CSEE Journal of Power and Energy systems*, vol. 6, no. 3, pp. 479–488, 2020.

[6] T. M. Gruzs, "A survey of neutral currents in three-phase computer power systems," *IEEE Transactions on Industry Applications*, vol. 26, no. 4, pp. 719–725, 1990.

[7] J. Spitaels, "Hazards of harmonics and neutral overloads," *Schneider Electric Data Center Science Center, White Paper*, vol. 26, p. 4, 2011.

[8] D. Sreenivasarao, P. Agarwal, and B. Das, "Neutral current compensation in three-phase, four-wire systems: A review," *Electric Power Systems Research*, vol. 86, pp. 170–180, 2012, https://doi.org/10.1016/j.epsr.2011.12.014.

[9] A. Negi, S. Surendhar, S. R. Kumar, and P. Raja, "Assessment and comparison of different neutral current compensation techniques in three-phase four-wire distribution system," in *2012 3rd IEEE International Symposium on Power Electronics for Distributed Generation Systems (PEDG)*. IEEE, 2012, pp. 423–430.

[10] W. H. Kersting, *Distribution system modeling and analysis*. CRC press, 2018.

[11] R. Ayyanar, A. Nagarajan, T. Overbye, and R. Bhana, "Distribution system analysis tools for studying high penetration of PV with grid support features," *Arizona State University, Tech. Rep*, 2013.

[12] T. A. Short, *Electric power distribution equipment and systems.* CRC press, 2018.

[13] M. Nick, R. Cherkaoui, and M. Paolone, "Optimal allocation of dispersed energy storage systems in active distribution networks for energy balance and grid support," *IEEE Transactions on Power Systems*, vol. 29, no. 5, pp. 2300–2310, 2014.

[14] A. Sharma, A. Kapoor, and S. Chakrabarti, "Impact of plug-in electric vehicles on power distribution system of major cities of india: A case study," 2019.

[15] J. Romero Agüero, "Improving the efficiency of power distribution systems through technical and non-technical losses reduction," in *PES T D 2012*, 2012, pp. 1–8.

[16] H. Markiewicz and A. Klajn, "Voltage disturbances standard EN 50160-voltage characteristics in public distribution systems," *Wroclaw University of Technology*, vol. 21, pp. 215–224, 2004.

[17] A. Broshi, "Monitoring power quality beyond EN 50160 and IEC 61000-4-30," in *2007 9th International Conference on Electrical Power Quality and Utilisation*, 2007, pp. 1–6.

[18] L.-M. Jiang, J.-X. Meng, Z.-D. Yin, Y.-X. Dong, and J. Zhang, "Research on additional loss of line and transformer in low voltage distribution network under the disturbance of power quality," in *2018 International Conference on Advanced Mechatronic Systems (ICAMechS)*, 2018, pp. 364–369.

[19] T. Degner, G. Arnold, T. Reimann, B. Engel, M. Breede, and P. Strauss, "Increasing the photovoltaic-system hosting capacity of low voltage distribution networks," in *Proceedings of 21st International Conference on Electricity Distribution*, 2011, pp. 1243–1246.

[20] H. Arghavani and M. Peyravi, "Unbalanced current-based tariff," *CIRED-Open Access Proceedings Journal*, vol. 2017, no. 1, pp. 883–887, 2017.

[21] E. Bentley, P. Suwanapingkarl, S. Weerasinghe, T. Jiang, G. Putrus, and D. Johnston, "The interactive effects of multiple EV chargers within a distribution network," in *2010 IEEE Vehicle Power and Propulsion Conference*. IEEE, 2010, pp. 1–6.

[22] T.-H. Chen, C. Yang, T. Hsieh, and S. Chen, "Case studies of the impact of voltage imbalance on power distribution systems and equipment," in *WSEAS International Conference. Proceedings. Mathematics and Computers in Science and Engineering*, no. 8, 2009.

[23] A. Njafi, I. Iskender, and N. Genc, "Evaluating and derating of three-phase distribution transformer under unbalanced voltage and unbalance load using finite element method," in *2014 IEEE 8th international power engineering and optimization conference (PEOCO2014)*. IEEE, 2014, pp. 160–165.

[24] M. Bollen, "Definitions of voltage unbalance," *IEEE Power Engineering Review*, vol. 22, no. 11, pp. 49–50, 2002.

[25] T.-H. Chen, C.-H. Yang, and N.-C. Yang, "Examination of the definitions of voltage unbalance," *International Journal of Electrical Power & Energy Systems*, vol. 49, pp. 380–385, 2013.

[26] I. P. E. Society, "Ieee standard test procedure for polyphase induction motors and generators." IEEE Power Engineering Society Piscataway, NJ, USA, 2004.

[27] "IEEE recommended practice for monitoring electric power quality," *IEEE Std 1159-2019 (Revision of IEEE Std 1159-2009)*, pp. 1–98, 2019.

[28] A. B. Baggini *et al.*, *Handbook of power quality*. Wiley Online Library, 2008.

[29] R. Arthur and R. Shanahan, "Neutral currents in three phase wye systems," vol. 16, 1996.

[30] H.-L. Jou, J.-C. Wu, K.-D. Wu, W.-J. Chiang, and Y.-H. Chen, "Analysis of zig-zag transformer applying in the three-phase four-wire distribution power system," *IEEE transactions on power delivery*, vol. 20, no. 2, pp. 1168–1173, 2005.

[31] Q. Song, Z. Yin, J. Xue, and L. Zhou, "Zero-sequence harmonics current minimization using zero-blocking reactor and zig-zag transformer." IEEE, 2008, pp. 1758–1764.

[32] R. Cutri and L. M. Junior, "A generalized instantaneous method for harmonics, positive and negative sequence detection/extraction," in *2007 IEEE Power Electronics Specialists Conference*. IEEE, 2007, pp. 2294–2297.

[33] V. Ramachandran, *Modeling of utility distribution feeder in OpenDSS with steady state impact analysis of distributed generation.* West Virginia University, 2011.

[34] W. Kersting, "A method to teach the design and operation of a distribution system," no. 7. IEEE, 1984, pp. 1945–1952.

[35] W. Kersting and W. Phillips, "Modeling and analysis of rural electric distribution feeders," *IEEE Transactions on Industry Applications*, vol. 28, no. 4.

[36] W. H. Kersting and W. H. Phillips, "Distribution feeder line models," in *Proceedings of 1994 IEEE Rural Electric Power Conference.* IEEE, 1994, pp. A4–1.

[37] W. Kersting and R. Green, "The application of Carson's equation to the steady-state analysis of distribution feeders," in *2011 IEEE/PES Power Systems Conference and Exposition.* IEEE, 2011, pp. 1–6.

[38] H. Keshtkar, S. K. Solanki, and J. M. Solanki, "Improving the accuracy of impedance calculation for distribution power system," *IEEE transactions on power delivery*, vol. 29, no. 2, pp. 570–579, 2013.

[39] J. R. Carson, "Wave propagation in overhead wires with ground return," *The Bell System Technical Journal*, vol. 5, no. 4, pp. 539–554, 1926.

[40] R. Olsen and T. Pankaskie, "On the exact, Carson and image theories for wires at or above the earth's interface," *IEEE Transactions on Power Apparatus and Systems*, no. 4, pp. 769–778, 1983.

[41] D. Woodhouse, "On the theoretical basis of Carson's equations," in *2012 IEEE International Conference on Power System Technology (POWERCON).* IEEE, 2012, pp. 1–6.

[42] K. Miu and M. Kleinberg, "Impact studies of unbalanced multi-phase distribution system component models," in *IEEE PES General Meeting.* IEEE, 2010, pp. 1–4.

[43] M. Z. Kamh and R. Iravani, "Unbalanced model and power-flow analysis of microgrids and active distribution systems," *IEEE Transactions on Power Delivery*, vol. 25, no. 4, pp. 2851–2858, 2010.

[44] B. Das, "Estimation of parameters of a three-phase distribution feeder," *IEEE transactions on power delivery*, vol. 26, no. 4, pp. 2267–2276, 2011.

[45] M. Stifter, B. Bletterie, D. Burnier, H. Brunner, and A. Abart, "Analysis environment for low voltage networks," in *2011 IEEE First International Workshop on Smart Grid Modeling and Simulation (SGMS)*. IEEE, 2011, pp. 61–66.

[46] H. Ravindra, M. O. Faruque, K. Schoder, R. Meeker, M. Steurer, and P. McLaren, "Modeling and validation of a utility feeder for study of voltage regulation in the presence of high PV penetration," in *2014 IEEE PES T&D Conference and Exposition*. IEEE, 2014, pp. 1–5.

[47] M. Baggu, R. Ayyanar, and D. Narang, "Feeder model validation and simulation for high-penetration photovoltaic deployment in the Arizona public service system," in *2014 IEEE 40th Photovoltaic Specialist Conference (PVSC)*. IEEE, 2014, pp. 2088–2093.

[48] A. Koirala, R. D'hulst, and D. Van Hertem, "Impedance modelling for European style distribution feeder," in *2019 International Conference on Smart Energy Systems and Technologies (SEST)*. IEEE, 2019, pp. 1–6.

[49] F. Dorfler and F. Bullo, "Kron reduction of graphs with applications to electrical networks," *Circuits and Systems I: Regular Papers, IEEE Transactions on*, vol. 60, no. 1, pp. 150–163, 2013.

[50] P. Radatz, N. Kagan, C. Rocha, J. Smith, and R. C. Dugan, "Assessing maximum DG penetration levels in a real distribution feeder by using OpenDSS," in *2016 17th International Conference on Harmonics and Quality of Power (ICHQP)*. IEEE, 2016, pp. 71–76.

[51] S. Heslop, I. MacGill, J. Fletcher, and S. Lewis, "Method for determining a PV generation limit on low voltage feeders for evenly distributed PV and load," *Energy Procedia*.

[52] B. Bletterie, S. Kadam, M. Stifter, A. Abart, D. B. de Castro, and H. Brunner, "Characterising LV networks on the basis of smart meter data and accurate network models," 2012.

[53] J. Giraldez, P. Gotseff, A. Nagarajan, R. Ueda, J. Shindo, and S. Suryanarayanan, "Distribution feeder modeling for time-series simulation of voltage management strategies," in *2018 IEEE/PES Transmission and Distribution Conference and Exposition (T&D)*. IEEE, 2018, pp. 1–5.

[54] M. R. Islam, H. Lu, M. Hossain, and L. Li, "Mitigating unbalance using distributed network reconfiguration techniques in distributed power generation

grids with services for electric vehicles: A review," *Journal of Cleaner Production*, vol. 239, 2019, https://doi.org/10.1016/j.jclepro.2019.117932.

[55] M. U. Hashmi, J. Horta, L. Pereira, Z. Lee, A. Bušić, and D. Kofman, "Towards phase balancing using energy storage," *arXiv preprint arXiv:2002.04177*, 2020.

[56] C. Liao and B. Yang, "Phases-controlled coordinated charging method for electric vehicles," *CES Transactions on Electrical Machines and Systems*, vol. 2, no. 1, pp. 3–12, 2018, https://doi.org/10.23919/TEMS.2018.8326447.

[57] M. R. Kikhavani, A. Hajizadeh, and A. Shahirinia, "Charging coordination and load balancing of plug-in electric vehicles in unbalanced low-voltage distribution systems," *IET Generation, Transmission & Distribution*, vol. 14, no. 3, pp. 389–399, 2019, https://doi.org/10.1049/iet-gtd.2019.0397.

[58] S. Das, D. Chatterjee, and S. K. Goswami, "A reactive power compensation scheme for unbalanced four-wire system using virtual Y-TCR model," *IEEE Transactions on Industrial Electronics*, vol. 65, no. 4, pp. 3210–3219, 2018, https://doi.org/10.1109/TIE.2017.2758720.

[59] N. Gupta, A. Swarnkar, and K. Niazi, "A novel method for simultaneous phase balancing and mitigation of neutral current harmonics in secondary distribution systems," *International Journal of Electrical Power & Energy Systems*, vol. 55, pp. 645–656, 2014.

[60] F. H. M. Rafi, M. Hossain, M. S. Rahman, and S. Taghizadeh, "An overview of unbalance compensation techniques using power electronic converters for active distribution systems with renewable generation," *Renewable and Sustainable Energy Reviews*, vol. 125, 2020, https://doi.org/10.1016/j.rser.2020.109812.

[61] L. Motta and N. Faúndes, "Active/passive harmonic filters: Applications, challenges & trends," ser. 2016 17th International Conference on Harmonics and Quality of Power (ICHQP), Belo Horizonte, Brazil, October 16–19 ,2016.

[62] X. Sun, R. Han, H. Shen, B. Wang, Z. Lu, and Z. Chen, "A double-resistive active power filter system to attenuate harmonic voltages of a radial power distribution feeder," *IEEE Transactions on Power Electronics*, vol. 3, no. 9, pp. 6203–6216, 2015, https://doi.org/10.1109/TPEL.2015.2500913.

[63] N. Pogaku and T. Green, "Harmonic mitigation throughout a distribution system: A distributed-generator-based solution," *IEE Proceedings-Generation, Transmission and Distribution*, vol. 153, no. 3, pp. 350–358, 2006.

[64] H. Yoshida and K. Wada, "Third-harmonic current suppression for power distribution systems under unbalanced installation of DG units," *IEEE Transactions on Industrial Electronics*, vol. 62, no. 9, pp. 5578–5585, 2015, https://doi.org/10.1109/TIE.2015.2415766.

[65] H. R. Baghaee, M. Mirsalim, G. B. Gharehpetian, and H. A. Talebi, "Unbalanced harmonic power sharing and voltage compensation of microgrids using radial basis function neural network-based harmonic power-flow calculations for distributed and decentralised control structures," *IET Generation, Transmission & Distribution*, vol. 12, no. 7, pp. 1518–1530, 2017, https://doi.org/10.1049/iet-gtd.2016.1277.

[66] M. Jedari, S. H. Fathi, and S. S. Dobakhshari, "An investigation on harmonics compensation under highly unbalanced non-linear loads in 3p4w distribution network for PV application," ser. IECON 2017-43rd Annual Conference of the IEEE Industrial Electronics Society, Beijing, China, October 29–November 1, 2017.

[67] J. Zeng, Z. Huang, Y. Ling, L. Yang, Z. Li, G. Qiu, B. Yang, and T. Yu, "Analysis and hardware implementation of virtual resistance based PV inverters for harmonics suppression," *IET Generation, Transmission & Distribution*, vol. 13, no. 20, pp. 4592–4603, 2019, https://doi.org/10.1049/iet-gtd.2019.0314.

[68] T. Fukami, T. Onchi, N. Naoe, and R. Hanaoka, "Compensation for neutral current harmonics in a three-phase four-wire system by a synchronous machine," *IEEE Transactions on Industry Applications*, vol. 38, no. 5, pp. 1232–1236, 2002.

[69] A. Sabir and M. Javaid, "Minimizing neutral currents in distribution microgrids using smart loads," *International Journal of Electrical Power & Energy Systems*, vol. 113, pp. 436–448, 2019, https://doi.org/10.1016/j.ijepes.2019.05.058.

[70] B. Singh, P. Jayaprakash, and D. Kothari, "Magnetics for neutral current compensation in three-phase four-wire distribution system," ser. 2010 Joint International Conference on Power Electronics, Drives and Energy Systems & 2010 Power India, New Delhi, India, December 20-23,2010.

[71] D. Sreenivasarao, P. Agarwal, and B. Das, "A T-connected transformer based hybrid D-STATCOM for three-phase, four-wire systems," *International Journal of Electrical Power & Energy Systems*, vol. 44, no. 1, pp. 964–970, 2013, https://doi.org/10.1016/j.ijepes.2012.08.019.

[72] S. C. L. Freitas, L. C. O. de Oliveira, P. da Silva Oliveira, B. Exposto, J. G. Oliveira Pinto, and J. L. Afonso, "Modeling, design, and experimental test of a zero-sequence current electromagnetic suppressor," *International Transactions on Electrical Energy Systems*, vol. 30, p. e12222, 2020, https://doi.org/10.1002/2050-7038.12222.

[73] B. Bletterie, S. Kadam, A. Zegers, and Z. Miletic, "On the effectiveness of voltage control with PV inverters in unbalanced low voltage networks," in *Proc. Int. Conf. CIRED*, 2015, pp. 1–55.

[74] Y. Zhou and H. Nian, "Zero-sequence current suppression strategy of open-winding PMSG system with common DC bus based on zero vector redistribution," *IEEE Transactions on industrial Electronics*, vol. 62, no. 6, pp. 3399–3408, 2014.

[75] W. Hu, C. Ruan, H. Nian, and D. Sun, "Zero-sequence current suppression strategy with common-mode voltage control for open-end winding PMSM drives with common DC bus," *IEEE Transactions on Industrial Electronics*, vol. 68, no. 6, pp. 4691–4702, 2020.

[76] B. V. Reddy and V. Somasekhar, "An SVPWM scheme for the suppression of zero-sequence current in a four-level open-end winding induction motor drive with nested rectifier-inverter," *IEEE Transactions on Industrial Electronics*, vol. 63, no. 5, pp. 2803–2812, 2015.

[77] X. Zhang and K. Wang, "Current prediction based zero sequence current suppression strategy for the semicontrolled open-winding PMSM generation system with a common DC bus," *IEEE Transactions on Industrial Electronics*, vol. 65, no. 8, pp. 6066–6076, 2017.

[78] X. Yuan, S. Zhang, C. Zhang, M. Degano, G. Buticchi, and A. Galassini, "Improved finite-state model predictive current control with zero-sequence current suppression for OEW-SPMSM drives," *IEEE Transactions on Power Electronics*, vol. 35, no. 5, pp. 4996–5006, 2019.

[79] Y. Luo, T. Xu, F. Meng, J. You, and X. Duan, "The research on the zero sequence circulating current suppression in parallel inverters." IEEE, 2012, pp. 1–5.

[80] R. Zhu, M. Liserre, Z. Chen, and X. Wu, "Zero-sequence voltage modulation strategy for multiparallel converters circulating current suppression," *IEEE Transactions on Industrial Electronics*, vol. 64, no. 3, pp. 1841–1852, 2016.

[81] W. Jiang, W. Ma, J. Wang, W. Wang, X. Zhang, and L. Wang, "Suppression of zero sequence circulating current for parallel three-phase grid-connected converters using hybrid modulation strategy," *IEEE Transactions on Industrial Electronics*, vol. 65, no. 4, pp. 3017–3026, 2017.

[82] Z. Liang, X. Lin, X. Qiao, Y. Kang, and B. Gao, "A coordinated strategy providing zero-sequence circulating current suppression and neutral-point potential balancing in two parallel three-level converters," *IEEE Journal of Emerging and Selected Topics in Power Electronics*, vol. 6, no. 1, pp. 363–376, 2017.

[83] P. P. Khera, "Application of zigzag transformers for reducing harmonics in the neutral conductor of low voltage distribution system," in *Conference Record of the 1990 IEEE Industry Applications Society Annual Meeting.* IEEE, 1990, pp. 1092–vol.

[84] S. R. Kumar, S. Surendhar, A. Negi, and P. Raja, "Zig zag transformer performance analysis on harmonic reduction in distribution load," in *International Conference on Electrical, Control and Computer Engineering 2011 (InECCE).* IEEE, 2011, pp. 107–112.

[85] S. De Freitas, L. De Oliveira, and J. De Souza, "Experimental analysis of an electromagnetic zero-sequence suppressor," in *PES T&D 2012.* IEEE, 2012, pp. 1–6.

[86] L. C. O. da Oliveira, R. N. da Oliveira, J. B. da Souza, and S. C. da Freitas, "Electromagnetic zero-sequence harmonics blocker: modeling and experimental analysis," *Journal of Energy and Power Engineering*, vol. 8, no. 8, 2014.

[87] H.-L. Jou, K.-D. Wu, J.-C. Wu, and W.-J. Chiang, "A three-phase four-wire power filter comprising a three-phase three-wire active power filter and a zig-zag transformer," *IEEE Transactions on Power Electronics*, vol. 23, no. 1, pp. 252–259, 2008.

[88] B. Singh, P. Jayaprakash, T. Somayajulu, and D. Kothari, "Reduced rating VSC with a zig-zag transformer for current compensation in a three-phase four-wire distribution system," *IEEE Transactions on Power Delivery*, vol. 24, no. 1, pp. 249–259, 2008.

[89] S. Choi and M. Jang, "Analysis and control of a single-phase-inverter–zigzag-transformer hybrid neutral-current suppressor in three-phase four-wire systems," *IEEE Transactions on Industrial Electronics*, vol. 54, no. 4, pp. 2201–2208, 2007.

[90] B. Singh, P. Jayaprakash, T. Somayajulu, D. Kothari, A. Chandra *et al.*, "Integrated three-leg VSC with a zig-zag transformer based three-phase four-wire DSTATCOM for power quality improvement." IEEE, 2008, pp. 796–801.

[91] R. C. Dugan, "Reference guide: The open distribution system simulator (OpenDSS)," *Electric Power Research Institute, Inc*, vol. 7, p. 29, 2012.

[92] F. Shahnia, R. Majumder, A. Ghosh, G. Ledwich, and F. Zare, "Voltage imbalance analysis in residential low voltage distribution networks with rooftop PVs," *Electric Power Systems Research*, vol. 81, no. 9, pp. 1805–1814, 2011.

[93] A. Canova, L. Giaccone, F. Spertino, and M. Tartaglia, "Electrical impact of photovoltaic plant in distributed network," *IEEE Transactions on industry applications*, vol. 45, no. 1, pp. 341–347, 2009.

[94] B. Bletterie, S. Kadam, R. Bolgaryn, and A. Zegers, "Voltage control with PV inverters in low voltage networks—in depth analysis of different concepts and parameterization criteria," *IEEE Transactions on Power Systems*, vol. 32, no. 1, pp. 177–185, 2016.

[95] A. T. Procopiou, C. Long, and L. F. Ochoa, "Voltage control in LV networks: An initial investigation," in *IEEE PES Innovative Smart Grid Technologies, Europe*, Oct 2014, pp. 1–6.

[96] A. P. Kenneth and K. Folly, "Voltage rise issue with high penetration of grid connected PV," *IFAC Proceedings Volumes*, vol. 47, no. 3, pp. 4959–4966, 2014.

[97] Kerala State Electricity Regulatory Commission, "Kerala electricity supply code, 2014," in *No.215/DD/TD(Rev)2014/KSERC*, 1 January 2014.

[98] A. Einfalt, F. Zeilinger, R. Schwalbe, B. Bletterie, and S. Kadam, "Controlling active low voltage distribution grids with minimum efforts on costs and engineering." IEEE, 2013, pp. 7456–7461.

[99] Y. Gong and A. Guzmán, "Integrated fault location system for power distribution feeders," *IEEE transactions on industry applications*, vol. 49, no. 3, pp. 1071–1078, 2013.

[100] W. Kersting and W. Phillips, "Modeling and analysis of rural electric distribution feeders," vol. 28, no. 4. IEEE, 1992, pp. 767–773.

[101] B. Bletterie, S. Kadam, M. Stifter, R. Pitz, and A. Abart, "Optimisation of LV networks with high photovoltaic penetration—balancing the grid with smart meters," *IEEE PowerTech 2013*, pp. 1–6, 2013.

[102] H. Lasso, C. Ascanio, and M. Guglia, "A model for calculating technical losses in the secondary energy distribution network," in *2006 IEEE/PES Transmission Distribution Conference and Exposition: Latin America*, 2006, pp. 1–6.

[103] R. C. Dugan, "The open distribution system simulator," in *Reference Guide, OpenDSS*. Electric Power Research Institute, 2013.

[104] W.H.Kersting, "A Method to Teach the Design and Operation of a Distribution System," vol. PAS-103, no. 7, July 1984, pp. 1945–1952.

[105] J. R. Carson, "Wave propagation in overhead wires with ground return," *Bell system technical journal*, vol. 5, no. 4, pp. 539–554, 1926.

[106] Bureau of Energy Efficiency, Government of India, Ministry of Power and Energy Management Centre-Kerala, "Identification of technical loss reduction and rationalization of secondary distribution system at selected typical three distribution transformers of kerala state electricity board," in *http:www.keralaenergy.gov.in*.

[107] W. H. Kersting, "Radial distribution test feeders," *IEEE Transactions on Power Systems*, vol. 6, no. 3, pp. 975–985, 1991.

[108] O. L. F. Petrou Kyriacos, Quiros-Tortos Jairo, "Controlling electric vehicle charging points for congestion management of UK LV networks," ser. IEEE Power and Energy Society Innovative Smart Grid Technologies Conference (ISGT), Washington, DC, February 18–20, 2015.

[109] F. Shahnia, R. Majumder, A. Ghosh, G. Ledwich, and F. Zare, "Voltage imbalance analysis in residential low voltage distribution networks with rooftop PVs," *Electric Power Systems Research*, vol. 81, no. 9, pp. 1805–1814, 2011.

[110] O. Ceylan, S. Paudyal, S. Dahal, and N. R. Karki, "Assessment of harmonic distortion on distribution feeders with electric vehicles and residential PVs," ser. 2017 7th International Conference on Power Systems (ICPS), Pune, India, December 21–23, 2017.

[111] M. A. H. Rafi, Y. Sun, and J. Bauman, "Impact of background voltage harmonic mitigation techniques on coupled frequencies in VSC-based EV fast charging,"

ser. 2019 IEEE Transportation Electrification Conference and Expo (ITEC), Detroit, MI, USA, June 19–21, 2019.

[112] L. Kutt, E. Saarijarvi, M. Lehtonen, H. Molder, and J. Niitsoo, "A review of the harmonic and unbalance effects in electrical distribution networks due to EV charging," ser. 12th International Conference on Environment and Electrical Engineering, Wroclaw, Poland, May 5–8, 2013.

[113] L. d. A. Bitencourt, B. S. Borba, B. H. Dias, R. S. Maciel, D. H. Dias, and L. W. Oliveira, "Electric vehicles charging optimization to improve the insertion considering the brazilian regulatory framework," *Energy Storage*, vol. 1, no. 4, pp. 1–13, 2019.

[114] O. Gul and M. Bayrak, "Power quality and neutral current problems from unbalanced and nonlinear loads in three phase power systems," ser. 15th International Conference on Electricity Distribution, France, 1999, pp. 1 – 4.

[115] G. Eduful and K. J. Atanga, "Analysis of high neutral currents and harmonic impacts on losses and capacities of distribution transformers," ser. Proceedings of the World Congress on Engineering, vol. 1, 29 June–1 July,2016.

[116] T. Klayklueng and S. Dechanupaprittha, "Impact analysis on voltage unbalance of EVs charging on a low voltage distribution system," ser. International Electrical Engineering Congress (iEECON), Chonburi, Thailand, March 19-21,2014.

[117] W. Kersting and W. Phillips, "Distribution feeder line models," *IEEE Transactions on Industry Applications*, vol. 31, no. 4, pp. 715–720, 1995, http://ieeexplore.ieee.org/document/395276.

[118] W. Kersting, "Using the IEEE comprehensive test feeder," ser. 2011 Rural Electric Power Conference, Chattanooga, TN, USA, April 10–13, 2011.

[119] "IEEE recommended practice for grounding of industrial and commercial power systems," *IEEE Std 142-2007 (Revision of IEEE Std 142-1991)*, 2007.

[120] A. Bonner, T. Grebe, E. Gunther, L. Hopkins, M. Marz, J. Mahseredjian, N. Miller, T. Ortmeyer, V. Rajagopalan, S. Ranade *et al.*, "Modeling and simulation of the propagation of harmonics in electric power networks. 1. concepts, models, and simulation techniques," *IEEE Power Engineering Review*, vol. 16, no. 1, pp. 452–465, 1996, https://doi.org/10.1109/61.484130.

[121] S. H. Hashemi, M. H. Ashouian, H. Pirpiran, and R. Karami, "Impact of distributed generation on unbalanced distribution networks," *IET Conference Publications*, 2013, https://doi.org/10.1049/cp.2013.1039.

[122] B. A. Schneider, Mather KP, B. C. Pal, C. W. Ten, G. J. Shirek, H. Zhu, J. C. Fuller, J. L. R. Pereira, L. F. Ochoa, L. R. De Araujo, R. C. Dugan, S. Matthias, S. Paudyal, T. E. McDermott, and W. Kersting, "Analytic considerations and design basis for the IEEE distribution test feeders," *IEEE Transactions on Power Systems*, vol. 33, no. 3, pp. 3181–3188, 2017.

[123] J. Balda, A. Oliva, D. McNabb, and R. Richardson, "Measurements of neutral currents and voltages on a distribution feeder," *IEEE Transactions on Power Delivery*, vol. 12, no. 4, pp. 1799–1804, 1997.

[124] W. Kersting, "A three-phase unbalanced line model with grounded neutrals through a resistance," ser. 2008 IEEE Power and Energy Society General Meeting-Conversion and Delivery of Electrical Energy in the 21st Century, Pittsburgh, PA, USA.

[125] D. W. Zipse, "The hazardous multigrounded neutral distribution system and dangerous stray currents," ser. IEEE Industry Applications Society 50th Annual Petroleum and Chemical Industry Conference, Houston, TX, USA, September 15-17, 2003, https://doi.org/10.1109/PCICON.2003.1242596.

[126] A. Deri, G. Tevan, A. Semlyen, and A. Castanheira, "The complex ground return plane a simplified model for homogeneous and multi-layer earth return," *IEEE Transactions on Power Apparatus and Systems*, no. 8, pp. 3686–3693, 1981.

[127] S. Das, S. Santoso, R. Horton, and A. Gaikwad, "Effect of earth current return model on transmission line fault location-a case study," in *2013 IEEE Power & Energy Society General Meeting*. IEEE, 2013, pp. 1–5.

[128] M. Mitolo, "Of electrical distribution systems with multiple grounded neutrals," *IEEE Transactions on Industry Applications*, vol. 46, no. 4, pp. 1541–1546, 2010.

[129] D. Sreenivasarao, P. Agarwal, and B. Das, "Neutral current compensation in three-phase, four-wire systems: A review," *Electric Power Systems Research*, vol. 86, pp. 170–180, 2012.

[130] O. U. Omeje, A. S. Alayande, T. O. Akinbulire, F. N. Okafor, and J. I. Ebelechi, "Propagation of current and voltage unbalance in electrical power networks," in *2019 IEEE PES/IAS PowerAfrica*. IEEE, 2019, pp. 493–498.

[131] S. Inoue, T. Shimizu, and K. Wada, "Control methods and compensation characteristics of a series active filter for a neutral conductor," *IEEE Transactions on Industrial Electronics*, vol. 54, no. 1, pp. 433–440, 2007.

[132] R. F. Buzo, L. C. O. de Oliveira, and F. B. Leão, "A method for dimensioning and designing the zero-sequence electromagnetic blocker considering system unbalance factor," *IEEE Transactions on Power Delivery*, vol. 35, no. 4, pp. 2089–2096, 2019.

[133] C. L. Fortescue, "Method of symmetrical co-ordinates applied to the solution of polyphase networks," *Transactions of the American Institute of Electrical Engineers*, vol. 37, no. 2, pp. 1027–1140, 1918.

[134] "IEEE recommended practice for monitoring electric power quality," *IEEE Std 1159-2019 (Revision of IEEE Std 1159-2009)*, pp. 1–98, 2019.

[135] A. Hobson, "The zero-flux current transformer [includes discussion]," *Transactions of the American Institute of Electrical Engineers. Part III: Power Apparatus and Systems*, vol. 72, no. 4, pp. 608–615, 1953.

[136] M. Shwedhi and M. Sultan, "Power factor correction capacitors; essentials and cautions," in *2000 Power Engineering Society Summer Meeting (Cat. No. 00CH37134)*, vol. 3. IEEE, 2000, pp. 1317–1322.

[137] T. M. Blooming and D. J. Carnovale, "Application of IEEE std 519-1992 harmonic limits." IEEE, 2006, pp. 1–9.

[138] P. Roncero-Sánchez and E. Acha, "Harmonic and imbalance voltage mitigation in smart grids: A DSTATCOM based solution," in *IEEE EUROCON 2015-International Conference on Computer as a Tool (EUROCON)*. IEEE, 2015, pp. 1–6.

[139] A. Banerji, S. K. Biswas, and B. Singh, "DSTATCOM control algorithms: a review," *International Journal of Power Electronics and Drive Systems*, vol. 2, no. 3, p. 285, 2012.

# List of Publications

## Referred Journals:

[**1**] "Power quality improvement utilizing neutral current in distribution systems," ***International Transactions on Electrical Energy Systems***, 2020 Nov, 18:e12703.DOI: 10.1002/2050-7038.12703 Online ISSN:2050-7038. © John Wiley & Sons Ltd.

[**2**] "Patent publication for Mutual Compensator Extractor," ***https://ipindia.gov.in/journal-patents.htm Part-1.pdf***, Published on 19/02/2021 , Page No.91.

[**3**] "A custom power device for zero sequence reduction and reactive power compensation," ***IEEE Transactions on Power Delivery***, manuscript ID: PESL-00117-2021. (Communicated)

## International Conferences:

[**1**] "More realistic Approximate LV Feeder model for quick decision on PV interconnection requests," ***IEEE PEDES 2016, IEEE International conference on power electronics, drives and energy systems***, Trivandrum, India, December 2016, 14–17.

[**2**] "Modeling of Power Distribution Feeder and Analysis of Small PV Plant Penetration in Kerala Low Voltage Distribution System," ***ICUE 2016, International Conference on Cogeneration, Small Power Plants and District Energy, BITEC***, Bang–Na, Thailand, September 2016, 14–16.

## Patents:

[**1**] "Patent application for Mutual Compensator Extractor," (Application referred u/s 12 for examination.) ***Patent Application Number–202041007106***, Date of filing 19/02/2020.

# Appendix A

**Carson's equations for computing self and mutual impedances of overhead conductors considering presence of earth** [10]

Self Impedance of Conductor i:

$$\hat{Z_{ii}} = \quad r_i + 4\omega P_{ii} G + j\left(X_i + 2\omega G \cdot ln\frac{S_{ii}}{RD_i} + 4\omega Q_{ii} G\right) \Omega/mile \tag{A.1}$$

Mutual Impedance between Conductor i and j:

$$\hat{Z_{ij}} = \quad 4\omega P_{ij} G + j\left(2\omega G \cdot ln\frac{S_{ij}}{D_{ij}} + 4\omega Q_{ij} G\right) \Omega/mile \tag{A.2}$$

where

$\hat{Z_{ii}}$ = self impedance of conductor i in $\Omega/mile$

$\hat{Z_{ij}}$ = mutual impedance between conductors i and j in $\Omega/mile$

$r_i$ = resistance of conductor i in $\Omega/mile$

$\omega = 2\Pi f$ = system angular frequency in radians per second

$G = 0.1609344 \times 10^{-3}\ \Omega/mile$

$RD_i$ = radius of conductor i in feet

$GMR_i$ = Geometric Mean Radius of conductor i in feet

$f$ = system frequency in Hertz

$\rho$ = resistivity of earth in Ω-meters

$D_{ij}$ = distance between conductors i and j in feet

$S_{ij}$ = distance between conductors i and image j in feet

$\theta_{ij}$ = angle between a pair of lines drawn from conductor i to its own image and to the image of conductor j

$$X_i = \quad 2\omega G \cdot ln\frac{RD_i}{GMR_i} \Omega/mile \tag{A.3}$$

$$P_{ij} = \quad \frac{\Pi}{8} - \frac{1}{3\sqrt{2}} k_{ij} cos(\theta_{ij}) + \frac{k_{ij}^2}{16} cos(2\theta_{ij}) \cdot \left(0.6728 + ln\frac{2}{k_{ij}}\right) \tag{A.4}$$

$$Q_{ij} = \quad -0.0386 + \frac{1}{2} \cdot ln\frac{2}{k_{ij}} + \frac{1}{3\sqrt{2}} k_{ij} cos(\theta_{ij}) \tag{A.5}$$

$$k_{ij} = \ 8.565 \times 10^{-4} \cdot S_{ij} \cdot \sqrt{\frac{f}{\rho}} \tag{A.6}$$

**Modified Carson's Equations**

Only two approximations are made in deriving the modified Carson's equations. These approximations involve the terms associated with $P_{ij}$ and $Q_{ij}$ by using only the first term of the variable $P_{ij}$ and the first two terms of $Q_{ij}$.

$$P_{ij} = \ \frac{\Pi}{8} \tag{A.7}$$

$$Q_{ij} = \ -0.03860 + \frac{1}{2} ln \frac{2}{k_{ij}} \tag{A.8}$$

Substitute for $X_i$

$$\hat{Z_{ii}} = \ r_i + 4\omega P_{ii} G + j \left( 2\omega G \cdot ln \frac{RD_i}{GMR_i} + 2\omega G \cdot ln \frac{S_{ii}}{RD_i} + 4\omega Q_{ii} G \right) \tag{A.9}$$

Combine terms and simplify :

Series Impedance of Overhead and Underground Lines

Substitute in the values of Π and G :

The frequency and earth resistivity can be now assumed:

$f$ = Frequency = 50 or 60 Hertz

$\rho$ = Earth resistivity = 100 Ohm-meter

# Appendix B

## Field measurement data

Sample of field measurement data collected for realistic feeder modelling of low voltage feeder at Kerala State Housing Board, Thiruvananthapuram

Time: 11.00 am

| Phase | a | b | c |
|---|---|---|---|
| Feeder head current (A) | 126 | 110 | 98 |
| Feeder head voltage (V) | 232 | 233 | 234 |
| Feeder tail voltage (V) | 206 | 208 | 211 |

Time: 01.00 pm

| Phase | a | b | c |
|---|---|---|---|
| Feeder head current (A) | 56 | 52 | 48 |
| Feeder head voltage (V) | 232 | 232 | 229 |
| Feeder tail voltage (V) | 226 | 227 | 221 |

Time: 04.00 pm

| Phase | a | b | c |
|---|---|---|---|
| Feeder head current (A) | 64 | 63 | 52 |
| Feeder head voltage (V) | 234 | 236 | 232 |
| Feeder tail voltage (V) | 232 | 230 | 228 |

Time: 06.00 pm

| Phase | a | b | c |
|---|---|---|---|
| Feeder head current (A) | 96 | 82 | 108 |
| Feeder head voltage (V) | 235 | 234 | 233 |
| Feeder tail voltage (V) | 212 | 215 | 209 |

# Appendix C

## Intermediate results of Fully Grounded Neutral(FGN) System and Single Grounded Neutral(SGN) Systems

Sample currents and voltages in a line section for Fully Grounded Neutral(FGN) System and Single Grounded Neutral(SGN) Systems

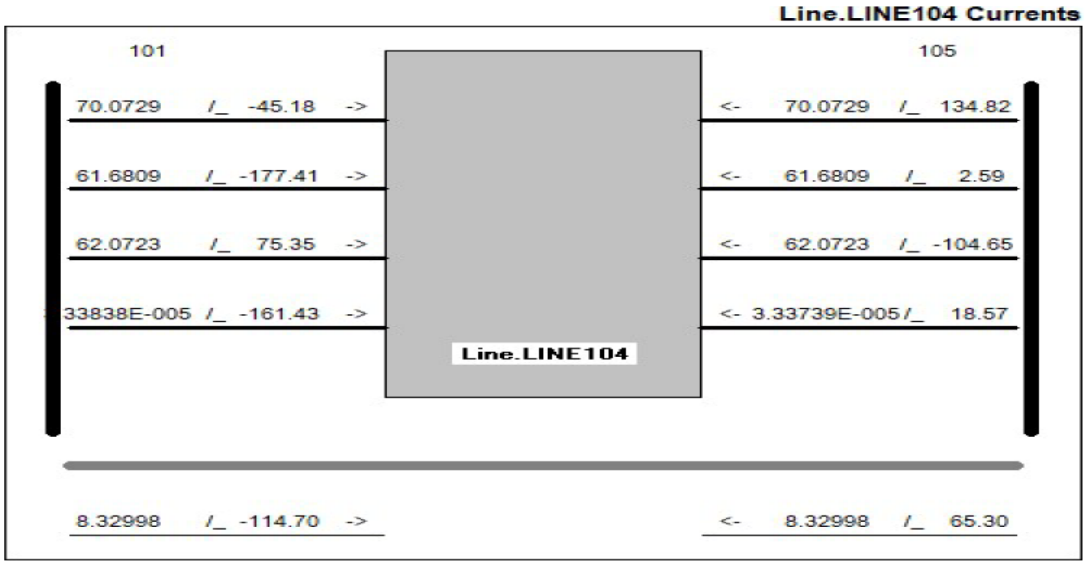


**Figure 6.1:** Currents through a FGN line section

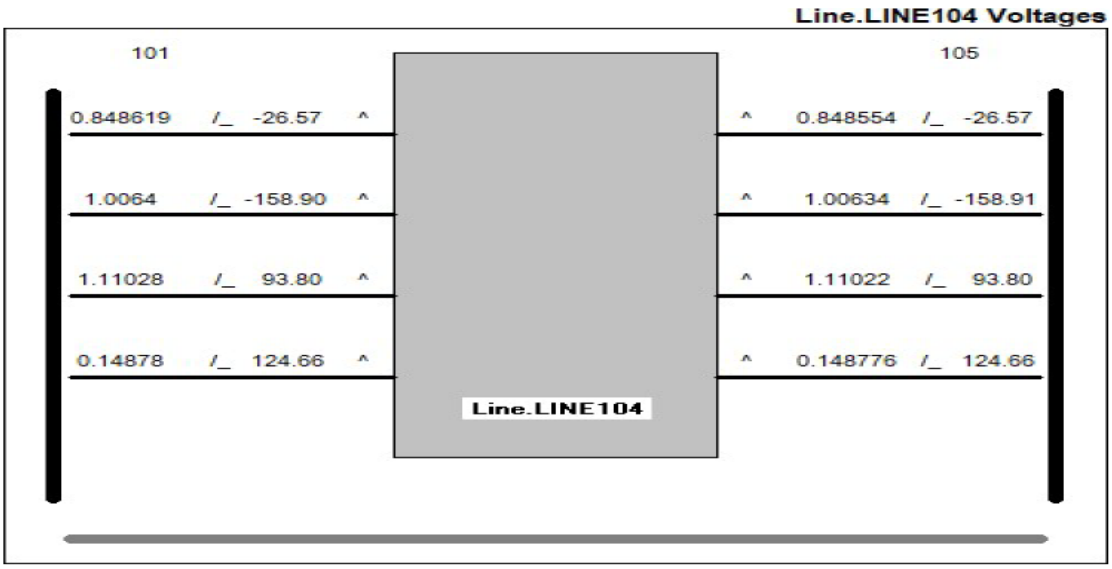


**Figure 6.2:** Voltages in a FGN line section

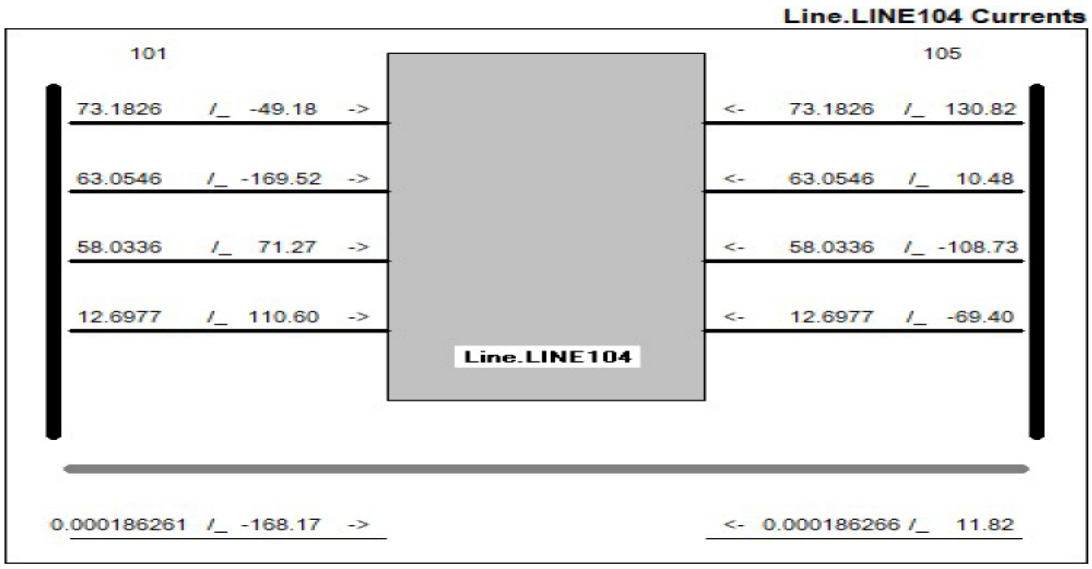


**Figure 6.3:** Currents through a SGN line section

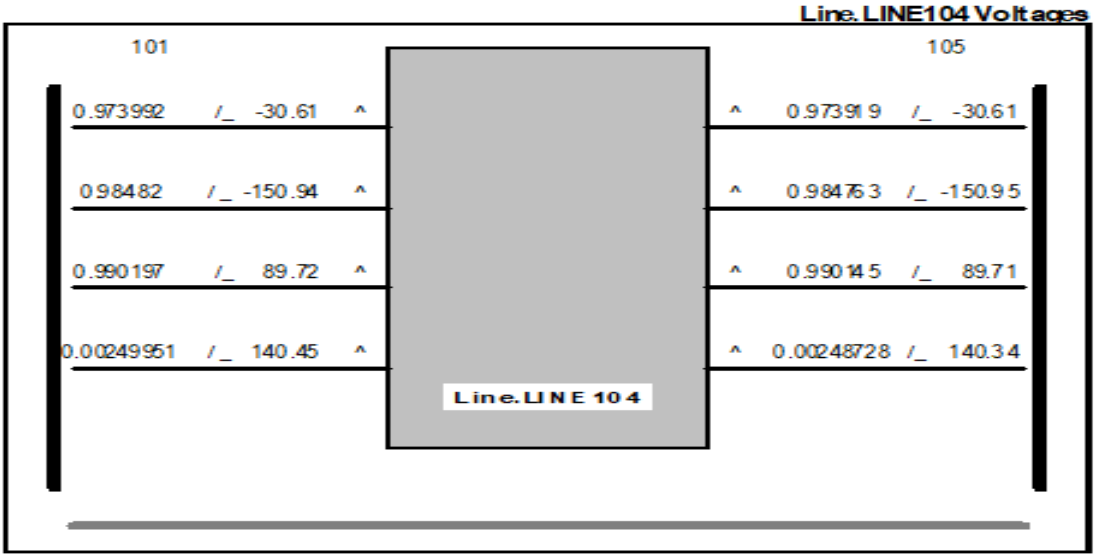


**Figure 6.4:** Voltages in a SGN line section